Departement für Kleintiere
Klinik für Kleintiermedizin
der Vetsuisse-Fakultät Universität Zürich

Direktorin: Prof. Dr. med. vet. Claudia Reusch, Dipl. ECVIM-CA

Arbeit unter der Leitung von:
Prof. Dr. med. vet. Felicitas Boretti Schär, Dipl. ACVIM & ECVIM-CA
Prof. Dr. med. vet. Nadja Sieber-Ruckstuhl, Dipl. ACVIM & ECVIM-CA

Characterization of canine plasma lipidome alterations due to prednisolone or tetracosactide treatment of healthy beagle dogs

Inaugural-Dissertation

zur Erlangung der Doktorwürde der
Vetsuisse-Fakultät der Universität Zürich

vorgelegt von

Susanne Spoerel

Tierärztin
von Hamburg, Deutschland

genehmigt auf Antrag von

Prof. Dr. med. vet. Felicitas Boretti Schär, Referentin
Prof. Dr. med. vet. Nadja Sieber-Ruckstuhl, Referentin
Prof. Dr. med. vet. Thomas Lutz, Korreferent

Zürich 2017

To my parents

Table of contents

Abstract

Lipidomic studies are gaining importance, as alterations in lipid metabolism have been recognized as being involved in the pathogenesis of several diseases.

This study aimed to characterize the plasma lipidome of healthy Beagle dogs using a targeted lipidomic approach and to evaluate alterations in the lipidome after short-term prednisolone and long-term tetracosactide treatment as a model of hypercortisolism. Both treatments led to significant lipidome alterations, however, they were more pronounced and more profound after long-term steroid excess. Lipid load was decreased after short-term and increased after long-term excess. In two detected lipid classes (cholesterol esters and sphingosine-1-phosphate) clear opposite effects were found. After long-term tetracosactide treatment, phosphatidylcholine and lysophosphatidylcholine species with an acyl chain length of <19 carbon atoms and low unsaturation were upregulated, whereas lipid species with a chain length of ≥19 carbon atoms and high unsaturation were downregulated.

We conclude that evaluation of the whole lipidome is crucial for a complete picture of plasma lipid changes, as the measurement of single lipid classes may obscure relevant alterations. The different findings depending on the duration and type of treatment are a first step in characterizing the influence of steroids on the lipid metabolism; however, the biological significance of these findings clearly has to be evaluated with further studies.

Zusammenfassung auf Deutsch

Lipidomanalysen gewinnen an Bedeutung, da erkannt wurde, dass Veränderungen im Lipidmetabolismus bei der Pathogenese verschiedener Erkrankungen eine Rolle spielen.

Die vorliegende Studie beschreibt das Plasmalipidom von Beaglen mit einer gezielten massenspektrometrischen Technik und charakterisiert Veränderungen nach Kurzzeit Prednisolon- und Langzeit Tetracosactidbehandlung als Model eines Hyperkortisolismus. Beide Therapien führten zu Lipidomveränderungen, wobei diese nach Langzeitsteroidexzess ausgeprägter und tiefgreifender waren. Die Lipidkonzentration war nach Kurzzeitsteroidexzess vermindert und nach Langzeitsteroidexzess erhöht. Bei Cholesterylestern und Sphingosin-1-phosphat wurden gegensätzliche Effekte je nach Behandlungslänge und -art gesehen. Zudem waren nach Langzeitsteroidexzess Phosphatidycholine und Lysophosphatidylcholine mit einer Acylkettenlänge von <19 Kohlenstoffatomen und geringem Unsättigungsgrad aufreguliert, während Spezies mit einer Acylkettenlänge von ≥19 Kohlenstoffatomen und hohem Unsättigungsgrad runterreguliert waren.

Lipidomanalysen sind wichtig für die Beurteilung von Lipidveränderungen, da die Messung einzelner Lipidklassen diese Änderungen eventuell nicht detektiert. Die abweichenden Ergebnisse basierend auf der Behandlungsdauer und -art sind erste Schritte bei der Charakterisierung des Einflusses von Steroiden auf den Lipidmetabolismus. Weitere Studien zur Beurteilung der biologischen Signifikanz dieser Veränderungen sind nötig.

Abbreviations

ACTH	adrenocorticotropic hormone
ADH	adrenal-dependent hyperadrenocorticism
BuMe	butanol/methanol
CE	cholesteryl ester
Cer	ceramide
CoV	coefficient of variation
CRH	corticotropin releasing hormone
DG	diacylgylcerol
DHCer	dihexosylceramide
DM	diabetes mellitus
ESI	electrospray ionization
FA	fatty acid
FC	fold change
GL	glycerolipids
GM3	GM3 ganglioside
GP	glycerophospholipids
GR	glucocorticoid receptor
HAC	hyperadrenocorticism
ISTD	internal standard
LC-MS	liquid chromatography mass spectrometry
LPC	lysophosphatidlycholine
LPL	lipoprotein lipase
LPE	lysophophatidylethanolamine
MHCer	monohexosylceramide
MG	monoacylglycerol
MRM	multiple reaction monitoring
MS	mass spectrometry
MS/MS	tandem mass spectrometry
MVA	mevalonic acid pathway
m/z	mass-to-charge ratio
OPLS-DA	orthogonal partial least squares discriminant analysis
PC	phosphatidylcholine
PDH	pituitary-dependent hyperadrenocorticism
PE	phosphatidylethanolamine
PG	phosphatidylglycerol
PI	phosphatidylinositol
PK	polyketide

PR	prenol lipid
PS	phosphatidylserine
SL	saccharolipid
SM	sphingomyeline
SP	sphingolipids
S1P	sphingosine-1-phosphate
ST	sterol lipids
TG	triacylglycerols
TQC	pooled quality control
VLDL	very low-density lipoprotein

Chapter One

Introduction

1.1 Lipids

Lipids are defined as hydrophobic or amphiphatic small molecules that may originate entirely or in part through carboanion-based condensations of thioesters and/or carbocation-based condensations of isoprene units (Fahy et al., 2009). Biological lipids refer to a broad range of naturally occurring molecules including fatty acids, eicosanoids, triglycerides, phospholipids, sphingolipids and fat-soluble vitamins (Dennis, 2009; Vance et al., 2008). They serve as signaling molecules and have biological functions as structural components of cell membranes as well as in energy storage.
The study of all fundamental lipid species in a defined sample type such as plasma or serum is defined as a lipidomic study, which is a characterization of the lipidome (Han and Gross, 2005; Oresic et al., 2008). The classification of lipids is commonly based on the LIPID MAPS Consortium recommendation. Referring to the LIPID MAPS Lipid Classification System, there are eight lipid categories, which are based on the chemical structure including the headgroup: fatty acyls, glycerolipids, glycerophospholipids, sphingolipids, saccharolipids, polyketides, sterol lipids and prenol lipids (table 1.1) (Fahy et al., 2005; Fahy et al., 2009). Each of the eight categories contains distinct lipid classes and subclasses (Schmelzer et al., 2007). The categories represent lipid structures from mammals and non-mammalian sources like plants, fungi and bacteria. Most of the categories are found in mammals apart from polyketides (PK), which are metabolites from plant and microbial sources and saccharolipids (SL), which are found in gram-negative bacteria. In the following, the focus is on lipid categories found in mammals.

Category	Abbreviation	Structures in Database
Fatty acyls	FA	7010
Glycerolipids	GL	7542
Glycerophospholipids	GP	9620
Sphingolipids	SP	4352
Sterol Lipids	ST	2835
Prenol Lipids	PR	1256
Saccharolipids	SL	1316
Polyketides	PK	6742
		40673 TOTAL

Table 1.1: Summary of lipid categories listed in the LIPID MAPS Lipid Classification System (modified based on (Fahy et al., 2009)), structures in database as of 01/30/17 (http://www.lipidmaps.org/data/structure/index.html).

1.1.1 Lipid categories found in mammals

Fatty acyls (FA) are lipids with a simple structure, as they consist of repeating series of methylene groups. They are synthesized by chain elongation of an acetyl-CoA primer with malonyl-CoA groups. The group of FA is diverse as it comprises fatty acids, eicosanoids, fatty alcohols and fatty amides. Especially fatty acids are widely used as building blocks for more complex lipid categories such as glycerolipids and sphingolipids (Han, 2016).

Glycerolipids (GL) consist of mono-, di- and tri-substituted glycerols. The main constituent during synthesis is α-glycerophosphate, which is then esterified with acyl-CoA. This leads to the synthesis of 1,2-diacyl phosphoglycerol, which is further dephosphorylated into diacylglycerol (DG). DG can be transformed either into monoacylglycerols (MG) or triacylglycerols (TG). TGs represent the main storage fat in mammalian tissues (Cohen and Spiegelman, 2016).

Glycerophospholipids (GP) (figure 1.1) are divided into subclasses based on their chemical properties, in detail by their polar head group situated at the sn-3 position of the glycerol backbone. GPs have several subclasses and their synthesis differs depending on their subclass affiliation. The subclasses are dominated by phosphatidylcholine (PC) (also known as lecithin), phosphatidylethanolamine (PE), phosphatidylinositol (PI) and phosphatidylserine (PS). PCs, PEs and PSs differ from each other only slightly and can be easily converted into each other (Püschel et al., 2011). GPs are amphiphilic and represent the main components of the cellular lipid bilayer and are therefore omnipresent (Vance et al., 2008).

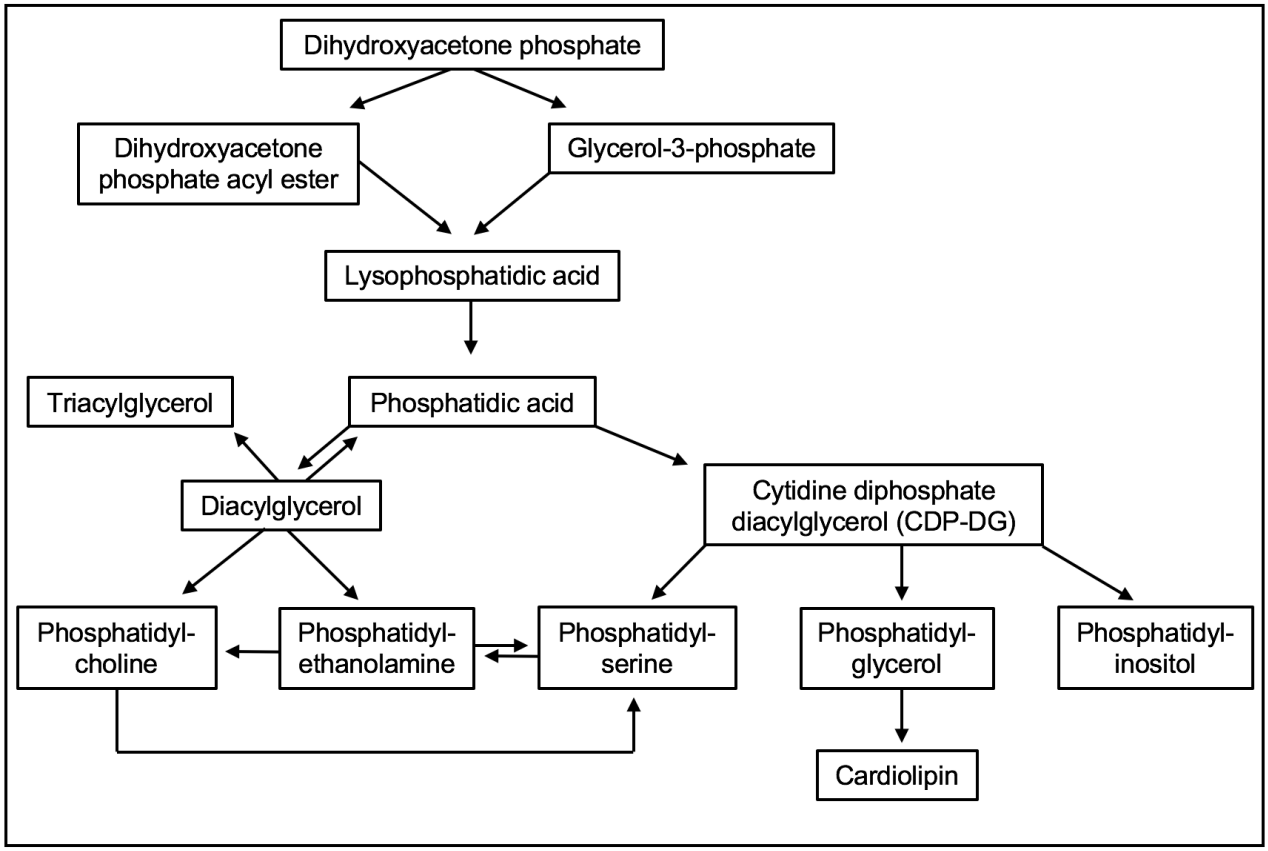

Figure 1.1: Major glycerophospholipid metabolic pathways (modified from (Zhang et al., 2015)).

The sphingolipid backbone is the common structural feature in all sphingolipids (SP) (Stryer, 1990). SPs are synthesized de novo from serine and palmitoyl-CoA followed by conversion into ceramides (Cer), phosphosphingolipids, glycosphingolipids (figure 1.2). The conversion leads to various structures of the subclasses, e.g.: firstly, the sphingoid bases with an amide-linked fatty acid such as Cer; secondly, more complex phosphosphingolipids, where the hydroxyl group of the sphingoid base is linked with various ligands such as choline; thirdly, glycosphingolipids, mainly found in the neural system, where sugar residues are linked β-glycosidically with the hydroxyl group of the sphingoid base (Püschel et al., 2011). SPs are found in cell membranes (Vance et al., 2008) and Cers are present on the epidermis, playing a role in stabilizing the lipid barrier of the skin. However, Cers can also act as signaling molecules (Püschel et al., 2011).

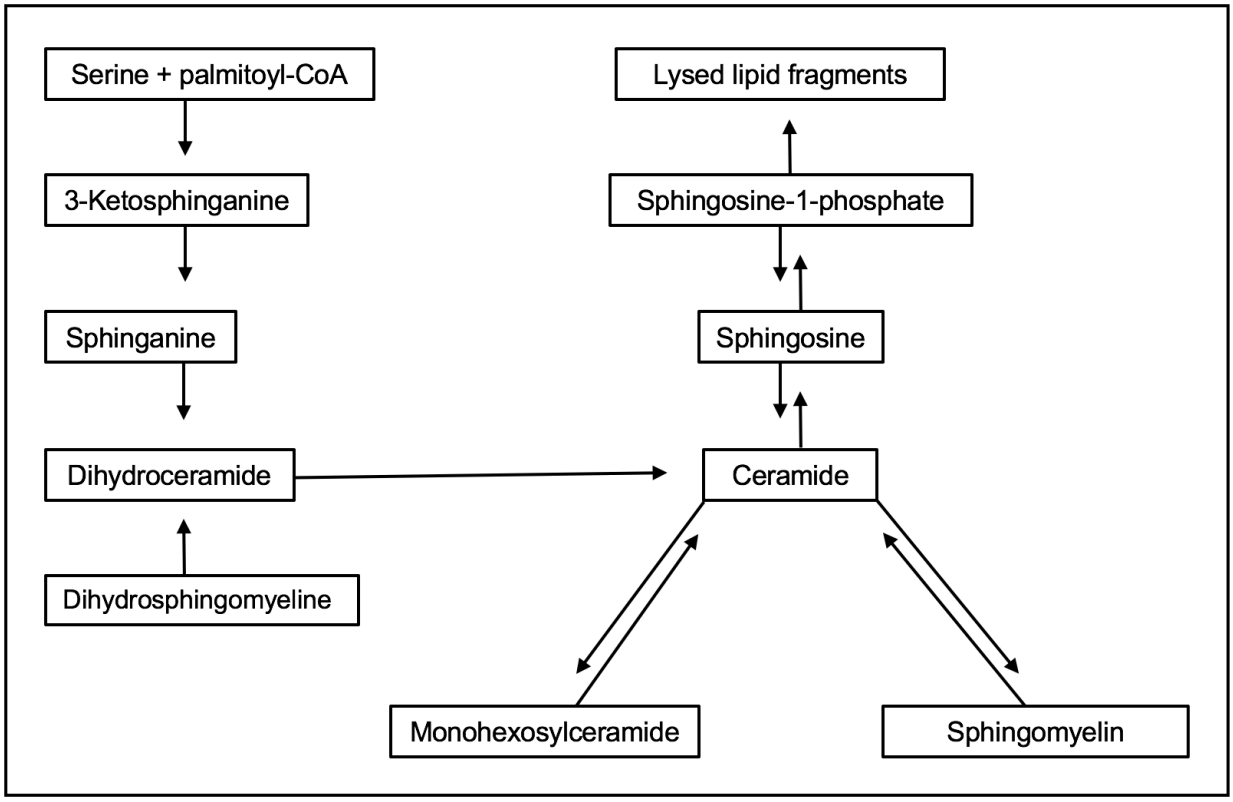

Figure 1.2: Conserved sphingolipid pathway: left: de novo biosynthesis; right: salvage pathway and complex sphingolipid biosynthesis (modified from (Zhang et al., 2015)).

Sterol lipids (ST) consist of cholesterol and its derivatives. Structurally, this group can be detected by their fused four-ring structure. Steroid hormones secreted from the adrenal cortex, testes and ovaries and placenta during pregnancy are products synthesized from cholesterol. Steroids with 18 carbon atoms (C18) include the estrogen family, whereas C19 steroids make up androgens. Progesterones as well as the glucocorticoids and mineralocorticoids are members of the C21 subclass. Cholesterol and its derivatives are ingested in large amounts, serve as signaling molecules such as hormones and play an important role in intestinal fat absorption after conversion into bile acids (Püschel et al., 2011). Cholesterol derivatives are also found in cellular membranes.

Prenol lipids (PR) are synthesized via the mevalonic acid (MVA) pathway from the five carbon precursors isopentenyl diphosphate and dimethylallyl diphosphate (Vance et al., 2008; Vance, 2002). Important members of the prenol lipids are carotenoids, quinones and hydroquinones (including vitamins E and K). They can

serve as antioxidants and play an important role in the transport of oligosaccharides across membranes.

1.1.2 Plasma lipids

In 2010, Quehenberger and coworkers were the first to publish work on the human plasma lipidome (Quehenberger et al., 2010). The lipid species they have found in human plasma belong to six of the eight existing lipid categories of which the most abundant categories were GP, ST and GL. A study performed in our lab investigating the plasma lipidome of dogs detected species belonging to seven of the eight existing categories, with only SL missing (Schmid, 2017). The fact that PKs were detected in canine plasma was explained by dietary intake of flavonides serving as plant pigments. Their origin remains unsolved. The three most abundant lipid classes in canine plasma were FAs, GPs and STs (Schmid, 2017). Generally, the variety of lipid species found in plasma is high, with more than 500 lipid species described in humans and over 400 in canines (Quehenberger et al., 2010; Schmid, 2017).

Alterations in the lipidome are found in association with various diseases. Therefore, many efforts are being made to establish possible biomarkers for several diseases e.g. obesity and cardiovascular disease (Bellis et al., 2014).
Going further into detail, an increase in lysophophatidylcholine (LPC) species was reported for obese patients (Pietiläinen et al., 2007; Schmitz and Ruebsaamen, 2010; Yang et al., 2005). LPC is an important component of oxidized low-density lipoprotein (Aiyar et al., 2007; Kougias et al., 2006), which induces apoptosis via oxidative stress, promoting atherogenesis. At the same time, ether phospholipids, known to have antioxidative properties, are decreased in those humans (Engelmann, 2004; Zoeller et al., 1999). Peroxidation of lipids has been suggested as promoting disease development, including atherosclerosis (Glass and Witztum, 2001).
Hypertension leads to a decrease in ether linked lipids (PC-O and PE-O) and free cholesterol (Graessler et al., 2009). While free cholesterol is an important factor leading to atherosclerotic plaque instability (Kolodgie et al., 2007), its role in plasma remains to be elucidated. It has been hypothesized that a deficiency of arachidonic acid-rich ether lipids could potentially contribute to the pathogenesis of essential hypertension (Graessler et al., 2009).
Moreover, insulin resistance shows a correlation with TGs, consisting of either saturated or monounsaturated fatty acids, possibly reflecting an increased hepatic de novo synthesis of those fatty acids (Kotronen et al., 2009).
The metabolic syndrome is a major and emerging public health and clinical challenge worldwide as a consequence of urbanization, exaggerated energy uptake, obesity and sedentary lifestyle (Kaur, 2014). It is defined as a group of factors, which, if altered considerably increase the risk of developing cardiovascular disease and type 2 diabetes mellitus (Kaur, 2014; Wilson et al., 2005). Identification of sufferers from this syndrome is possible if three of the following factors are present: hypertension, dyslipidemia, impaired fasting glucose and abdominal obesity (Alberti et al., 2009; Kaur, 2014; Wilson et al., 2005).

1.2 Mass spectrometry based lipidomics

Along with the vast fields of genomics and proteomics, lipidomics is emerging as a new field in the 21st century. Estimations predict between 10,000 and 100,000 distinct chemical structures in the lipidomics field. The complexity of lipidomics is high as there is no genetic code for lipids but their synthesis relies on enzymes, which are

influenced by the biological system as well as by dietary intake. First reports of mass spectrometric (MS) based analysis of complex lipid mixtures were published by Kim et al. and Han and Gross in the 1990s (Han and Gross, 1994; Kim et al., 1994).

MS can be divided into “untargeted” and “targeted” approaches. Untargeted analysis can be conducted with time-of-flight MS and Orbitrap MS and has high mass accuracy and resolution. Its aim is to screen for any lipid in the sample, which is an important approach in biomarker detection. Within a given mass-to-charge ratio (m/z) the sample is screened for lipids either in positive or negative mode. Even though it has a high mass accuracy and resolution, the disadvantage of this method is that only very abundant lipid species can be detected due to limited experimental time. In a targeted approach, ions with a specific m/z and specific retention time are detected.

Shot-gun lipidomics as a targeted technique is based on the identification of a given precursor ion m/z and, in the case of tandem MS, depends on a characteristic fragment ion m/z. Single state MS (no fragmentation of molecule) can be used to study a lipid profile in general. For further characterization of the lipid profile, tandem MS (MS/MS) screens for lipids with a given precursor and fragment ion m/z and retention time. Multiple reaction monitoring (MRM) coupled with MS/MS makes (semi)quantitative analysis of targeted lipid species possible (figure 1.3). Even though new molecules cannot be detected with this technique, its major advantage is that molecules at all abundance ranges above noise level can be detected. The mass accuracy and resolution in a targeted approach is as high as in an untargeted approach (Hyötyläinen and Orešič, 2015).
Challenges in MS still remain; for example, the detection of low abundant lipid species as well as configurations of double bonds, which cannot be determined by MS/MS. The configuration of double bonds makes a clear distinction of lipid species with geometric isomerism possible (identical chemical formula but double bond either in cis- or trans-conformation). At the same time improvements are being made such as the identification of so far uncharacterized lipids, which is possible due to MS’s high resolution as well as discrimination of lipids with similar mass and chemical structures. Even close similarities such as isomers (same chemical formula but different structure) and isobars (different molecules with the same mass) can be distinguished.

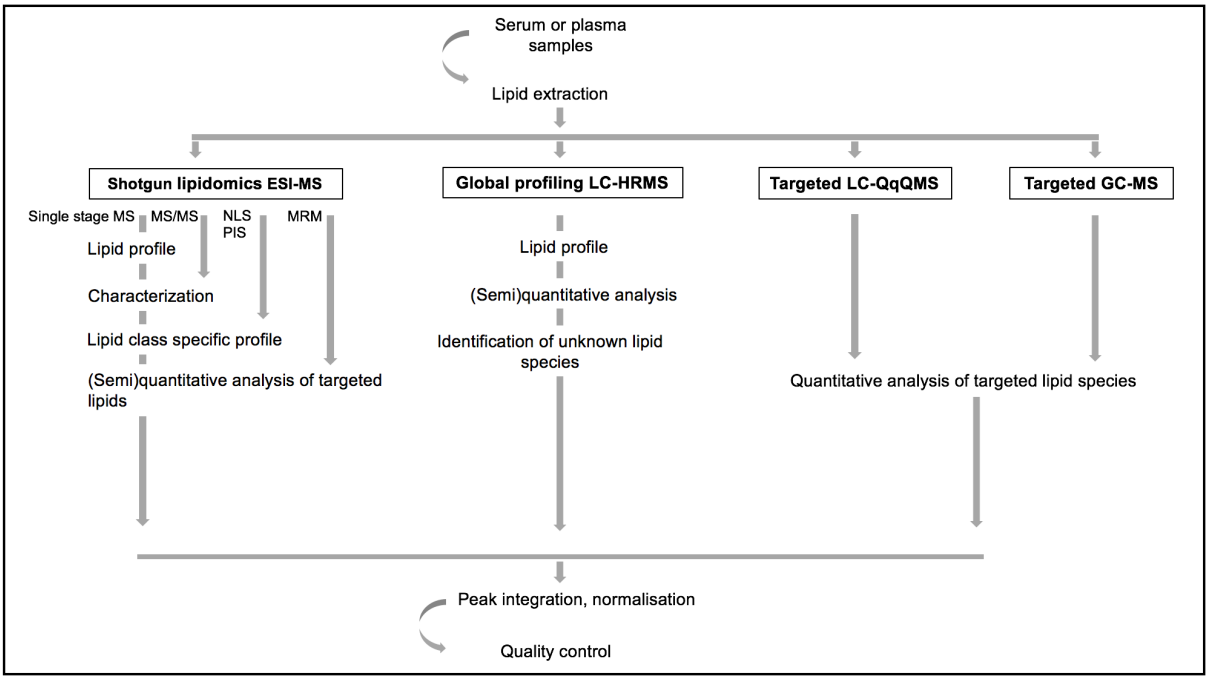

Figure 1.3: Methods used for lipidomic analysis of serum and plasma samples. Used abbreviations: ESI: electrospray ionization, HRMS: high resolution mass spectrometry, LC: liquid chromatography, GC: gas chromatography, MRM: multiple reaction monitoring, NLS: neutral loss scanning, PIS: precursor ion scanning, QqQMS: triple-quadrupole mass spectrometry (adapted from (Hyötyläinen and Orešič, 2015).

1.3 Hyperlipidemia

Hyperlipidemia is defined as an elevation of plasma cholesterol, TGs or both, or a low high-density lipoprotein level. It is known to contribute to the development of atherosclerosis in humans. There are two forms: primary and secondary hyperlipidemia. Primary hyperlipidemia is based on genetic abnormalities, whereas secondary hyperlipidemia results from underlying diseases. Among all chronic disease states, secondary hyperlipidemia is seen as the second most frequent abnormality (CDC, 2009). The etiology of human secondary hyperlipidemia is diverse, as diets rich in fats, alcohol excess, weight gain, administration of drugs (e.g. glucocorticoids, estrogens, antihypertensives) and hypothyroidism are known to be underlying conditions (Nelson, 2013; Stone, 1994). Hyperlipidemia is an important component of the metabolic syndrome and an important risk factor in the development of type II diabetes (Meikle and Christopher, 2011). Furthermore, hyperlipidemia is considered a serious state in humans due to its well-known subsequent elevated risk for cardiovascular disease (Nelson, 2013), which is the leading cause of morbidity and mortality worldwide. Thus, extensive research has been undertaken in human medicine, while in veterinary medicine up to now studies are only limited (Boynosky and Stokking, 2014; Chiers et al., 2010; Hess et al., 2003; Xenoulis and Steiner, 2010).

1.3.1 Canine Hyperlipidemia

The underlying causes of hyperlipidemia in dogs are divided into physiologic postprandial hyperlipidemia, rare primary hyperlipidemia caused by genetic abnormalities and common secondary hyperlipidemia due to underlying diseases such as endocrinopathies (e.g. as diabetes mellitus (DM), hypothyroidism and

hyperadrenocorticism), pancreatitis, obesity and lymphoma (Xenoulis and Steiner, 2010).
Interestingly, naturally occurring canine atherosclerosis seems to be a rare disease with just a few case reports published (Boynosky and Stokking, 2014; Chiers et al., 2010) and only 30 dogs with atherosclerotic lesions detected in a retrospective clinical study (Hess et al., 2003). This is remarkable especially as obesity is a problem with consistently increasing significance in small animals (German, 2006). Hess and coworkers (Hess et al., 2003) have shown that certain endocrine diseases are associated with a higher risk of the development of atherosclerosis, namely DM and hypothyroidism, while others such as hyperadrenocorticism are not. This is of interest, as not only diabetes and hypothyroidism but also hyperadrenocorticism are associated with hyperlipidemia. The reason for this phenomenon is so far unknown.

1.4 Hyperadrenocorticism

Cortisol excess is the main characteristic in the disease called hyperadrenocorticism (HAC), which is nowadays one of the most commonly diagnosed endocrinopathies in dogs (Mooney and Peterson, 2004). An excess of cortisol can result from chronic, excessive glucocorticoid therapy (iatrogenic HAC) or from high levels of endogenously produced cortisol due to a malfunction of the hypothalamic-pituitary-adrenal axis (naturally occurring HAC). Generally, naturally occurring HAC is divided into two forms depending on the localization of the neoplastic lesion causing the disease: Neoplasia of the anterior pituitary gland (pituitary-dependent hyperadrenocorticism, PDH) occurring in 80% of canine patients with spontaneous HAC, or the adrenal gland (adrenal-dependent hyperadrenocorticism, ADH) (Mooney and Peterson, 2004). In PDH, high amounts of adrenocorticotropic hormone (ACTH) are secreted, leading to an increase in cortisol production by the adrenal glands. At the same time, the physiological negative-feedback loop is impaired as the neoplastic cells are neither responsive to high cortisol levels nor to the decreased secretion of corticotropin releasing hormone (CRH). In the case of ADH, the neoplastic cells in the adrenal gland produce high amounts of cortisol. Such production is hyporesponsive to the negative-feedback loop of decreased ACTH levels (Prélaud et al., 2005).
Clinical symptoms are a wide-ranging, as with most endocrinopathies. An overview of symptoms in dogs is summarized in Table 1.2.

General condition	polydipsia
	polyuria
	polyphagia
	lethargy
	abdominal enlargement (“potbelly”)
	panting
	muscle weakness, muscle wasting
	hepatomegaly
Urinary tract	recurrent urinary tract infections
Endocrinology	diabetes mellitus
Dermatology	alopecia (especially truncal)
	thin skin
	pyoderma
	comedones
	bruising
	dermal atrophy (especially close to scars)
	calcinosis cutis
Cardiology	hypertension
	pulmonary thromboembolism
Neurology	pseudomyotonia
	facial nerve palsy

Table 1.2: Symptoms of hyperadrenocorticism listed in approximate decreasing order of frequency (adapted from (Feldman, 2015))

1.5 Corticosteroids

1.5.1 Receptor

As a member of the steroid hormone family, cortisol exhibits its effects at cell level via nuclear receptors, namely the glucocorticoid receptor (GR). Unliganded GR are present in the cytoplasm in a complex bond with several heat shock proteins and chaperone complexes (Oakley and Cidlowski, 2011). Dissociation from the complex and translocation into the nucleus results after ligand binding.
Glucocorticoid-activated GR regulates gene expression firstly by binding directly to DNA, secondly by tethering itself to other DNA-bound transcription factors and thirdly by binding to the DNA directly, interacting with neighboring DNA-bound transcription factors (Oakley and Cidlowski, 2011).

1.5.2 Systemic effects

The effects of cortisol in vivo are multifaceted and at times contradictory. Physiological levels of cortisol are essential to facilitate the complex metabolism of carbohydrates, proteins and lipids (Mooney and Peterson, 2004). Moreover, they have anti-inflammatory characteristics. Excessive cortisol levels cause muscle loss by protein breakdown as well as systemic insulin resistance (Lee et al., 2014). Biochemical and molecular mechanisms of these effects still remain poorly understood (Ljung et al., 2000). We focus in the following on cortisol’s pathophysiological function, especially on adipose tissue. Freedman et al, highlighted the important role of cortisol in lipid metabolism as early as 1986 (Freedman et al., 1986). Adrenalectomized Zucker rats were protected from high-fat induced obesity, which was reversible by supplementation of hydrocortisone (Freedman et al., 1986). Increase in lipid uptake is facilitated by cortisol through activating the enzyme

lipoprotein lipase (LPL) (Appel and Fried, 1992; Fried et al., 1993; Ottosson et al., 1994). LPL hydrolyses triglycerides bound to very low-density lipoproteins (VLDL) and chylomicrons and therefore increases the release of fatty acids from VLDL and chylomicrons in the blood when activated (Peckett et al., 2011). Furthermore, it has been shown in vitro that preadipocytes and adipose stromal cells are stimulated by cortisol and dexamethasone to differentiate into mature adipocytes (Hauner et al., 1989). Lipogenesis due to excess cortisol varies depending on the localization of adipose tissue as seen in HAC: significant increase in central, especially visceral, adipose tissues, whereas peripheral subcutaneous fat depots decrease (Geer et al., 2010; Rockall et al., 2003). At the same time, cortisol is also widely referred to as lipolytic. The lipolytic effect on mature adipocytes is generally explained by the increased transcription and expression of the lipase proteins adipose triglyceride lipase and hormone-sensitive lipase (Campbell et al., 2011; Slavin et al., 1994; Xu et al., 2009). However, the results differ depending on the experimental model systems used, as well as on the concentration and duration of cortisol treatment. Due to the similarities between metabolic abnormalities in central obesity and cortisol excess, it has been hypothesized that disorders in cortisol metabolism play essential roles in the development of obesity and the pathogenesis of obesity-related diseases (Lee et al., 2014).

1.5.3 Therapeutic usage

Corticosteroids are widely used in human and veterinary medicine, because of their potent anti-inflammatory and immunosuppressive effects. The term corticosteroids normally refers to glucocorticoids, which vary in potency (table 1.3), durations of action and relative glucocorticoids (measured by anti-inflammatory activity) vs mineralocorticoid (measured by sodium retention) activities. Their mechanism of action is similar to endogenous cortisol. Their anti-inflammatory effects are mediated on one hand, by stabilizing lysosomal membranes to reduce the release of proteolytic enzymes by damaged cells, and on the other hand by depressing the phagocytic abilities of white blood cells to reduce further release of inflammatory materials (Mooney and Peterson, 2004). Their immunosuppressive effects are mediated by interference with signaling from the key inflammatory transcriptional regulators (NF-κB and AP-1) (Heck et al., 1994; Jonat et al., 1990; Wang et al., 2013; Yang-Yen et al., 1990).

Indications for the use of corticosteroids in human and veterinary medicine are numerous, including asthma, systemic lupus erythematosus, hemolytic anemia, rheumatoid arthritis, psoriasis, inflammatory bowel disease, nephritic syndrome, cancer, leukemia, organ transplantation, autoimmune hepatitis, hypersensitivity reactions, cardiogenic and septic shock and glucocorticoid deficiency diseases like Addison's disease.

Substance grouped by duration of action	Glucocorticoid activity (Cortisol =1)	Mineralocorticoid action
Short activity:		
Cortisol/Hydrocortisone	1	1
Cortisone	0.8	0.8
Medium long activity:		
Prednisolone	4	0.8
Prednisone	4	0.8
Long activity:		
Dexamethasone	25	0.75
Flumethasone	700	0

Table 1.3: Comparison of corticosteroids: duration of action, glucocorticoid activity and mineralocorticoid action (modified from (Diseases and Services, 2014))

1.6 Aim of this study

Based on the information given above, two objectives were addressed in the present work:

Firstly, to characterize the plasma lipidome of healthy Beagle dogs using a targeted lipidomic approach.
Secondly, to evaluate alterations in the plasma lipidome after short-term prednisolone and long-term tetracosactide treatment of healthy Beagle dogs.

Chapter Two

Materials and Methods

2.1 Animals

In this study healthy beagle dogs were used. All dogs were considered healthy based on the results of a physical examination, complete blood count and biochemical analysis of serum and urine. The dogs were housed in groups of 2-4 in standard kennels at a university facility, fed dry adult maintenance dog food (Josera, Adult Sensitive, Kleinheubach, Germany), and given access to water ad libidum. Blood was collected from the jugular vein into lithium heparin tubes (Vacuette Greiner bio-one, Frickenhausen, Germany) after 12 hours of fasting. The samples were centrifuged immediately after collection (1862 x g, 10 min, 4°C) and plasma was stored at -80°C.
For the first experiment (short-term prednisolone treatment), 8 Beagles (5 intact males, 2 intact and 1 spayed female), aged between 7 and 58 months (median 25.5 months) and weighing between 9 and 15.5 kg (median 12.5 kg) were used. Dogs were treated with 50 mg/d prednisolone (Streuli Pharma AG, Uznach, Switzerland, Pharmacode 0718393) orally twice daily for 3 consecutive days. Blood samples were collected before the start of treatment and on day 4, 12 hours after the last prednisolone administration.
For the second experiment (long-term tetracosactide treatment), 6 Beagles (4 intact males, 1 intact and 1 spayed female), aged between 23 and 88 months (median 71.5 months) and weighing between 14 and 19.8 kg (median 15.85 kg) were used. All dogs were infused using minipumps (model: 2ML4, Alzet, Durect Corporation, Cupertino, CA, USA) subcutaneously implanted in the subcutaneous area of dorsolateral neck for 25 weeks with synthetic tetracosactide (Bachem AG, Bubendorf, Switzerland, catalogue number: 4042686). Every four weeks the pumps were replaced with increasing doses of tetracosactide. The dogs were divided into two groups (low-dose and high-dose group), with three dogs in each group (one female and two males). The high-dose group received a starting dose of 1.95 ± 0.28 µg kg^{-1} d^{-1} tetracosactide, increased to 10.3 ± 0.1 µg kg^{-1} d^{-1}. The low-dose group received a starting dose of 0.31 ± 0.04 µg kg^{-1} d^{-1} tetracosactide, increased to 6.3 ± 0.76 µg kg^{-1} d^{-1}. Blood sampling was conducted before and at regular intervals up to 25 weeks after start of treatment. Moreover, the successful induction of HAC was tested with an ACTH stimulation test and a low-dose dexamethasone suppression test 25 weeks after start of treatment. For the ACTH stimulation test, 5 µg kg^{-1} synthetic tetracosactide (Synacthen ®, Novartis Pharma Schweiz AG, Bern, Switzerland, Pharmacode: 6748610) were injected intravenously and plasma cortisol measured 0 and 1 hour after injection. For the low-dose dexamethasone test, 0.01 mg kg^{-1} dexamethasone (Dexadreson ®, MSD Animal Health GmbH, Luzern, Switzerland, ATCvet number: QH02AB02) were injected intravenously and plasma cortisol measured 0, 4 and 8 hours after injection.
Blood samples obtained before treatment ensured that each animal served as its own control.

Both studies were approved by the Cantonal Veterinary Office of Zurich (TVB 133/2013 and 276/2014), and conducted in accordance with guidelines established by the Animal Welfare Act of Switzerland.

2.2 Lipid extraction

A stock solution was prepared for each standard lipid by dissolving standard lipids in butanol/methanol (BuMe) (1:1, v/v) (table 2.1). Aliquots of each stock solution were transferred to a glass Erlenmeyer flask to create the internal standard mix. Plasma lipids were extracted using a modified version of the butanol/methanol method (Alshehry et al., 2015). Plasma samples were thawed on ice. Then, 10 µl plasma was transferred to Eppendorf tubes (Eppendorf, Hamburg, Germany) and 2,6-di-tert-butyl-4-methylphenol (BHT) (Sigma-Aldrich Saint Louis, MO, USA, Cat. No.: B1378) 1 µl 10 mM in ethanol (Sigma-Aldrich, 02854) was added to prevent oxidation. Next, 90 µl 1-butanol:methanol (1:1, v/v) (Sigma-Aldrich, 34867; 34860, respectively) containing the internal standards (table 2.1) were added, followed by vortexing for 10 seconds. The samples were sonicated (Sonorex Digiplus DL 255H, Bandelin electronic GmbH & Co. KG, Berlin, Germany) at room temperature, maintained by the addition of ice cubes for 30 minutes at 40 kHz, and precipitants were removed by centrifugation (14000 x g, 10 min, 4°C). Finally, 90 µl of supernatant was transferred into Sarstedt micro tubes (Sarstedt AG & Co, Nümbrecht, Germany, 72.694.006) and dried under a nitrogen stream at 37°C (Dri-Block D8-3D, Techne Sample Concentrator, Bibby Scientific Limited, Stone, UK). Samples were stored at -80°C until further analysis.

Before analysis, reconstitution of dried lipid extracts was performed by placing them on ice and adding 90 µl of 1-butanol:methanol (1:1, v/v). The samples were vortexed for 30 seconds and sonicated (Brandson Ultrasonic CPXH Series) for 10 minutes at room temperature for precipitation. After sonication, samples were vortexed for 30 seconds and centrifuged (20,800 x g, 10 min, 4°C). Then, 80 µl supernatant were transferred into microvolume glass inserts (Agilent Technologies, Santa Clara, CA, USA, 5182-0549) for analysis.

Table 2.1: Internal standard lipids

Internal Standard Mix	Internal Standard (Abbreviation)	Final conc. in mix (ng/ml)	Supplier; Cat. No.
Sterol lipid, D6 cholesterol ester	CE 18:0 d6	100	CDN Isotopes; D-2139
Glycerolipid, d5TAG	d5TAG 48:0/16:0 16:0 16:0	100	CDN Isotopes D-5815
Glycerolipid, 12:0 DG	DG 24:0 (12:0)	100	Avanti Lipids; 800821P
Glycerophospholipid, DMPC	PC 14:0 14:0	100	Avanti Lipids; 850345P
Glycerophospholipid, 20:0 LPC	LPC 20:0	50	Avanti Lipids; 855777P
Glycerophospholipid, PI 12:0/13:0	PI 12:0 13:0	50	Avanti Lipids; LM-1500
Glycerophospholipid, DMPE	PE 14:0 14:0	50	Avanti Lipids; 850745P
Glycerophospholipid, 14:0 Lyso LPE	PE 14:0 (0:0)	50	Avanti Lipids; 856735P
Glycerophospholipid, DMPS, 14:0 PS	PS 14:0 14:0	50	Avanti Lipids; 840033P

Internal Standard Mix	Internal Standard (Abbreviation)	Final conc. in mix (ng/ml)	Supplier; Cat. No.
Glycerophospholipid, DMPG, 14:0 PG	PG 14:0 14:0	50	Avanti Lipids; 840445P
Sphingolipid, 12:0 SM	SM d18:1/C12:0	50	Avanti Lipids; 860583P
Sphingolipid, C8GluCer	DHCer 8:0	50	Avanti Lipids; 860540P
Sphingolipid, C17Cer	Cer d18:1/C17:0	50	Avanti Lipids; 860517P
Sphingolipid, DiHexosylCer 16:0 d3	DHC 16:0 d3	50	Matreya LLC; 1534
Sphingolipid, MHC 16:0 d3	MHC d18:1/16:0 d3	50	Matreya LLC; 1533
THC 18:0 d3	THC 18:0 d3	50	Matreya LLC; 1537

Table 2.1: Internal standard lipids
Components of the internal standard mix and their abbreviations: The final concentration of the internal standard in the mix varied depending on the individual internal standard (column 3). Suppliers and catalogue number are given in the right column.

2.3 Mass spectrometry

2.3.1 Chemicals and instruments

All chemicals used for liquid chromatography mass spectrometry (LC-MS) were LC-MS grade. Acetonitrile, formic acid and isopropanol were obtained from Fisher Scientific (Fisher Scientific, Hampton, NH, USA, A955-4, A117-50 and A461-4, respectively) and non LC-MS grade ammonium formate 10 M in H_2O from Sigma Aldrich (Sigma-Aldrich, 78314). Unless otherwise noted, the LC was performed using Agilent Technologies 1290 infinity series pumps.

2.3.2 Panel 1 and 2

Panel 1 and 2 were measured with different MS instruments and parameters and had different dynamic MRM lists (table 5.9 and 5.10 respectively).
Mobile phase A consisted of 40% (v/v) acetonitrile, 60% MilliQ water and 10mM ammonium formate, mobile phase B of 10% acetonitrile, 90% isopropanol and 10 mM ammonium formate. Analytes were eluted with the following gradient: 80% A 20% B from 0 to 1.99 min; 40% A 60% B from 2 to 6.99 min; 0% A and 100% B from 7 to 9 min; 80% A and 20% B from 9.01 to 10.8 min. The flow rate was set to 0.4 ml/min and the column oven to 40°C. Samples (2 µl panel 1 and 1 µl panel 2) were injected onto an Agilent Zorbax RRHD Eclipse Plus C18 (2.1 x 50 mm, particle size 1.8 µm, pore size 95 Å).
MS was conducted with a Triple Quadrupole (model no.: 6460 for panel 1, model no.: 6495 for panel 2) LC-MS operated in positive mode for panel 1 and in positive and negative mode for panel 2 with electrospray ionization (ESI) (detailed information table 5.5 and 5.6 respectively). All analyses were performed in dynamic MRM mode with a unit mode of 0.7 dalton. Data acquisition was carried out using Agilent MassHunter software (version B.06.00).

2.3.3 Panel 3

The chromatographic separation of TAG was undertaken on an Agilent LC1100 HPLC system (Agilent Technologies) and was done isocratically, using a mobile phase of chloroform:methanol (Fischer Scientific, chloroform: AC383770025) (1:1 v:v) containing 2 mM ammonium acetate (Sigma Aldrich, 17843) at a flow rate of 128 µL/min for 25 min; oven temperature 25°C. The stationary phase consisted of an Agilent Zorbax Eclipse XDB-C18 Silica column, length 150 mm, internal diameter 3 mm, particle size 1.8 µm and pore size 80 Å. Injection volume was 10 µl.
Mass spectrometry was undertaken on an ABSciex 4000QTrap (Applied Biosystems MDS SCIEX, Washington D.C. USA) in single-ion monitoring (SIM) mode with a unit mode of 0.7 dalton fitted with an ESI source. Parameters were as follows: source voltage 5.0 kV, source temperature 250°C, drying gas: nitrogen, gas 1 flow 40, gas 2 flow 30, curtain gas flow 10 (for detailed information, see table 5.7). Data acquisition was carried out using Analyst software (Applied Biosystems MDS SCIEX) (version 1.6.2).

2.3.4 Panel 4

Sphingosine-1-phosphate (S1P) analysis was performed according to the method described by (Narayanaswamy et al., 2014). To 50 µl of reconstituted lipid extracts, 50 µl of internal standard ($^{13}C_2D_2$–S1P; Toronto Research Chemicals, Toronto, Canada), 20 ng/ml in 1-butanol:methanol (1:1, v/v) were added and vortexed for 5 seconds. Under a chemical hood, 20 µl of TMS-Diazomethane (2 M in hexane, Acros Organics, NJ, USA, AC385330050) were added for derivatization, followed by an incubation in a thermomixer (Eppendorf thermomixer C, Hamburg, Germany) for 20 min at 25°C and 700 rpm and subsequent brief vortexing. To stop the reaction and to inactivate remaining TMS-Diazomethane, 1 µl of 100% acetic acid (Merck Millipore, Darmstadt, Germany, 100063) was added. Derivates were centrifuged at 20,800 x g for 10 minutes at 7°C. Finally, 100 µl of the supernatant was used for analysis.

Mobile phase A consisted of 50% (v/v) acetonitrile, containing 50% (v/v) 25 mM ammonium formate solution (in water, pH 4.6, adjusted using formic acid and mobile phase B 95% (v/v) acetonitrile containing 5% (v/v) 25 mM ammonium formate solution. Formic acid (Fluka Chemie GmbH, Buchs, Switzerland, 14265) was used to adjust the pH. Analytes were eluted with the following gradient: 0.1% A, 99.9% B from 0 to 4.99 min; 60% A, 40% B from 5 to 5.49 min; 90% A, 10% B from 5.5 to 6.59 min and 0.1 % A 99.9% B 6.6 to 8.6 min.
The column oven was set to 60°C and the flow rate to 0.4 ml/min. Samples (5 µl) were injected onto a Waters ACQUITY UPLC BEH HILIC (2.1 x 100mm, particle size 1.7 µm, pore size 130 Å) analytical column.
Mass spectrometry was performed using static MRM (table 5.11) on an Agilent Technologies 6490 Triple Quadrupole LC/MS operated in positive mode with an ESI source (detailed information table 5.8). Ions were isolated using a “unit” (0.7 dalton) mass selection window.
Data acquisition was performed using Agilent MassHunter software (version B.06.00).

2.3.5 Quality control

Pooled quality control (TQC, technical quality control) samples were injected and measured before the first and last sample as well as after every fourth sample, or sixth sample in the case of panel 3, to monitor technical accuracy during each run. Samples were pooled by taking off a defined volume from each sample. Panel 4

included TQCs including a volume of each sample. The other three panels had separate TQCs for each experimental group (prednisolone and tetracosactide).

2.3.6 MS data processing

For panel 4, raw LC-MS data were imported in Skyline software (version 3.5) (MacLean et al., 2010).
Lipids with no or low (< 100 count intensity) peak areas were deleted.
For panel 1 and 2, raw LC-MS data were imported in MassHunter QQQ Quantitative Analysis. For panel 4, raw LC-MS data were imported in Analyst software (version 1.6.2).

Unless otherwise noted, data was processed in Microsoft Excel (Redmond, Washington, USA). Normalized intensities were calculated by dividing the raw peak area of the analyte by the raw peak area of the corresponding internal standard (ISTD) (tables 5.12-5.15). This ratio was used to calculate the concentration of measured lipids.
For panel 1, PE(P-acyl length:number of double bonds) with or without a head group attached were used as qualifiers and the same lipid species with a FA-adduct of a PE(P-acyl length:number of double bonds) were used as quantifiers. For panel 2, lipid species measured with a loss of H_2O were used as qualifiers and their corresponding lipids without water loss as quantifiers. For panel 4, the m/z 60.08 product was used as a quantifier (due to its high intensity) and m/z 113 was used as a qualifier. The qualifier represents the mono-methylated phosphate and was used to discriminate between penta-methylated species generated by the derivatization reaction.

2.4 Statistical analysis

Coefficient of variation (CoV) was determined for every experimental group (tetracosactide and prednisolone for panel 1,2,3) and for all samples (panel 4) by dividing the standard deviation of TQCs by the mean of the TQCs. Lipid species with a CoV <20% were reported as recommended by the FDA (U.S. Department of Health and Human Services, 2001). A binary logarithm of fold change (log2FC) determined by the following equation: log2FC = log2(mean value of group after treatment)-log2(mean value of group before treatment). Then the FC was determined with the following equation: FC = ^{2}log2FC. The standard deviation of measured lipid species based on FC was determined and indicated as error bars in bar charts depicting the FC created with GraphPad (GraphPad Software, Version 6.00, La Jolla California USA). Significant changes between results from dogs before and after treatment were determined by a paired, two-tailed Student's t-test with a p-value <0.05 considered significant. P-values were used to create volcano plots. Unless otherwise noted, statistical analyses were performed using MetaboAnalyst 3.0 online Software (Canada) (Xia et al., 2015). The false discovery rate was determined and a q-value of <0.05 considered as a significant change. Significant q-values are marked with stars in bar charts and used for the creation of heat maps. For all panels, a summary of detected lipids was created (supplementary table 5.18). This summary includes lipids measured in panel 1-4. As some lipid classes were measured in two or more panels, the results of lipid classes from just one of the panels were included in the summary to rule out overlap from the four panels. From this summary, volcano plots were created (GraphPad Software). The volcano plots depict lipid species with a p-value <0.05 (y-axis) and a FC >1.5 for upregulated lipid species and FC <-1.5 for downregulated lipid species (x-axis). A multivariate pattern recognition technique, in

this case a supervised (orthogonal partial least-squares discriminant analysis, OPLS-DA) score plot was applied to lipid concentration data to discriminate between sample features of healthy dogs and dogs during treatment. A supervised multivariate pattern recognition technique was implemented as the categories of samples (control or treated) were known, whereas unsupervised methods are used when the category of the sample is unknown and the aim is to find an appropriate category. A heat map based on Pearson's distance and Ward clustering algorithm of lipids with significant q-values was created to depict concentration changes of the individual dogs during treatment.

Chapter Three

Results

3.1 Clinical characteristics of the dogs

During treatment with prednisolone, all dogs showed polyuria, polydipsia and polyphagia. Increases in alkaline phosphatase levels were found in 6 out of 8 dogs and increases in alanine transaminase levels in 3 out of 8 (supplementary table 5.1-5.4).
During treatment with tetracosactide, all dogs showed elevated alkaline phosphatase and alanine transaminase levels, and reacted positively in the ACTH stimulation and low-dose dexamethasone suppression test. Four out of 6 dogs showed elevated lipase levels and 5 out of 6 dogs showed polyuria and polydipsia. The two groups with different tetracosactide doses were used, because the optimal tetracosactide dose necessary to induce typical clinical signs of HAC was not known before starting the experiment. As all dogs from the two groups showed laboratory and clinical findings associated with HAC, they were pooled into one group in the following MS analysis.

3.2 Quality control

All four panels had different numbers of lipid species used for screening. The following results are based on lipid species with a CoV <20%. The CoV varied depending on the panel, as depicted in table 3.1.

Panel no.	**Lipid species in MRM list**	**Detectable lipid species**	**Lipid species with CoV <20%**		**Percentage of detectable lipid species CoV<20%**	
			Pred	ACTH	Pred	ACTH
1	454	211	176	179	83.4%	84.8%
2	221	117	71	76	60.7%	65%
3	44	27	25	8	92.5%	29.6%
4	29	6	5	5	83.3%	83.3%

Table 3.1: Evaluation of quality control: Overview of different panels in rows: the columns show lipid species number in the MRM or SIM list (only quantifier; qualifier excluded), number of detectable lipid species, number of lipid species with CoV <20% for prednisolone (Pred) and tetracosactide (ACTH) group and the percentage of detectable lipid species with CoV <20% for prednisolone (Pred) and tetracosactide (ACTH) group are described. Lipids with a CoV >20% had a low signal-to-noise-ratio, which is another reason for exclusion from the list of reported lipid species.

3.3 Canine plasma lipidome

All lipid species described in the following subchapter were found in treated and untreated animals of the corresponding group. After a targeted LC-MS approach of BuMe extracted lipids, a total number of 225 and 210 lipid species were revealed in the plasma of dogs of the prednisolone group and of the tetracosactide group, respectively. The lipid species detected in untreated and treated dogs of the prednisolone and tetracosactide group represented 4 out of the 8 known lipid categories, namely GL, GP, SP and ST. FA, PR, SL and PK could not be detected. The distribution of detected lipid species within lipid categories showed the following pattern:
prednisolone group: 11.11% GL, 53.33% GP, 28% SP, 7.56% ST;
tetracosactide group: 3.81% GL, 56.19% GP, 31.91% SP, 8.09% ST (table 3.2)

Category	Main Class	Number of detected lipids prednisolone group	Number of detected lipids tetracosactide group
Glycerolipids (GL)		**25**	**8**
	Triradylglycerols	25	8
Glycerophospho-lipids (GP)		**120**	**118**
	Glycerophosphocholines	79	77
	Gylcerophosphoethanolamines	28	26
	Glycerophosphoinositols	12	14
	Gylcerophosphoserines	1	1
Sphingolipids (SP)		**63**	**67**
	Ceramides	25	28
	Phosphosphingolipids	21	21
	Acidic glycosphingolipids	12	13
	Sphingoid bases	5	5
Sterol lipids (ST)		**17**	**17**
	Sterols	17	17

Table 3.2: Overview of canine plasma lipid species revealed after BuMe lipid extraction and use of a targeted LC-MS approach: Lipid species represented 4 out of 8 lipid categories and several main classes.

3.4 Treatment induced alterations

When all lipid classes detected in each treatment group are added up and comparing the overall lipid concentration before and during treatment, the prednisolone group shows a decrease in lipid concentration, whereas the tetracosactide group shows an increase in lipid concentration (supplementary table 5.18). The OPLS-DA model was used to investigate, whether there are signals in the dataset that can clearly discriminate between samples of dogs before treatment (labeled “control”) and samples of treated dogs (labeled “disease”). The results of the OPLS-DA analyses revealed that both prednisolone and tetracosactide treatment clearly altered the plasma lipidomic pattern (figure 3.1).

Additionally, treatment induced alterations were exposed in volcano plots: after short-term prednisolone treatment, 24 significantly changed lipids were downregulated (FC < -1.5) and 22 significantly changed lipids were upregulated (FC > 1.5), resulting in a total number of 46 significantly changed lipids out of 225 lipid detected lipid species (figure 3.2). All PIs measured were listed as significantly changed downregulated (FC < -1.5) lipids.
After long-term tetracosactide treatment, 55 significantly changed lipids were downregulated (FC < -1.5) and 21 significantly changed lipids were upregulated (FC > 1.5), resulting in a total number of 76 significantly changed lipids out of 210 detected lipid species (figure 3.3).
Comparison of the significantly changed lipid species with a FC > 1.5 or FC < -1.5 in the two treatment groups resulted in a total number of 12 identical lipid species. Ten of those 12 showed the same pattern of change and 2 (PC 38:3 and PC (P-36:5)) showed the opposite pattern of change (table 3.3).

	Upregulation		Downregulation	
Lipid species	**Prednisolone**	**Tetracosactide**	**Prednisolone**	**Tetracosactide**
LPC 19:0			x	x
MHCer d18:1/C16:1	x	x		
MHCer d18:1/C18:0	x	x		
MHCer d18:1/C20:0	x	x		
PC 37:4			x	x
PC 38:3		x	x	
PC 39:5			x	x
PC (P-36:5)	x			x
PI 36:4			x	x
PI 38:4			x	x
PI 38:5			x	x
PI 40:5			x	x

Table 3.3: Pattern of change of lipid species after prednisolone and tetracosactide treatment. Lipid species with a p-value of <0.05 and FC <-1.5 and FC >1.5 are listed.

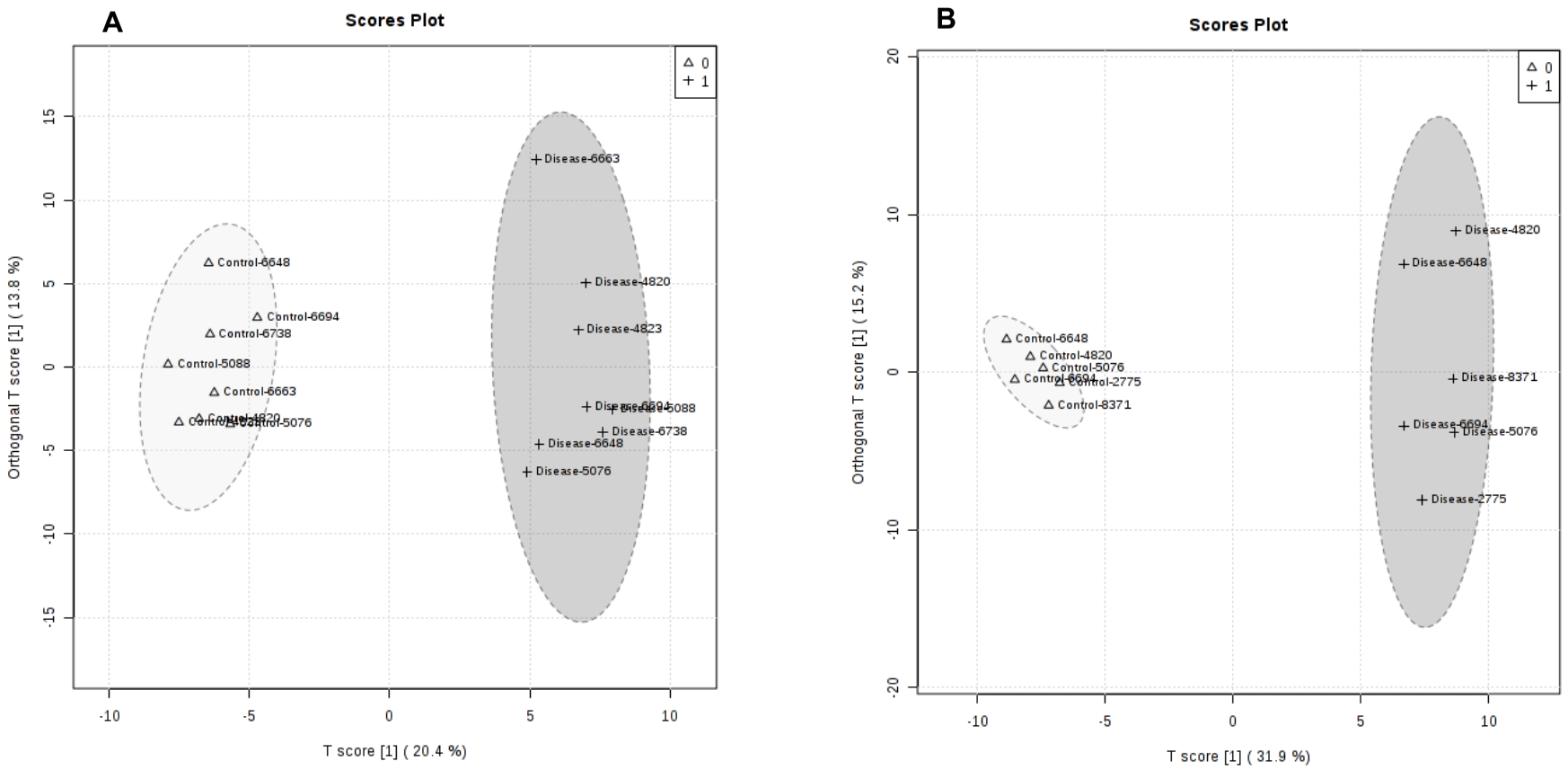

Figure 3.1: OPLS-DA plots for classification of samples from dogs before treatment (labeled “control”) and dogs during treatment (labeled “disease”). The plot on the left (A) depicts the results from the prednisolone treated dogs and on the right (B), the results from tetracosactide treated dogs.

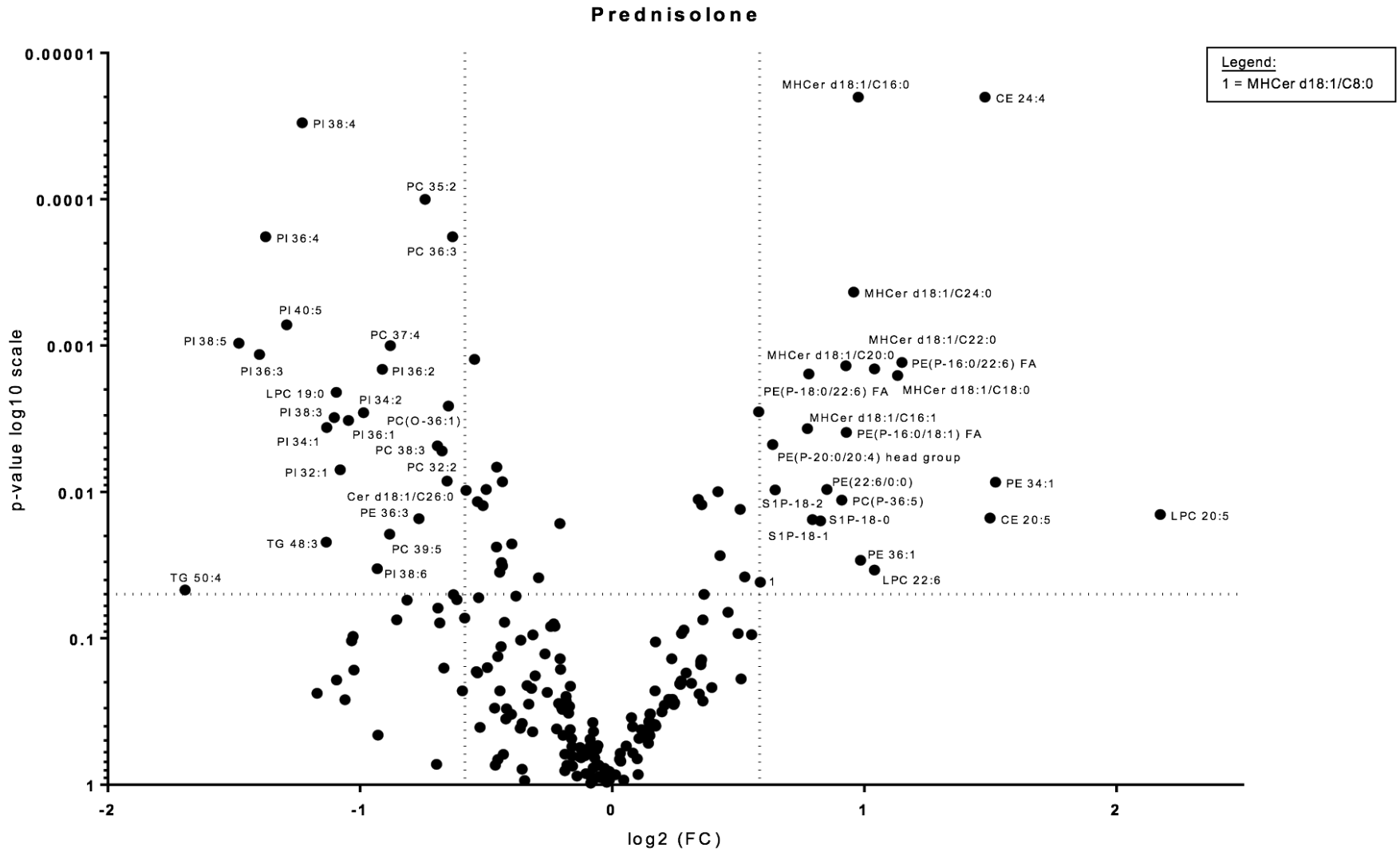

Figure 3.2: Volcano plot depicting lipid species with a p-value of <0.05 (y-axis, log10 scale) and FC <-1.5 and FC >1.5 (x-axis) after prednisolone treatment.

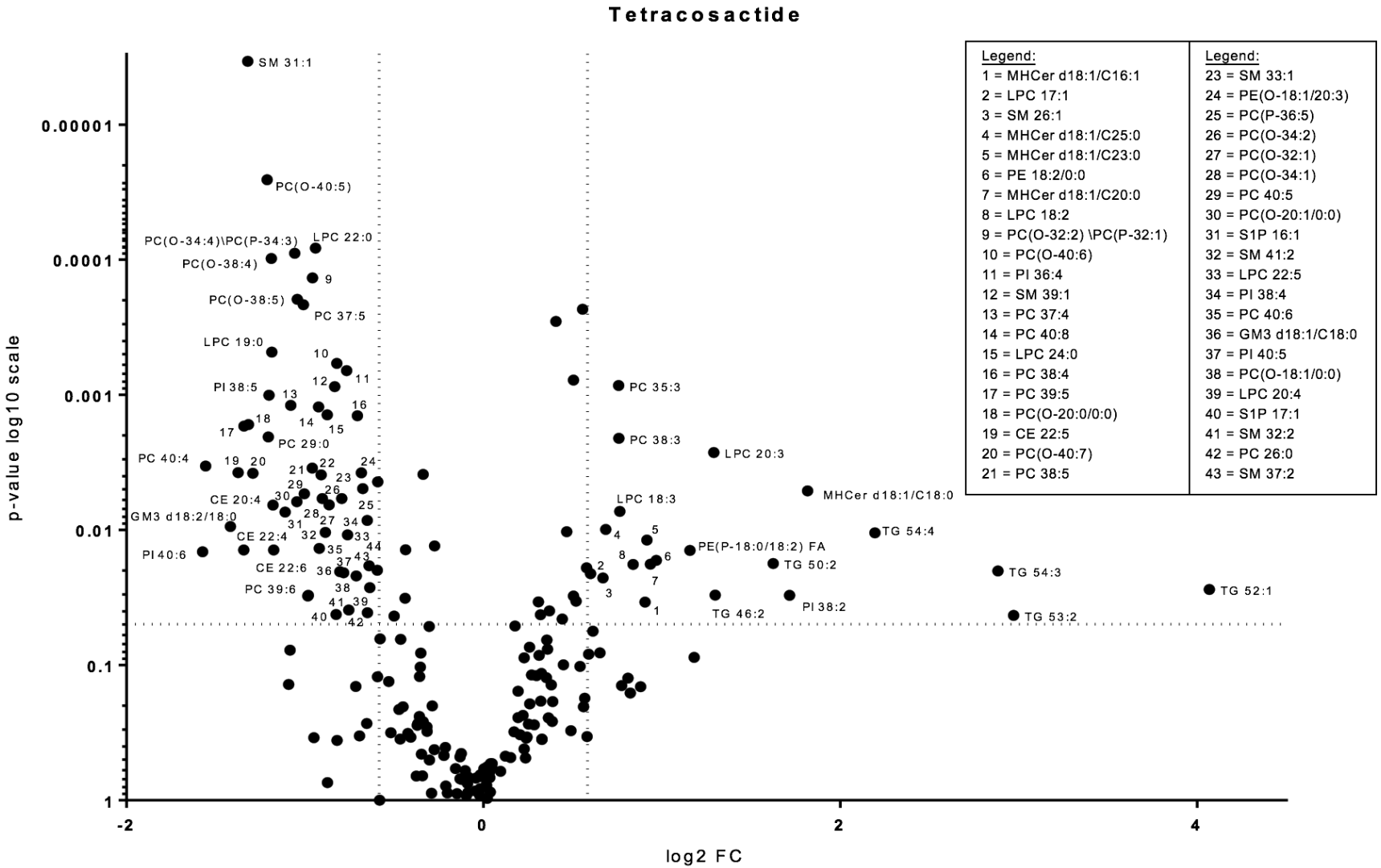

Figure 3.3: Volcano plot depicting lipid species with a p-value of <0.05 (y-axis, log10 scale) and FC <-1.5 and FC >1.5 (x-axis) after tetracosactide treatment.

3.5 Hierarchical clustering analysis

Hierarchical clustering was performed with heat maps. They directly showed the variation of the lipid species with a significant q-value in the two groups. The heat map illustrates the relatively increased (red) or decreased (blue) values in the dogs before (control group) and during treatment (treated group) (figure 3.4 A and B). The significant lipid species showed an overall consistent pattern of change: Firstly, the lipid species concentration (indicated with colors: blue: low concentration; red: high concentration) revealed a clear separation between control samples and samples of treated dogs. Secondly, the individual members of the groups (control and treated) showed a consistent pattern of change within their group.

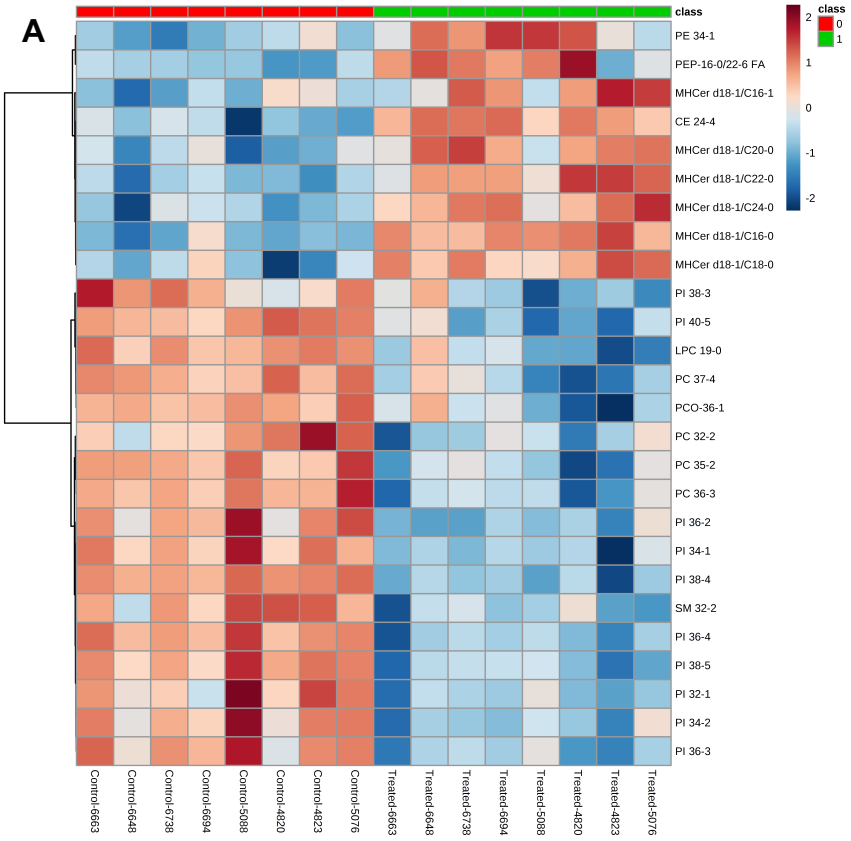

Figure 3.4 A: Hierarchically clustered heat maps using Pearson distance, based on logarithmic normalized lipid concentrations with a q-value <0.05, listed in rows, from the results of 8 dogs before treatment (control) and after prednisolone treatment (treated) dogs in columns. All values are shown after auto-scaling. Blue represents a lower lipid concentration, whereas red represents a higher lipid concentration.

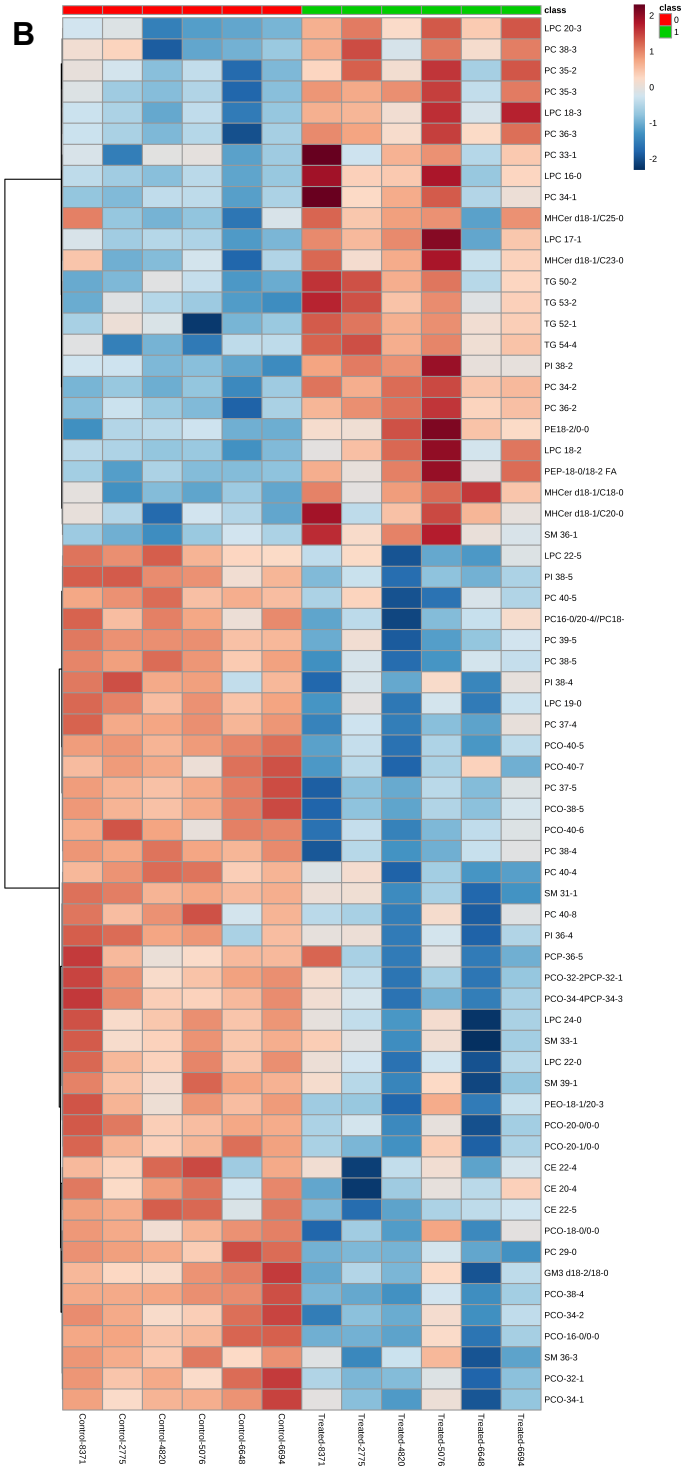

Figure 3.4 B: Hierarchically clustered heat maps using Pearson distance, based on logarithmic normalized lipid concentrations with a q-value <0.05, listed in rows, from the results of 6 dogs before treatment (control) and after tetracosactide treatment (treated) in columns. All values are presented after auto-scaling. Blue represents a lower lipid concentration, whereas red represents a higher lipid concentration.

3.6 Comparison of selected lipid classes in prednisolone and tetracosactide treated dogs

3.6.1. Lysophosphatidylcholines (LPC) and phosphatidylcholines (PC)

In animals undergoing long-term tetracosactide treatment, an effect on the chain length and the degree of unsaturation of LPCs and PCs could be shown:
LPCs with a chain length of <19 carbon atoms and up to 3 double bonds were upregulated (90% of the reported LPC species with these characteristics were upregulated; 4 of them with a significant q-value), whereas species with a chain length of ≥19 carbon atoms and up to 6 double bonds were downregulated (72% of the reported LPC species with these characteristics were downregulated; four of them with a significant q-value, one with a significant q-value was upregulated) (figure 3.5).

These effects could not be detected in the samples from prednisolone treated dogs.

PCs with less than 37 carbon atoms and up to 5 double bonds were upregulated (71% of the reported PC species with these characteristics were upregulated; 6 of them had a significant q-value, 2 with a significant q-value were downregulated), whereas PCs with ≥37 carbon atoms and up to 8 double bonds were downregulated (93% of the reported PC species with these characteristics were downregulated; 6 of them had significant q-values, and one with a significant q-value was upregulated) (Figure 3.6).

These effects could not be detected in the samples from prednisolone treated dogs.

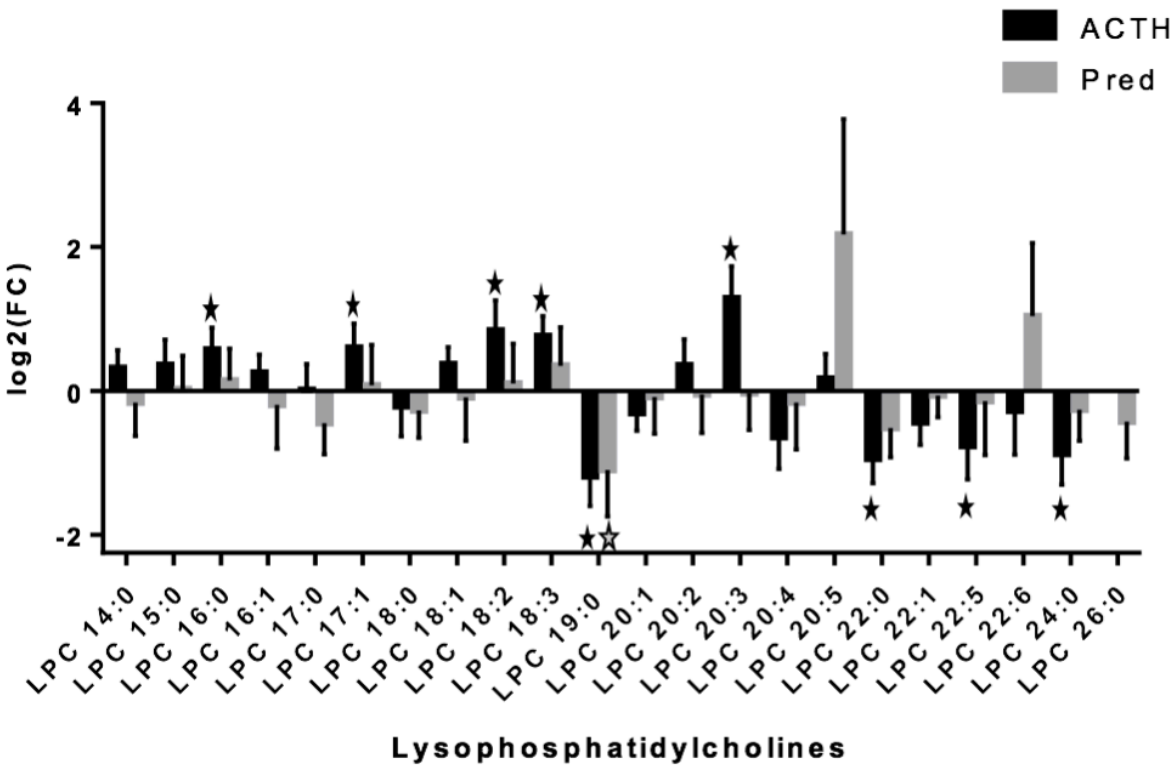

Figure 3.5: Lysophosphatidylcholine (LPC) species: Log2 FC (y-axis) depicted together with the standard deviation of the FC as error bar: Results of tetracosactide (ACTH) treated dogs are depicted in black, whereas results of prednisolone treated dogs are depicted in grey. Significant q-values are marked with a star.

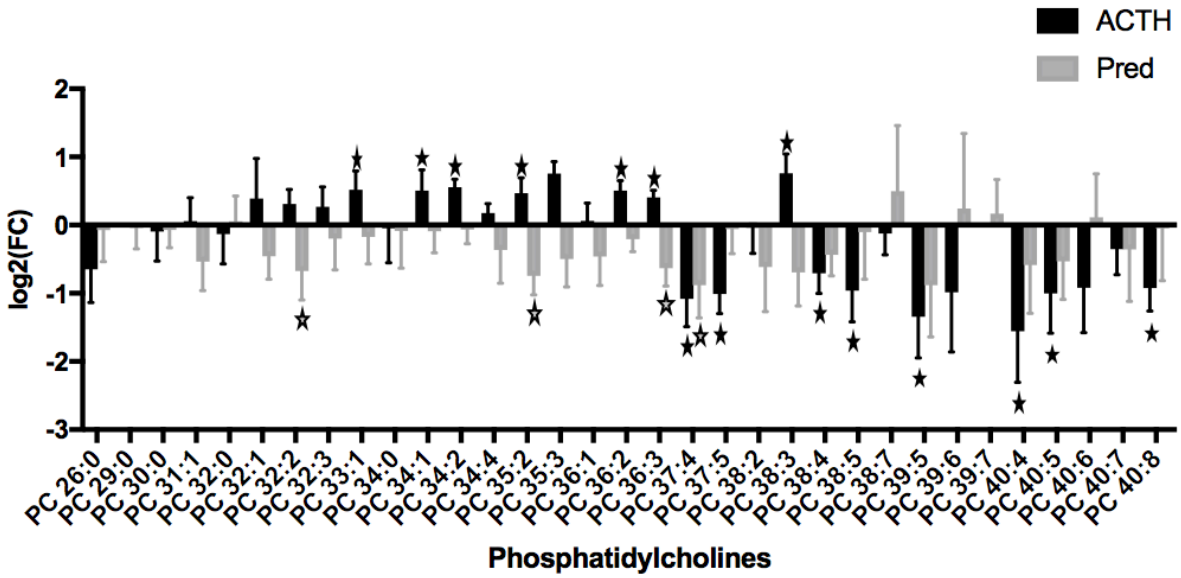

Figure 3.6: Phosphatidylcholine (PC) species: Log2 FC (y-axis) depicted together with the standard deviation of the FC as error bars: Results of tetracosactide (ACTH) treated dogs are depicted in black, whereas results of prednisolone treated dogs are depicted in grey. Significant q-values are marked with a star.

3.6.2 Cholesteryl esters and sphingosine-1-phosphate

An opposing effect of short-term prednisolone treatment compared to long-term tetracosactide treatment of the dogs could be demonstrated in selected lipid species, mainly cholesteryl esters (CE) and sphingosine-1-phosphate (S1P).

Short-term prednisolone treatment led to an upregulation of CE species (77% of reported species, one of them with a significant q-value), whereas long-term tetracosactide treatment led to a downregulation (77% of reported CE species, three of them with a significant q-value) (figure 3.7).

For S1P species, the same opposing effect of the different treatments was observed: All reported S1P species were upregulated after short-term prednisolone treatment, whereas all reported S1P species were downregulated after long-term tetracosactide treatment (figure 3.8).

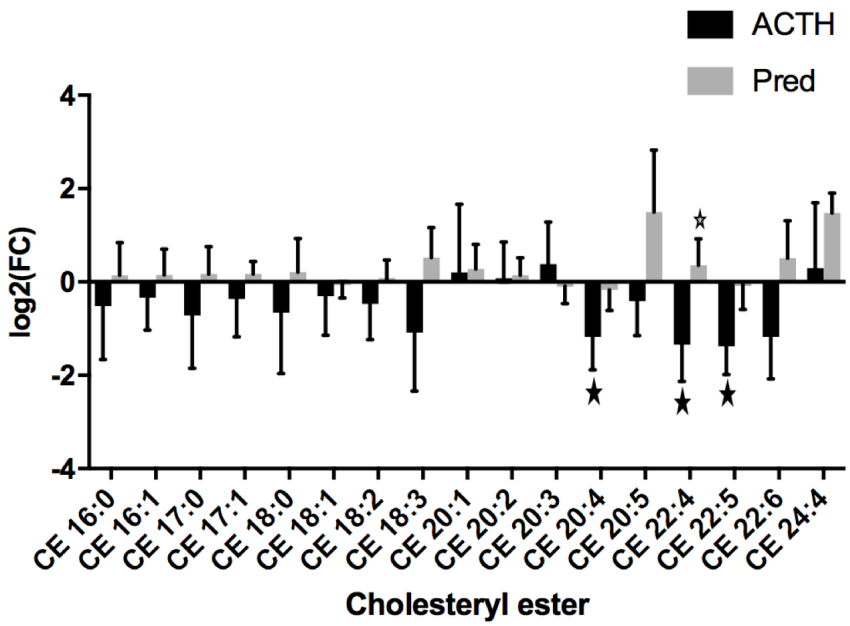

Figure 3.7: Cholesteryl ester (CE) species: Log2 FC (y-axis) depicted together with the standard deviation of the FC as error bars: Results for tetracosactide (ACTH) treated dogs are depicted in black, whereas results for prednisolone treated dogs are depicted in grey. Significant q-values are marked with a star.

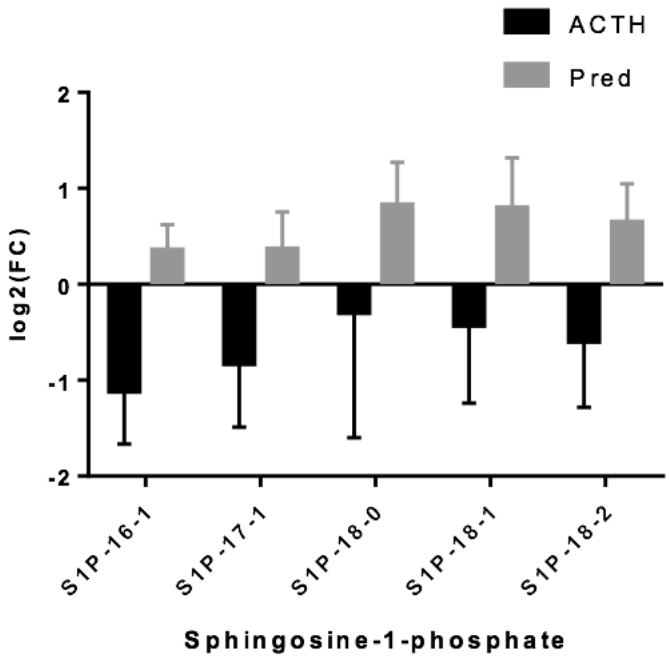

Figure 3.8: S1P species: Log2 FC (y-axis) depicted together with the standard deviation of the FC as error bars: Results for tetracosactide (ACTH) treated dogs are depicted in black, whereas results for prednisolone treated dogs are depicted in grey. No significant q-values were detected.

Chapter Four

Discussion

This study aimed to reveal the effects of prednisolone or tetracosactide treatment on the plasma lipidome of healthy beagle dogs.

4.1 Beagle plasma lipidome

Plasma lipid species could be detected originating from 4 out of 8 lipid categories (table 3.2) defined by the LIPID MAPS Consortium. This contrasted with earlier findings, which identified lipid species from 7 out of 8 lipid categories in canine plasma (Schmid, 2017). Several reasons for this discrepancy have to be considered: First, detection of lipids with MS is dependent on the method of lipid extraction. In this study the BuMe lipid extraction method was used, which leads for example to a loss of eicosanoids during extraction (data not shown). Second, the detection of lipid species depends on the approach selected: in the case of an untargeted approach, the sample is screened for any lipid species within a given time and given m/z-range. This can lead to the detection of prior unreported lipid species, but might not detect present lipid species with a low abundance. A targeted approach screens for all lipid species included in the MRM or SIM list and can also detect lipid species with low abundance. Therefore, the greater variety in lipid species of canine plasma detected in the previous study is probably due to the fact that, on the one hand, a different lipid extraction method (MTBE method) and, on the other, an untargeted approach were used. Thus we can conclude that the plasma lipids reported in this targeted study describe the canine plasma lipidome independently of a lipid's abundance, in contrast to the earlier canine plasma lipidome description, which was based on an untargeted approach. The prior detected lipid categories PK, SL, FA and PR in canine plasma were not included in the MRM or SIM lists of this study. A comparison between the categories of detected lipid species in the two studies is difficult because, as mentioned above, the lipid extraction methods, the MS equipment as well as the mobile phases for LC were different in the two studies.
It should be noted that prior studies have suggested that the Beagle plasma lipidome shows broad variance (Lloyd et al., 2017), which is consistent with findings of the urinary metabolome of this breed (Beckmann et al., 2010). However, as Beagle dogs are the most common breed used in veterinary and human medicine research, as well as in pharmaceutical research, the characterization of the plasma lipidome of this breed is crucial.

4.2. Comparison of the human and Beagle plasma lipidome

In comparison with the human plasma lipidome described by Quehenberger and coworkers (Quehenberger et al., 2010), the lipid classes (CE, TG, LPE, PE, LPC, PC, PI, PS, phosphatidylglycerol (PG), sphingomyeline (SM), monohexosylceramide (MHCer), Cer) included in our study resemble the human lipid species: Lipid species showed the following overlapping in detection within lipid classes comparing the human and canine plasma lipidome: CE 63.6%, TG 83.3%, LPE 85.7%, PE 28.9%, LPC 75%, PC 61.3%, PI 78.9%, PS 5%, PG 6.3%, SM 65%, MHCer 17.1% and Cer 36.6% (supplements table 5.18).
Free FA, eicosanoids and related metabolites, DG, phosphatidic acid and total sterol could not be compared as they were not measured in the canine plasma. Contrariwise, plasmologens of PE and PC and PC (O), GM3 ganglioside and dihexosylceramide could not be compared, as they were not detected in human plasma and could therefore not be compared with our results (supplements table 5.18).

4.3 Alterations of the Beagle plasma lipidome due to the influence of steroids

The findings revealed remarkable alterations in the canine plasma lipidome due to the effects of prednisolone or tetracosactide treatment.
The heat maps displayed a clear separation within the prednisolone and tetracosactide group between the control samples and samples from treated dogs. This supports the finding that the two treatments lead to a disturbance of the canine lipid profile. They showed a consistent pattern of change during treatment with only slight deviations, most likely due to biological variance.
After prednisolone treatment, all detected phosphatidylinositol (PI) species were significantly downregulated and after tetracosactide treatment 42% of detected PI species were downregulated (figure 3.2 and 3.3, table 3.3). This is unexpected as steroids are negatively linked to PI degradation: Steroids exhibit their primary anti-inflammatory mechanism via lipocortin-1 synthesis. Lipocortin-1 suppresses phospholipase A_2 and therefore arachidonic acid dependent synthesis of eicosanoids and related inflammatory lipids. PI hydrolysis takes place by phospholipase A_2 and most likely phospholipase C (Hong and Deykin, 1981; Shibata et al., 1988; Smith and Waite, 1992) so that PI represents one of the primary sources of arachidonic acid in animal tissues. Therefore, it was expected that PI concentrations would be increased due to steroid's inhibition of phospholipase A_2. Here we detected the opposite effect. Reasons for this remarkable effect remain to be elucidated.
Interestingly, there were several remarkable differences between prednisolone and tetracosactide treated dogs: prednisolone treatment led to a lower number of significant lipid species with a FC > 1.5 or FC < -1.5 depicted in the volcano plot compared to tetracosactide treatment. This suggests that short-term steroid treatment leads to less marked and less profound alterations in lipid metabolism. Of course it should be noted that not only the duration of steroid excess but also the type of steroid might have played a role in altering the plasma lipidome.
Lipidomics is often utilized in biomarker research for the detection of various diseases (Missmer et al., 2006; Pietiläinen et al., 2007).
In this study significant and highly upregulated or downregulated lipid species were depicted by volcano plots with the same pattern of change in the two treatment groups. They could possibly be used as biomarkers for short-term or long-term steroid excess. Further investigations are needed to verify the usefulness of these possible biomarkers.

As lipidomics is an important tool in biomarker research for coronary artery disease, it is noteworthy that Cer d18:1/16:0 is associated with lipid burden in coronary angiography and predictive for 1-year clinical outcome (Cheng et al., 2014). Moreover, Cer d18:1/16:0, Cer d18:1/18:0, Cer d18:1/24:1 are suggested as potential risk stratifiers for coronary artery disease (Tarasov et al., 2014). All three lipid species have been detected in the plasma of dogs treated with prednisolone or tetracosactide.
Cer d18:1/16:0 and Cer d18:1/24:1 were decreased after tetracosactide treatment and increased after prednisolone treatment in canine plasma. Cer d18:1/18:0 was increased during treatment of dogs with prednisolone or tetracosactide. In a hamster model for atherosclerosis Cer d18:1/24:1 was increased in hamster plasma after a high-fat diet (Jové et al., 2014). The fact that out of three potential risk stratifiers for human coronary artery disease all were detected but just one (Cer d18:1/18:0) was increased in dogs after long-term steroid excess might be a potential explanation for the relative resistance of dogs to atherosclerosis (Boynosky and Stokking, 2014; Chiers et al., 2010; Hess et al., 2003; Xenoulis and Steiner, 2010).

To further understand the lipidomic differences between control samples and samples from treated dogs, the reported lipids data were analyzed using hierarchical clustering. Hierarchical clustering analysis based on Pearson distance supported the hypothesis that long-term steroid treatment or excess due to HAC is needed for profound plasma lipidome changes, by showing a distinct clustering of control samples and samples of treated dogs in the tetracosactide group, whereas the clustering of control samples and samples of treated dogs was less distinct in the prednisolone group. This supports that short-term high steroid influence results in less distinct patterns of change in lipid metabolism of dogs than long-term high steroid influence. It can be hypothesized that alterations in the lipid metabolism need time, as they are dependent on enzymatic activities, since lipid synthesis completely depends on enzymes. It has already been reported that the transcription and translation as well as the activity of enzymes involved in lipid synthesis are influenced by steroid hormones (Brenner, 1990; Tvrdik et al., 1997).

4.4 Steroid effects on hydrocarbon chain length and degree of unsaturation

Taking a closer look at the detected patterns of change in lipid classes, LPCs and PCs exhibited a two-sided effect within their lipid class after tetracosactide treatment: Low unsaturated lipid species with hydrocarbon chains of <19 C-atoms were upregulated; conversely, high unsaturated lipid species with hydrocarbon chains of ≥19 C-atoms were downregulated. This effect could be a result of the activity of elongases and desaturases. In 1987, it was already shown by Mandon and coworkers (Mandon et al., 1987) that steroids influence the activity of desaturases in the liver and adrenal glands of rats: they were able to show that steroids and ACTH have a depressing effect on Δ5- and Δ6-desaturases. Depressing the activity of these enzymes leads to a reduced synthesis of C18:3n-6, C18:4n-3, C20:3n-6, C20:4n-3, C24:5n-6 and C24:6n-3 FA. The fatty acids C20:3n-6 and C20:4n-3 are precursors of arachidonic acid and eicosanoids. As steroids are well known for their anti-inflammatory functions, and as arachidonic acid and eicosanoids are well established for mounting inflammatory responses, this regulatory pathway might in part explain the anti-inflammatory characteristics of steroids in a physiological state. Additionally, there is evidence based on estimation of the activity of Δ5- and Δ6-desaturases that the enzyme activities reflect each other in serum and in the liver

but not in adipose tissue (Kotronen et al., 2010). This directly links the serum lipidome to liver metabolism. It has already been reported that one subtype (ELOVL3) out of 7 known elongase subtypes is influenced by glucocorticoids (Tvrdik et al., 1997), as glucocorticoids induce the expression of ELOVL3. Interestingly, Nguyen et al. (Nguyen et al., 2016) have suggested that changes in fatty acid chain length and lipid saturation lead to the alteration of the lipid function based on their increase in different cell lines. One mechanism by which acyl chains can change lipid function is by changing the physical properties of cell membranes. Moreover, it has been shown that an arachidonoyl chain (20:4 FA) bound to PC oscillates during the cell cycle and delays cell cycle progression (Koeberle et al., 2013). Another hint that acyl chains play a functional role is that they are very unevenly distributed among different lipid classes. Even within the same organism the composition of specific lipids differs in various organs (D'Souza and Epand, 2014). The findings of the current study suggest that steroids could influence lipid metabolism by modulating enzyme activities, namely elongase and desaturase activities, whose substrates are the basic building units of every lipid structure. Further studies in the global plasma FA composition are needed to verify this hypothesis.
Concerning implications in atherogenic disease of LPCs and PCs, there are the following findings:
Stegemann et al. (Stegemann et al., 2014) showed that PC 38:3 is the only PC detectable in the arteries of patients with atherosclerosis but not in the arteries of healthy patients. In the present study PC 38:3 was increased after tetracosactide treatment and decreased after prednisolone treatment. In a study conducted to induce atherosclerosis in hamsters on a high-fat diet, it was shown that PC 40:6 was significantly increased in atherogenic hamster plasma (Jové et al., 2014). PC 40:6 was decreased after tetracosactide treatment in this study. These findings might be an additional explanation of the relative resistance of dogs with HAC to the development of atherosclerosis.
Moreover, comparing the results from tetracosactide treated dogs with results from a study on hyperlipidemia induced by feeding rats a high fat diet revealed the following: for LPC 18:1, LPC 18:2, LPC 18:3 and LPC 20:3 the same pattern of change (upregulation) was detected in the rat plasma (Miao et al., 2015). This suggests that feeding rats a high fat diet leads to similar patterns of change in some lipid species of the LPC class as in long-term tetracosactide treated dogs. In general, LPCs are known to have both pro- and anti-atherogenic properties (Schmitz and Ruebsaamen, 2010) and there are studies suggesting that the chain-length of PCs is associated with particular lipid functions based on their presence in different blood cells (Leidl et al., 2008). Further investigations are needed, as the current knowledge on lipid function is restricted to the lipid classes, but detailed information on functions of individual lipid species is lacking.

4.5 Opposite effects depending on type of treatment (prednisolone vs. tetracosactide)

There were several interesting differences between prednisolone and tetracosactide treated dogs. Contrasting effects between the two were seen for example in cholesteryl esters:
Short-term prednisolone treatment led to an upregulation, while tetracosactide led to a downregulation in 77% of this species.
Going into greater detail about possible pathological effects, it was shown that CE 16:1, which was also detected in this study, was among the lipids most consistently

related to the incidence of cardiovascular disease (Stegemann et al., 2014). CE 16:1 was decreased after tetracosactide treatment, providing further evidence for the relative resistance of dogs with HAC to cardiovascular disease.
An S1P panel was included in the current study, as this molecule is of interest for its multiple functions such as regulating lymphocyte trafficking and its impacts on the vascular barrier and important aspects of disease states such as inflammation and cancer (Cyster and Schwab, 2012; Fyrst and Saba, 2010; Hla, 2004; Maceyka et al., 2012; Rivera et al., 2008). So far, the pro- and anti-atherogenic effects of S1P have been observed in animal models of atherosclerosis (Potì et al., 2014).
Another example for a contrasting effect of the type of treatment was found in S1P species: After prednisolone treatment, all S1P species were upregulated, whereas after tetracosactide treatment they all were downregulated. Generally, the S1P species detected in canine plasma resemble the S1P species found in human plasma: in both species S1P-16:1, -18:0, -18:1 and -18:2 can be detected. However, S1P-20:1 is only present in human plasma and S1P-17:1 is only found in canine plasma. Interestingly, the effect of tetracosactide treatment on S1P species seen in this study was equal to that found in an in-vitro study performed by Ozbay et al. (Ozbay et al., 2004): They could show that ACTH treatment of adrenocortical cells (H295R) leads to a rapid decrease of S1P, ceramide and sphingosine concentrations, which mirrors the findings of this study: 100% of the reported S1P species, 75% of the reported ceramide species and 80% of reported SM species were downregulated after tetracosactide treatment. SMs and S1P are dependent on sphingosine, as sphingosine serves as their molecular backbone. Therefore, decreases in SM and S1P concentrations are probably a result of decreased sphingosine concentrations.
A study in mice on glucocorticoid treatment during acute lung inflammation supports the findings of our study: dexamethasone treatment of mice significantly increased circulating plasma S1P levels. This may be dependent on the glucocorticoid receptor in macrophages (Vettorazzi et al., 2015).

After long-term tetracosactide treatment, all dogs tested positive for HAC as shown in a positive ACTH stimulation test as well as in the low-dose dexamethasone suppression test.
It is noteworthy, however, that just one of the six dogs exhibited hypercholesterolemia and hypertriglyceridemia (supplementary table 5.3), although hyperlipidemia is a common laboratory finding in dogs with HAC. However, currently the finding of hyperlipidemia in canine patients is limited to the evaluation of serum cholesterol and triglyceride levels, as they are included in standard laboratory testing. Interestingly, in all but one dog of this study hyperlipidemia was detected only when all concentrations of the detected lipid classes of all four lipid categories were added up. This leads to the conclusion that the evaluation of the whole lipidome is crucial for a complete picture of plasma lipid changes, as the measurement of single lipid classes (e.g. CE, TAG) may obscure relevant plasma lipidomic modifications. The same conclusion was also drawn by Quehenberger and coworkers (Quehenberger et al., 2010) based on their studies on the human plasma lipidome: the human lipidome revealed more relevant information (e.g. biomarkers) than single lipid classes included in general blood chemistry in humans (CE, TAG, low-density lipoprotein, high-density lipoprotein).
Interestingly, after prednisolone treatment, none of the dogs exhibited hypercholesterolemia or hypertriglyceridemia, and calculations of the total lipid concentration based on all lipid classes measured revealed a decrease in total lipid load of canine plasma. Reasons for this decrease remain unknown but indicate that

short-term steroid excess might lead to a reverse effect on plasma lipid load compared with the long-term effect of steroid excess.

4.6 Quality control

Quality control needs to be implemented in order to verify the reliability of reported lipid species. In this study the CoV varied depending on the panel type (table 3.1). The underlying cause for these differences might be the different number of TQCs measured per panel, and in a few cases additionally a different number per group (prednisolone and tetracosactide) within one panel. The lower the number of measured TQCs, the higher the susceptibility of CoV values to negative influence by outlying values from TQCs. One example is panel 3, where just 29.6% of measured lipid species in the tetracosactide group passed the quality control (CoV <20%), as just 3 TQCs were measured in this group (4 measured TQCs in prednisolone group). Another reason for high variance within measurement of the same lipid species in one panel is a low signal-to-noise ratio, another feature of quality control. The lower the detected signal of lipid species, the less reliable is the signal. Thus, panels comprising lipid species with low signal intensities had more lipid species which did not pass the quality control.

4.7 Limitations

The study is limited by the presence of biological variance, as the animals in this study were of different sexes and ages and were line-breed dogs. If the study had been conducted with an age and sex matched inbred mouse strain, the biological variance would be expected to be smaller. The rather limited number of dogs included in this study might have amplified the biological variance. Moreover, we only included beagle dogs, a breed reported to exhibit high inbreed variance in urine metabolites as well as in the plasma lipidome (Beckmann et al., 2010; Lloyd et al., 2017). Therefore, transfer of the results of the current study to other dog breeds should be done with caution. In addition, there was no separate and independent control group of Beagle dogs included in this study. Instead, each animal served as its own control. Concerning statistical measurements, the correction for multiple testing was not implemented for volcano plots. The report of raw p-values with possibly false positives was approved in order to be able to investigate pathways in future. In order to assess even more lipid categories of the canine plasma lipidome, further studies are needed with various lipid extraction methods to provide the best extraction method for lipid classes of interest, which were not successfully extracted with the BuMe method, such as eicosanoids.

4.8 Summary

In summary, the canine plasma lipidome resembles the human plasma lipidome. Distinct canine plasma lipidome alterations were found after short-term prednisolone or long-term tetracosactide treatment. The latter treatment led to a more profound pattern of change in the canine plasma lipidome than short-term prednisolone treatment. Our targeted approach of a lipidomic study of canine plasma exposed lipid species from 4 out of 8 lipid categories. Distinct patterns of changes were found in LPC and PC, as after tetracosactide treatment, low unsaturated lipid species with fatty acyl chains <19 C-atoms were upregulated, whereas high unsaturated lipid species with fatty acyl chains ≥19 C-atoms were downregulated. Another distinct

pattern of change was found in CE and S1P depending on the type and duration of steroid excess, as short-term steroid excess led to upregulation and long-term steroid excess to downregulation of species within these lipid classes. The overall lipid load in canine plasma decreased after short-term prednisolone treatment and increased after long-term tetracosactide treatment.

4.9 Outlook

Our findings will stimulate further investigations in lipidomic studies in veterinary medicine. Further studies should include dogs exhibiting spontaneous HAC in order to test the validity of the HAC dog model evaluated in the present study. Additionally, as client owned dogs with HAC possibly remain undiagnosed for an even longer time than 25 weeks, these dogs exhibit a longer chronic exposure to steroid excess. This may reveal other interesting lipidomic findings. Another aspect would be to assess the continuous changes in the plasma lipidome after the onset of treatment for HAC, as well as long-term implications of therapeutic treatment on the plasma lipidome.

References

Aiyar, N., J. Disa, Z. Ao, H. Ju, S. Nerurkar, R. N. Willette, C. H. Macphee, D. G. Johns, and S. A. Douglas, 2007, Lysophosphatidylcholine induces inflammatory activation of human coronary artery smooth muscle cells: Mol Cell Biochem, v. 295, p. 113-20.

Alberti, K. G., R. H. Eckel, S. M. Grundy, P. Z. Zimmet, J. I. Cleeman, K. A. Donato, J. C. Fruchart, W. P. James, C. M. Loria, S. C. Smith, I. D. F. T. F. o. E. a. Prevention, L. n. Hational Heart, and Blood Institute, A. H. Association, W. H. Federation, I. A. Society, and I. A. f. t. S. o. Obesity, 2009, Harmonizing the metabolic syndrome: a joint interim statement of the International Diabetes Federation Task Force on Epidemiology and Prevention; National Heart, Lung, and Blood Institute; American Heart Association; World Heart Federation; International Atherosclerosis Society; and International Association for the Study of Obesity: Circulation, v. 120, p. 1640-5.

Alshehry, Z. H., C. K. Barlow, J. M. Weir, Y. Zhou, M. J. McConville, and P. J. Meikle, 2015, An Efficient Single Phase Method for the Extraction of Plasma Lipids: Metabolites, v. 5, p. 389-403.

Appel, B., and S. K. Fried, 1992, Effects of insulin and dexamethasone on lipoprotein lipase in human adipose tissue: Am J Physiol, v. 262, p. E695-9.

Beckmann, M., D. P. Enot, D. P. Overy, I. M. Scott, P. G. Jones, D. Allaway, and J. Draper, 2010, Metabolite fingerprinting of urine suggests breed-specific dietary metabolism differences in domestic dogs: Br J Nutr, v. 103, p. 1127-38.

Bellis, C., H. Kulkarni, M. Mamtani, J. W. Kent, G. Wong, J. M. Weir, C. K. Barlow, V. Diego, M. Almeida, T. D. Dyer, H. H. Göring, L. Almasy, M. C. Mahaney, A. G. Comuzzie, S. Williams-Blangero, P. J. Meikle, J. Blangero, and J. E. Curran, 2014, Human plasma lipidome is pleiotropically associated with cardiovascular risk factors and death: Circ Cardiovasc Genet, v. 7, p. 854-63.

Boynosky, N. A., and L. Stokking, 2014, Atherosclerosis associated with vasculopathic lesions in a golden retriever with hypercholesterolemia: Can Vet J, v. 55, p. 484-8.

Brenner, R. R., 1990, Endocrine control of fatty acid desaturation: Biochem Soc Trans, v. 18, p. 773-5.

Campbell, J. E., A. J. Peckett, A. M. D'souza, T. J. Hawke, and M. C. Riddell, 2011, Adipogenic and lipolytic effects of chronic glucocorticoid exposure: Am J Physiol Cell Physiol, v. 300, p. C198-209.

CDC, 2009, National Ambulatory Medical Care Survey Summary Tables.

Cheng, J. M., H. M. Garcia-Garcia, S. P. de Boer, I. Kardys, J. H. Heo, K. M. Akkerhuis, R. M. Oemrawsingh, R. T. van Domburg, J. Ligthart, K. T. Witberg, E. Regar, P. W. Serruys, R. J. van Geuns, and E. Boersma, 2014, In vivo detection of high-risk coronary plaques by radiofrequency intravascular ultrasound and cardiovascular outcome: results of the ATHEROREMO-IVUS study: Eur Heart J, v. 35, p. 639-47.

Chiers, K., V. Vandenberge, and R. Ducatelle, 2010, Accumulation of advanced glycation end products in canine atherosclerosis: J Comp Pathol, v. 143, p. 65-9.

Cohen, P., and B. M. Spiegelman, 2016, Cell biology of fat storage: Mol Biol Cell, v. 27, p. 2523-7.

Cyster, J. G., and S. R. Schwab, 2012, Sphingosine-1-phosphate and lymphocyte egress from lymphoid organs: Annu Rev Immunol, v. 30, p. 69-94.

D'Souza, K., and R. M. Epand, 2014, Enrichment of phosphatidylinositols with specific acyl chains: Biochim Biophys Acta, v. 1838, p. 1501-8.
Dennis, E. A., 2009, Lipidomics joins the omics evolution: Proc Natl Acad Sci U S A, v. 106, p. 2089-90.
Diseases, N. I. o. D. a. D. a. K., and U. S. D. o. H. a. H. Services, 2014, Drug record Corticosteroids, https://livertox.nih.gov/resource.html, National Library of Medicine, p. LiverTox Clinical and Research Information on Drug-Induced Liver Injury.
Engelmann, B., 2004, Plasmalogens: targets for oxidants and major lipophilic antioxidants: Biochem Soc Trans, v. 32, p. 147-50.
Fahy, E., S. Subramaniam, H. A. Brown, C. K. Glass, A. H. Merrill, R. C. Murphy, C. R. Raetz, D. W. Russell, Y. Seyama, W. Shaw, T. Shimizu, F. Spener, G. van Meer, M. S. VanNieuwenhze, S. H. White, J. L. Witztum, and E. A. Dennis, 2005, A comprehensive classification system for lipids: J Lipid Res, v. 46, p. 839-61.
Fahy, E., S. Subramaniam, R. C. Murphy, M. Nishijima, C. R. Raetz, T. Shimizu, F. Spener, G. van Meer, M. J. Wakelam, and E. A. Dennis, 2009, Update of the LIPID MAPS comprehensive classification system for lipids: J Lipid Res, v. 50 Suppl, p. S9-14.
Feldman, E. C., Nelson, R.W., Reusch, C., Scott-Moncrieff, J.C., 2015, Canine and Feline Endocrinology, Elsevier.
Freedman, M. R., B. A. Horwitz, and J. S. Stern, 1986, Effect of adrenalectomy and glucocorticoid replacement on development of obesity: Am J Physiol, v. 250, p. R595-607.
Fried, S. K., C. D. Russell, N. L. Grauso, and R. E. Brolin, 1993, Lipoprotein lipase regulation by insulin and glucocorticoid in subcutaneous and omental adipose tissues of obese women and men: J Clin Invest, v. 92, p. 2191-8.
Fyrst, H., and J. D. Saba, 2010, An update on sphingosine-1-phosphate and other sphingolipid mediators: Nat Chem Biol, v. 6, p. 489-97.
Geer, E. B., W. Shen, D. Gallagher, M. Punyanitya, H. C. Looker, K. D. Post, and P. U. Freda, 2010, MRI assessment of lean and adipose tissue distribution in female patients with Cushing's disease: Clin Endocrinol (Oxf), v. 73, p. 469-75.
German, A. J., 2006, The growing problem of obesity in dogs and cats: J Nutr, v. 136, p. 1940S-1946S.
Glass, C. K., and J. L. Witztum, 2001, Atherosclerosis. the road ahead: Cell, v. 104, p. 503-16.
Graessler, J., D. Schwudke, P. E. Schwarz, R. Herzog, A. Shevchenko, and S. R. Bornstein, 2009, Top-down lipidomics reveals ether lipid deficiency in blood plasma of hypertensive patients: PLoS One, v. 4, p. e6261.
Han, X., 2016, Lipidomics Comprehensive Mass Spectrometry of Lipids: Hoboken, New Jersey, USA, John Wiley & Sons, Inc.
Han, X., and R. W. Gross, 1994, Electrospray ionization mass spectroscopic analysis of human erythrocyte plasma membrane phospholipids: Proc Natl Acad Sci U S A, v. 91, p. 10635-9.
Han, X., and R. W. Gross, 2005, Shotgun lipidomics: multidimensional MS analysis of cellular lipidomes: Expert Rev Proteomics, v. 2, p. 253-64.
Hauner, H., G. Entenmann, M. Wabitsch, D. Gaillard, G. Ailhaud, R. Negrel, and E. F. Pfeiffer, 1989, Promoting effect of glucocorticoids on the differentiation of human adipocyte precursor cells cultured in a chemically defined medium: J Clin Invest, v. 84, p. 1663-70.
Heck, S., M. Kullmann, A. Gast, H. Ponta, H. J. Rahmsdorf, P. Herrlich, and A. C. Cato, 1994, A distinct modulating domain in glucocorticoid receptor monomers

in the repression of activity of the transcription factor AP-1: EMBO J, v. 13, p. 4087-95.
Hess, R. S., P. H. Kass, and T. J. Van Winkle, 2003, Association between diabetes mellitus, hypothyroidism or hyperadrenocorticism, and atherosclerosis in dogs: J Vet Intern Med, v. 17, p. 489-94.
Hla, T., 2004, Physiological and pathological actions of sphingosine 1-phosphate: Semin Cell Dev Biol, v. 15, p. 513-20.
Hong, S. L., and D. Deykin, 1981, The Activation of Phosphatidylinositol-hydrolyzing Phopholipase A_2 during Prostagladin Synthesis in Transformed Mouse BALB/3T3 Cells The Activation of Phosphatidylinositol-hydrolyzing Phopholipase A2 during Prostagladin Synthesis in Transformed Mouse BALB/3T3 Cells The Journal of Biological Chemistry, v. 256, p. 5215-5219.
Hyötyläinen, T., and M. Orešič, 2015, Optimizing the lipidomics workflow for clinical studies--practical considerations: Anal Bioanal Chem, v. 407, p. 4973-93.
Jonat, C., H. J. Rahmsdorf, K. K. Park, A. C. Cato, S. Gebel, H. Ponta, and P. Herrlich, 1990, Antitumor promotion and antiinflammation: down-modulation of AP-1 (Fos/Jun) activity by glucocorticoid hormone: Cell, v. 62, p. 1189-204.
Jové, M., A. Naudí, M. Portero-Otin, R. Cabré, S. Rovira-Llopis, C. Bañuls, M. Rocha, A. Hernández-Mijares, V. M. Victor, and R. Pamplona, 2014, Plasma lipidomics discloses metabolic syndrome with a specific HDL phenotype: FASEB J, v. 28, p. 5163-71.
Kaur, J., 2014, A comprehensive review on metabolic syndrome: Cardiol Res Pract, v. 2014, p. 943162.
Kim, H. Y., T. C. Wang, and Y. C. Ma, 1994, Liquid chromatography/mass spectrometry of phospholipids using electrospray ionization: Anal Chem, v. 66, p. 3977-82.
Koeberle, A., H. Shindou, S. C. Koeberle, S. A. Laufer, T. Shimizu, and O. Werz, 2013, Arachidonoyl-phosphatidylcholine oscillates during the cell cycle and counteracts proliferation by suppressing Akt membrane binding: Proc Natl Acad Sci U S A, v. 110, p. 2546-51.
Kolodgie, F. D., A. P. Burke, G. Nakazawa, Q. Cheng, X. Xu, and R. Virmani, 2007, Free cholesterol in atherosclerotic plaques: where does it come from?: Curr Opin Lipidol, v. 18, p. 500-7.
Kotronen, A., T. Seppänen-Laakso, J. Westerbacka, T. Kiviluoto, J. Arola, A. L. Ruskeepää, H. Yki-Järvinen, and M. Oresic, 2010, Comparison of lipid and fatty acid composition of the liver, subcutaneous and intra-abdominal adipose tissue, and serum: Obesity (Silver Spring), v. 18, p. 937-44.
Kotronen, A., V. R. Velagapudi, L. Yetukuri, J. Westerbacka, R. Bergholm, K. Ekroos, J. Makkonen, M. R. Taskinen, M. Oresic, and H. Yki-Järvinen, 2009, Serum saturated fatty acids containing triacylglycerols are better markers of insulin resistance than total serum triacylglycerol concentrations: Diabetologia, v. 52, p. 684-90.
Kougias, P., H. Chai, P. H. Lin, A. B. Lumsden, Q. Yao, and C. Chen, 2006, Lysophosphatidylcholine and secretory phospholipase A2 in vascular disease: mediators of endothelial dysfunction and atherosclerosis: Med Sci Monit, v. 12, p. RA5-16.
Lee, M. J., P. Pramyothin, K. Karastergiou, and S. K. Fried, 2014, Deconstructing the roles of glucocorticoids in adipose tissue biology and the development of central obesity: Biochim Biophys Acta, v. 1842, p. 473-81.
Leidl, K., G. Liebisch, D. Richter, and G. Schmitz, 2008, Mass spectrometric analysis of lipid species of human circulating blood cells: Biochim Biophys Acta, v. 1781, p. 655-64.

Ljung, T., G. Holm, P. Friberg, B. Andersson, B. A. Bengtsson, J. Svensson, M. Dallman, B. McEwen, and P. Björntorp, 2000, The activity of the hypothalamic-pituitary-adrenal axis and the sympathetic nervous system in relation to waist/hip circumference ratio in men: Obes Res, v. 8, p. 487-95.
Lloyd, A. J., M. Beckmann, T. Wilson, K. Tailliart, D. Allaway, and J. Draper, 2017, Ultra high performance liquid chromatography-high resolution mass spectrometry plasma lipidomics can distinguish between canine breeds despite uncontrolled environmental variability and non-standardized diets: Metabolomics, v. 13, p. 15.
Maceyka, M., K. B. Harikumar, S. Milstien, and S. Spiegel, 2012, Sphingosine-1-phosphate signaling and its role in disease: Trends Cell Biol, v. 22, p. 50-60.
MacLean, B., D. M. Tomazela, N. Shulman, M. Chambers, G. L. Finney, B. Frewen, R. Kern, D. L. Tabb, D. C. Liebler, and M. J. MacCoss, 2010, Skyline: an open source document editor for creating and analyzing targeted proteomics experiments: Bioinformatics, v. 26, p. 966-8.
Mandon, E. C., I. N. de Gómez Dumm, M. J. de Alaníz, C. A. Marra, and R. R. Brenner, 1987, ACTH depresses delta 6 and delta 5 desaturation activity in rat adrenal gland and liver: J Lipid Res, v. 28, p. 1377-83.
Meikle, P. J., and M. J. Christopher, 2011, Lipidomics is providing new insight into the metabolic syndrome and its sequelae: Curr Opin Lipidol, v. 22, p. 210-5.
Miao, H., H. Chen, S. Pei, X. Bai, N. D. Vaziri, and Y. Y. Zhao, 2015, Plasma lipidomics reveal profound perturbation of glycerophospholipids, fatty acids, and sphingolipids in diet-induced hyperlipidemia: Chem Biol Interact, v. 228, p. 79-87.
Missmer, S. A., L. Suarez, M. Felkner, E. Wang, A. H. Merrill, K. J. Rothman, and K. A. Hendricks, 2006, Exposure to fumonisins and the occurrence of neural tube defects along the Texas-Mexico border: Environ Health Perspect, v. 114, p. 237-41.
Mooney, C. T., and M. E. Peterson, 2004, BSAVA Manual of Canine and Feline Endocrinology: Quedgeley, UK, British Small Animal Veterinary Association.
Narayanaswamy, P., S. Shinde, R. Sulc, R. Kraut, G. Staples, C. H. Thiam, R. Grimm, B. Sellergren, F. Torta, and M. R. Wenk, 2014, Lipidomic "deep profiling": an enhanced workflow to reveal new molecular species of signaling lipids: Anal Chem, v. 86, p. 3043-7.
Nelson, R. H., 2013, Hyperlipidemia as a risk factor for cardiovascular disease: Prim Care, v. 40, p. 195-211.
Nguyen, A., S. A. Rudge, Q. Zhang, and M. J. Wakelam, 2016, Using lipidomics analysis to determine signalling and metabolic changes in cells: Curr Opin Biotechnol, v. 43, p. 96-103.
Oakley, R. H., and J. A. Cidlowski, 2011, Cellular processing of the glucocorticoid receptor gene and protein: new mechanisms for generating tissue-specific actions of glucocorticoids: J Biol Chem, v. 286, p. 3177-84.
Oresic, M., V. A. Hänninen, and A. Vidal-Puig, 2008, Lipidomics: a new window to biomedical frontiers: Trends Biotechnol, v. 26, p. 647-52.
Ottosson, M., K. Vikman-Adolfsson, S. Enerbäck, G. Olivecrona, and P. Björntorp, 1994, The effects of cortisol on the regulation of lipoprotein lipase activity in human adipose tissue: J Clin Endocrinol Metab, v. 79, p. 820-5.
Ozbay, T., A. H. Merrill, and M. B. Sewer, 2004, ACTH regulates steroidogenic gene expression and cortisol biosynthesis in the human adrenal cortex via sphingolipid metabolism: Endocr Res, v. 30, p. 787-94.
Peckett, A. J., D. C. Wright, and M. C. Riddell, 2011, The effects of glucocorticoids on adipose tissue lipid metabolism: Metabolism, v. 60, p. 1500-10.

Pietiläinen, K. H., M. Sysi-Aho, A. Rissanen, T. Seppänen-Laakso, H. Yki-Järvinen, J. Kaprio, and M. Oresic, 2007, Acquired obesity is associated with changes in the serum lipidomic profile independent of genetic effects--a monozygotic twin study: PLoS One, v. 2, p. e218.
Potì, F., M. Simoni, and J. R. Nofer, 2014, Atheroprotective role of high-density lipoprotein (HDL)-associated sphingosine-1-phosphate (S1P): Cardiovasc Res, v. 103, p. 395-404.
Prélaud, P., D. Rosenberg, and P. d. Fornel, 2005, Endokrinologische Diagnostik in der Kleintierpraxis, Schlütersche Verlagsgesellschaft.
Püschel, G., H. Kühn, T. Kietzmann, W. Höhne, B. Christ, D. Doenecke, and J. Koolman, 2011, Taschenlehrbuch Biochemie: Stuttgart, Georg Thieme Verlag KG.
Quehenberger, O., A. M. Armando, A. H. Brown, S. B. Milne, D. S. Myers, A. H. Merrill, S. Bandyopadhyay, K. N. Jones, S. Kelly, R. L. Shaner, C. M. Sullards, E. Wang, R. C. Murphy, R. M. Barkley, T. J. Leiker, C. R. Raetz, Z. Guan, G. M. Laird, D. A. Six, D. W. Russell, J. G. McDonald, S. Subramaniam, E. Fahy, and E. A. Dennis, 2010, Lipidomics reveals a remarkable diversity of lipids in human plasma: J Lipid Res, v. 51, p. 3299-305.
Rivera, J., R. L. Proia, and A. Olivera, 2008, The alliance of sphingosine-1-phosphate and its receptors in immunity: Nat Rev Immunol, v. 8, p. 753-63.
Rockall, A. G., S. A. Sohaib, D. Evans, G. Kaltsas, A. M. Isidori, J. P. Monson, G. M. Besser, A. B. Grossman, and R. H. Reznek, 2003, Computed tomography assessment of fat distribution in male and female patients with Cushing's syndrome: Eur J Endocrinol, v. 149, p. 561-7.
Schmelzer, K., E. Fahy, S. Subramaniam, and E. A. Dennis, 2007, The lipid maps initiative in lipidomics: Methods Enzymol, v. 432, p. 171-83.
Schmid, F., 2017, Canine Lipoprotein Separation and Characterization of the Canine Lipidome with Comparison between Healthy and Prednisolone Treated Beagles, Inaugural Dissertation, University of Zurich, Switzerland (in progress), Zurich, Switzerland.
Schmitz, G., and K. Ruebsaamen, 2010, Metabolism and atherogenic disease association of lysophosphatidylcholine: Atherosclerosis, v. 208, p. 10-8.
Shibata, Y., Y. Abiko, and H. Takiguchi, 1988, Phospholipase A2 in macrophage plasma membrane releases arachidonic acid from phosphatidylinositol: Biochim Biophys Acta, v. 971, p. 121-6.
Slavin, B. G., J. M. Ong, and P. A. Kern, 1994, Hormonal regulation of hormone-sensitive lipase activity and mRNA levels in isolated rat adipocytes: J Lipid Res, v. 35, p. 1535-41.
Smith, D. M., and M. Waite, 1992, Phosphatidylinositol hydrolysis by phospholipase A2 and C activities in human peripheral blood neutrophils: J Leukoc Biol, v. 52, p. 670-8.
Stegemann, C., R. Pechlaner, P. Willeit, S. R. Langley, M. Mangino, U. Mayr, C. Menni, A. Moayyeri, P. Santer, G. Rungger, T. D. Spector, J. Willeit, S. Kiechl, and M. Mayr, 2014, Lipidomics profiling and risk of cardiovascular disease in the prospective population-based Bruneck study: Circulation, v. 129, p. 1821-31.
Stone, N. J., 1994, Secondary causes of hyperlipidemia: Med Clin North Am, v. 78, p. 117-41.
Stryer, L., 1990, Biochemie, v. 3: Heidelberg, Spektrum der Wissenschaft Verlangsgesellschaft mbH.
Tarasov, K., K. Ekroos, M. Suoniemi, D. Kauhanen, T. Sylvänne, R. Hurme, I. Gouni-Berthold, H. K. Berthold, M. E. Kleber, R. Laaksonen, and W. März, 2014,

Molecular lipids identify cardiovascular risk and are efficiently lowered by simvastatin and PCSK9 deficiency: J Clin Endocrinol Metab, v. 99, p. E45-52.
Tvrdik, P., A. Asadi, L. P. Kozak, J. Nedergaard, B. Cannon, and A. Jacobsson, 1997, Cig30, a mouse member of a novel membrane protein gene family, is involved in the recruitment of brown adipose tissue: J Biol Chem, v. 272, p. 31738-46.
U.S. Department of Health and Human Services, F. a. D. A., Center for Drug Evaluation and Research, Center for Veterinary Medicine, 2001, Guidance for Industry, Bioanalytical Method Validation.
Vance, D. E., J. E. Vance, and editors, 2008, Biochemistry of Lipids, Lipoproteins and Membranes, Elsevier B.V.
Vance, D. E. V. a. J. E., 2002, Biochemistry of Lipids, Lipoproteins and Membranes: Sphingolipids: metabolism and cell signaling.
Vettorazzi, S., C. Bode, L. Dejager, L. Frappart, E. Shelest, C. Klaßen, A. Tasdogan, H. M. Reichardt, C. Libert, M. Schneider, F. Weih, N. Henriette Uhlenhaut, J. P. David, M. Gräler, A. Kleiman, and J. P. Tuckermann, 2015, Glucocorticoids limit acute lung inflammation in concert with inflammatory stimuli by induction of SphK1: Nat Commun, v. 6, p. 7796.
Wang, B., K. Palomares, N. Parobchak, J. Cece, M. Rosen, A. Nguyen, and T. Rosen, 2013, Glucocorticoid receptor signaling contributes to constitutive activation of the noncanonical NF-κB pathway in term human placenta: Mol Endocrinol, v. 27, p. 203-11.
Wilson, P. W., R. B. D'Agostino, H. Parise, L. Sullivan, and J. B. Meigs, 2005, Metabolic syndrome as a precursor of cardiovascular disease and type 2 diabetes mellitus: Circulation, v. 112, p. 3066-72.
Xenoulis, P. G., and J. M. Steiner, 2010, Lipid metabolism and hyperlipidemia in dogs: Vet J, v. 183, p. 12-21.
Xia, J., I. V. Sinelnikov, B. Han, and D. S. Wishart, 2015, MetaboAnalyst 3.0--making metabolomics more meaningful: Nucleic Acids Res, v. 43, p. W251-7.
Xu, C., J. He, H. Jiang, L. Zu, W. Zhai, S. Pu, and G. Xu, 2009, Direct effect of glucocorticoids on lipolysis in adipocytes: Mol Endocrinol, v. 23, p. 1161-70.
Yang, L. V., C. G. Radu, L. Wang, M. Riedinger, and O. N. Witte, 2005, Gi-independent macrophage chemotaxis to lysophosphatidylcholine via the immunoregulatory GPCR G2A: Blood, v. 105, p. 1127-34.
Yang-Yen, H. F., J. C. Chambard, Y. L. Sun, T. Smeal, T. J. Schmidt, J. Drouin, and M. Karin, 1990, Transcriptional interference between c-Jun and the glucocorticoid receptor: mutual inhibition of DNA binding due to direct protein-protein interaction: Cell, v. 62, p. 1205-15.
Zhang, H., N. Abraham, L. A. Khan, and V. Gobel, 2015, RNAi-based biosynthetic pathway screens to identify in vivo functions of non-nucleic acid-based metabolites such as lipids: Nat Protoc, v. 10, p. 681-700.
Zoeller, R. A., A. C. Lake, N. Nagan, D. P. Gaposchkin, M. A. Legner, and W. Lieberthal, 1999, Plasmalogens as endogenous antioxidants: somatic cell mutants reveal the importance of the vinyl ether: Biochem J, v. 338 (Pt 3), p. 769-76.

Supplements

Table of contents, supplementary tables

Digital tables (provided on a CD-ROM)

Tables 5.1-5.3: Clinical characteristics of dogs: Age, gender, dosage of treatment, blood chemistry results, endocrine test results, symptoms are listed in rows. Abbreviations: Treatm. = treatment; Fruct. = fructosamine; Crea = creatinine; Chol = cholesterol; TG = triglycerides; ALKP = Alkaline phosphatase; ALAT = alanine transaminase, CK = creatine kinase; Na = sodium; K = potassium; Cl = chloride; Ca = calcium; P = phosphate; PU = polyuria; PD polydipsia; PP = polyphagia; M.W. = muscle wasting; C. obesity = central obesity

Table 5.1 Demographic data dogs

DogID	Exp.	Treatm.	Age	Gender	Sex	Neutered	Dose	DoseUnit
2775	ACTH	None	83	M	M	No	0	ug/kg/d
4820	ACTH	None	72	F	F	No	0	ug/kg/d
5076	ACTH	None	71	F_neut	F	Yes	0	ug/kg/d
6648	ACTH	None	23	M	M	No	0	ug/kg/d
6694	ACTH	None	23	M	M	No	0	ug/kg/d
8371	ACTH	None	88	M	M	No	0	ug/kg/d
2775	ACTH	ACTH	83	M	M	No	10.3	ug/kg/d
4820	ACTH	ACTH	72	F	F	No	6.3	ug/kg/d
5076	ACTH	ACTH	71	F_neut	F	Yes	10.3	ug/kg/d
6648	ACTH	ACTH	23	M	M	No	6.3	ug/kg/d
6694	ACTH	ACTH	23	M	M	No	10.3	ug/kg/d
8371	ACTH	ACTH	88	M	M	No	6.3	ug/kg/d
4820	Pred	None	58	F	F	No	0	mg/kg/d
4823	Pred	None	43	F	F	No	0	mg/kg/d
5076	Pred	None	56	F_neut	F	Yes	0	mg/kg/d
5088	Pred	None	43	M	M	No	0	mg/kg/d
6648	Pred	None	8	M	M	No	0	mg/kg/d
6663	Pred	None	7	M	M	No	0	mg/kg/d
6694	Pred	None	7	M	M	No	0	mg/kg/d
6738	Pred	None	8	M	M	No	0	mg/kg/d
4820	Pred	Pred	58	F	F	No	50	mg/kg/d
4823	Pred	Pred	43	F	F	No	50	mg/kg/d
5076	Pred	Pred	56	F_neut	F	Yes	50	mg/kg/d
5088	Pred	Pred	43	M	M	No	50	mg/kg/d
6648	Pred	Pred	8	M	M	No	50	mg/kg/d
6663	Pred	Pred	7	M	M	No	50	mg/kg/d
6694	Pred	Pred	7	M	M	No	50	mg/kg/d
6738	Pred	Pred	8	M	M	No	50	mg/kg/d

Table 5.2 Blood chemistry dogs (1)

DogID	Exp.	Treatm.	Bilirubin	Glucose	Fruct.	Urea	Crea.	Protein	Albumin	Globulin
2775	ACTH	None	2.5	5.4	268	3.5	55	59	35	24
4820	ACTH	None	2.5	5.2	288	3.1	48	63	37	26
5076	ACTH	None	2.5	5.5	287	2.9	62	57	36	21
6648	ACTH	None	2.5	6	304	3.7	75	61	37	25
6694	ACTH	None	2.5	7.1	326	4.1	81	65	40	25
8371	ACTH	None	2.5	6.3	272	4.1	56	62	34	27
2775	ACTH	ACTH	2.5	5.3	194	2.1	19	55	25	30
4820	ACTH	ACTH	2.5	6.8	233	1.2	NA	60	36	24
5076	ACTH	ACTH	2.5	6.9	205	1.5	16	56	33	23
6648	ACTH	ACTH	2.5	5.1	238	2.3	27	59	36	24
6694	ACTH	ACTH	2.5	5.6	248	3	31	61	39	22
8371	ACTH	ACTH	2.5	5.9	191	6	71	47	15	33
4820	Pred	None	2.5	5.2	243	4.1	51	59	38	21
4823	Pred	None	2.5	5.8	281	4.7	48	62	38	24
5076	Pred	None	2.5	5.5	264	4.1	69	59	38	21
5088	Pred	None	2.5	6.3	305	5.7	69	61	39	22
6648	Pred	None	2.5	5.4	244	5	73	55	39	16
6663	Pred	None	2.5	5.5	241	5.2	76	55	35	19
6694	Pred	None	2.5	5.5	282	5.9	77	52	38	15
6738	Pred	None	2.5	5.6	260	5.9	76	55	36	20
4820	Pred	Pred	2.5	4	273	4.2	47	63	41	22
4823	Pred	Pred	2.5	5.3	284	4.5	41	64	41	23
5076	Pred	Pred	2.5	5.3	278	4.4	48	63	42	21
5088	Pred	Pred	2.5	5.3	263	5.8	50	55	33	22
6648	Pred	Pred	5.1	3.4	239	4.4	49	58	24	34
6663	Pred	Pred	9.1	2.7	223	6	40	55	23	31
6694	Pred	Pred	2.5	3.7	280	5.6	58	60	41	19
6738	Pred	Pred	2.5	4.1	294	5.1	55	64	41	23

Table 5.3 Blood chemistry dogs (2)

DogID	Exp.	Treatm.	Chol	TG	ALKP	Lipase	ALAT	CK	Na	K	Cl	Ca	P
2775	ACTH	None	4.5	0.4	47	23	37	167	147	4.1	112	2.53	1.2
4820	ACTH	None	4.9	0.5	62	42	45	128	146	4	109	2.71	1.26
5076	ACTH	None	6.1	0.4	57	40	44	107	146	3.9	111	2.57	1.22
6648	ACTH	None	4.7	0.2	41	22	44	691	150	3.7	110	2.77	1.39
6694	ACTH	None	5.5	0.2	47	48	73	599	151	3.4	112	2.76	1.43
8371	ACTH	None	5.6	0.2	68	28	64	565	147	3.7	109	2.61	1.22
2775	ACTH	ACTH	6.6	1.3	206	57	127	248	146	4.3	107	2.34	1.71
4820	ACTH	ACTH	4.5	0.6	1004	194	326	151	145	4.1	100	2.49	1.27
5076	ACTH	ACTH	8.1	1	665	1866	672	154	140	4.7	96	2.34	1.28
6648	ACTH	ACTH	2.7	0.3	182	397	406	201	146	3.9	102	2.62	1.12
6694	ACTH	ACTH	5	0.4	161	141	154	92	146	3.9	103	2.58	1.27
8371	ACTH	ACTH	9.5	3.3	685	91	140	135	151	3.5	111	2.12	2.62
4820	Pred	None	5.5	0.8	42	41	31	100	144	3.6	105	2.6	1.09
4823	Pred	None	4.7	1.4	109	77	35	144	147	3.7	109	2.59	1.19
5076	Pred	None	6.3	0.7	58	52	35	221	149	3.6	112	2.55	1.36
5088	Pred	None	5.7	0.6	40	54	63	140	148	3.7	108	2.6	1.33
6648	Pred	None	5	0.3	74	40	35	172	147	3.9	110	2.81	2.23
6663	Pred	None	6	0.5	93	29	29	166	146	3.7	109	2.8	2.01
6694	Pred	None	5.7	0.3	71	56	47	190	147	3.8	111	2.65	1.97
6738	Pred	None	6.9	0.4	72	25	32	108	143	3.7	108	2.7	1.78
4820	Pred	Pred	5.8	1.2	114	85	70	48	148	3.8	98	2.59	1.22
4823	Pred	Pred	3.4	0.5	157	104	49	140	150	3.2	103	2.37	1.1
5076	Pred	Pred	4.5	0.7	139	78	51	89	147	4.1	100	2.58	1.42
5088	Pred	Pred	4.1	0.3	113	107	151	77	151	3.7	99	2.35	1.52
6648	Pred	Pred	5.7	0.3	160	32	178	141	152	4.2	93	2.55	2.6
6663	Pred	Pred	4	0.2	84	123	57	118	154	3.9	93	2.46	3.48
6694	Pred	Pred	5.7	0.2	94	106	111	75	150	3.8	99	2.87	1.46
6738	Pred	Pred	6.9	0.5	101	56	70	89	150	3.8	95	2.84	1.39

Table 5.4 Endocrine tests and clinical symptoms

DogID	Exp.	Treatm.	ACTH, StimLDDS	Cortisol Basal	PU	PD	PP	M.W.	C. Obesity	Other symptoms
2775	ACTH	None	not done	2.5	No	No	No	No	No	fuzzy hair
4820	ACTH	None	not done	2.5	No	No	No	No	No	
5076	ACTH	None	not done	1.9	No	No	No	No	No	dandruff
6648	ACTH	None	not done	2.6	No	No	No	No	No	
6694	ACTH	None	not done	5.4	No	No	No	No	No	
8371	ACTH	None	not done	11.9	No	No	No	No	No	dandruff
2775	ACTH	ACTH	positive	7	Yes	Yes	No	No	No	
4820	ACTH	ACTH	positive	46.3	Yes	Yes	No	Yes	Yes	pot belly
5076	ACTH	ACTH	positive	10.1	Yes	Yes	No	Yes	Yes	big belly, soft, not painful
6648	ACTH	ACTH	positive	8.6	Yes	Yes	No	Yes	No	
6694	ACTH	ACTH	positive	9.5	Yes	Yes	No	Yes	No	
8371	ACTH	ACTH	positive	16.1	No	No	No	No	No	dandruff
4820	Pred	None	not done	1.7	No	No	No	No	No	
4823	Pred	None	not done	1.8	No	No	No	No	No	
5076	Pred	None	not done	1.3	No	No	No	No	No	
5088	Pred	None	not done	1.5	No	No	No	No	No	
6648	Pred	None	not done	1.6	No	No	No	No	No	
6663	Pred	None	not done	1.1	No	No	No	No	No	
6694	Pred	None	not done	1.1	No	No	No	No	No	
6738	Pred	None	not done	1.6	No	No	No	No	No	
4820	Pred	Pred	not done	0.3	Yes	Yes	Yes	No	No	
4823	Pred	Pred	not done	0.3	Yes	Yes	Yes	No	No	
5076	Pred	Pred	not done	0.3	Yes	Yes	Yes	No	No	
5088	Pred	Pred	not done	2.3	Yes	Yes	Yes	No	No	
6648	Pred	Pred	not done	0.5	Yes	Yes	Yes	No	No	
6663	Pred	Pred	not done	1.4	Yes	Yes	Yes	No	No	
6694	Pred	Pred	not done	0.4	Yes	Yes	Yes	No	No	
6738	Pred	Pred	not done	0.5	Yes	Yes	Yes	No	No	

Table 5.4 A: Reference ranges of blood chemistry

Short Name	Full Name	Unit	LowerRefLimit	UpperRefLimit
Bilirubin	Total bilirubin	umol/l	0	3.5
Glucose	Glucose in Plasma	mmol/l	4.1	5.9
Fructosamin	Fructosamine	umol/l	207	324
Urea	Urea	mmol/l	3.8	9.4
Creatinin	Creatinine	umol/l	50	119
Protein	Protein (Biuret)	g/l	56	71
Albumin	Albumin (CobasC)	g/l	29	37
Globulin	Globulin (calculated)	g/l		
Chol	Cholesterol	mmol/l	3.5	8.6
TAG	Trigylcerides	mmol/l	0.4	1.5
ALKP	Alkaline Phosphatase	U/l	20	98
Lipase	Lipase (CobasC)	U/l	24	108
ALAT	Alkaline transaminase (GPT)	U/l	20	93
CK	Creatine kinase	U/l	51	191
Na	Sodium indirect (CobasC)	mmol/l	145	152
K	Potassium	mmol/l	4.3	5.3
Cl	Chloride indirect (CobasC)	mmol/l	107	118
Ca	Calcium	mmol/l	2.4	2.8
Protein	Phosphate	mmol/l	1	1.6
Cortisol	Cortisol basal	mcg/dl	0	2

Table 5.5: Detailed information of panel 1 measured on Agilent 6460 Triple Quadrupole LC-MS based on acquisition method report.

Panel 1

Scan Parameters		
Data Stg	Centroid	
Threshold	0	
Source Parameters		
Parameter	Value (+)	Value (-)
Gas Temp (°C)	300	300
Gas Flow (l/min)	5	5
Nebuliser (psi)	45	45
SheathGasHeater	250	250
SheathGasFlow	11	11
Capillary (V)	3500	3500
VCharging	500	500
HiP Sampler		
Draw Speed	20.0 µL/min	
Eject Speed	40.0 µL/min	
Draw Positon Offset	0.0 mm	
Wait Time After Drawing	3.0 s	
Sample Flush Out Factor	5	
Vial/Well bottom sensing	Yes	
Injection Mode	Injection with needle wash	
Injection Volume	2 µL/min	
Automatic Delay Volume Reduction	No	
Enable Overlapped Injection	No	
Quat Pump		
Flow	0.4 mL/min	
Use Solvent Types	Yes	
Low Pressure Limit	0.00 bar	
High Pressure Limit	1200.00 bar	
Max. Flow Ramp Up	100.000 mL/min^2	
Max. Flow Ramp Down	100.000 mL/min^2	
Automatic Stroke Calculation	Yes	
Stoptime Mode	Time set	
Stoptime Mode	10.8	
Temperature Control Mode	Temperature Set	
Temperature Control Mode	40.00°C	
Enable Analysis Left Temperature On	Yes	
Enable Analysis Left Temperature Value	0.80°C	
Right Temperature Control Mode	Combined	
Enable Right Temperature On	Yes	
Enable Analysis Right Temperature Value	0.80°C	

Table 5.6: Detailed information of panel 2 measured on Agilent 6495 Triple Quadrupole LC-MS based on acquisition method report.

Panel 2

Scan Parameters		
Data Stg	Centroid	
Threshold	0	
Source Parameters		
Parameter	Value (+)	Value (-)
Gas Temp (°C)	200	200
Gas Flow (l/min)	12	12
Nebuliser (psi)	25	25
SheathGasHeater	250	250
SheathGasFlow	12	12
Capillary (V)	3500	3000
VCharging	500	1500
HiP Sampler		
Draw Speed	50.0 µL/min	
Eject Speed	100.0 µL/min	
Draw Positon Offset	1.0mm (-)	
Wait Time After Drawing	0.0 s	
Sample Flush Out Factor	5	
Vial/Well bottom sensing	Yes	
Injection Mode	Injection with needle wash	
Injection Volume	1 µL/min	
Automatic Delay Volume Reduction	No	
Enable Overlapped Injection	No	
Quat Pump		
Flow	0.4 mL/min	
Use Solvent Types	Yes	
Low Pressure Limit	0.00 bar	
High Pressure Limit	1200.00 bar	
Max. Flow Ramp Up	100.000 mL/min^2	
Max. Flow Ramp Down	100.000 mL/min^2	
Automatic Stroke Calculation	Yes	
Stoptime Mode	Time set	
Stoptime Mode	10.8	
Temperature Control Mode	Temperature Set	
Temperature Control Mode	40.00°C	
Enable Analysis Left Temperature On	Yes	
Enable Analysis Left Temperature Value	0.80°C	
Right Temperature Control Mode	Temperature Set	
Enable Right Temperature On	Yes	
Enable Analysis Right Temperature Value	0.80°C	

Table 5.7: Detailed information of panel 3 measured on AB Sciex 4000 QTrap LC-MS based on acquisition method report.

Panel 3

Source Parameters	
Vacuum Gauge (10e-5 Torr)	2.6
Source Type	Turbo Spray
Source Temperature	250°C at setpoint
Start of run pressure (psi)	1364.66
HiP Sampler	
Draw Speed	200.0 µL/min
Eject Speed	200.0 µL/min
Injection Volume	10 µL/min
LC Binary pump	
Min. pressure (Psi)	0
Max. pressure	5801
Dead volume (µL)	40
Max. flow Ramp (ml/min^2)	100
Max. Pressure Ramp (psi/sec)	290
Max Flow Ramp Up (ml/min^2)	100
Max Flow Ramp Down (ml/min^2)	100

Table 5.8: Detailed information of panel 4 measured on Agilent 6490 Triple Quadrupole LC-MS based on acquisition method report.

Panel 4

Scan Parameters		
Data Stg	Centroid	
Threshold	0	
Source Parameters		
Parameter	Value (+)	Value (-)
Gas Temp (°C)	200	200
Gas Flow (l/min)	12	12
Nebuliser (psi)	25	25
SheathGasHeater	400	400
SheathGasFlow	12	12
Capillary (V)	3500	3000
VCharging	500	1500
HiP Sampler		
Draw Speed	50.0 µL/min	
Eject Speed	100.0 µL/min	
Draw Positon Offset	1.0mm (-)	
Wait Time After Drawing	0.0 s	
Sample Flush Out Factor	5	
Vial/Well bottom sensing	Yes	
Injection Mode	Standard injection	
Injection Volume	5 µL/min	
Automatic Delay Volume Reduction	No	

Panel 4

Enable Overlapped Injection	No
Quat Pump	
Flow	0.4 mL/min
Use Solvent Types	Yes
Low Pressure Limit	0.00 bar
High Pressure Limit	1000.00 bar
Max. Flow Ramp Up	100.000 mL/min^2
Max. Flow Ramp Down	100.000 mL/min^2
Automatic Stroke Calculation	Yes
Stoptime Mode	Time set
Stoptime Mode	9.00 min
Temperature Control Mode	Temperature Set
Temperature Control Mode	60.00°C
Enable Analysis Left Temperature On	Yes
Enable Analysis Left Temperature Value	0.80°C
Right Temperature Control Mode	Temperature Set
Enable Analysis Right Temperature Value	0.80°C

Table 5.9: MRM list of panel 1 including compound group, compound name, precursor ion and product ion (in unit respectively), retention time, collision energy and cell accelerator voltage settings. TGs of this panel were not included in summary of measured lipids but TGs of panel 3.

Compound Group	Compound Name	Precursor Ion	Product Ion	Ret Time (min)	Delta Ret Time	Collision Energy	Cell Accelerator Voltage
BMP	BMP 14:0 14:0	684.5	285.2	4.4	1	17	5
BMP	BMP 18:1 18:1	792.6	339.3	5.25	1	17	5
CE	CE 14:0	614.6	369.3	8.211	0.7	10	5
CE	CE 15:0	628.6	369.3	8.4	0.7	10	5
CE	CE 16:0	642.6	369.3	8.5	0.7	10	5
CE	CE 16:1	640.6	369.3	8.2	0.7	10	5
CE	CE 16:2	638.6	369.3	8.1	0.7	10	5
CE	CE 17:0	656.6	369.3	8.5	0.7	10	5
CE	CE 17:1	654.6	369.3	8.4	0.7	10	5
CE	CE 18:0	670.7	369.3	8.38	0.7	10	5
CE	CE 18:0-d6 (IS)	676.7	375.3	8.6	0.7	10	5
CE	CE 18:1	668.6	369.3	8.3	0.5	10	5
CE	CE 18:2	666.6	369.3	8.2	0.7	10	5
oxCE	CE 18:2 +2O NH4	698.6	369.4	7	1	10	5
oxCE	CE 18:2 +O NH4	682.6	369.4	7.5	1	10	5
CE	CE 18:3	664.6	369.3	8.1	0.7	10	5
CE	CE 20:1	696.7	369.3	8.6	0.7	10	5
CE	CE 20:2	694.7	369.3	8.36	0.7	10	5
CE	CE 20:3	692.6	369.3	8.15	0.7	10	5
CE	CE 20:4	690.6	369.3	8.2	0.7	10	5
CE	CE 20:5	688.6	369.3	8	0.7	10	5
CE	CE 22:0	726.7	369.3	8.9	1	10	5
CE	CE 22:1	724.7	369.3	8.611	1	10	5
CE	CE 22:4	718.7	369.3	8.25	0.7	10	5
CE	CE 22:5	716.6	369.3	8.12	0.7	10	5
CE	CE 22:6	714.6	369.3	8	0.7	10	5
CE	CE 24:0	754.7	369.3	9.2	0.7	10	5
CE	CE 24:1	752.7	369.3	8.9	0.7	10	5
CE	CE 24:4	746.7	369.3	8.4	0.7	10	5
CE	CE 24:5	744.7	369.3	8.4	0.7	10	5

Compound Group	Compound Name	Precursor Ion	Product Ion	Ret Time (min)	Delta Ret Time	Collision Energy	Cell Accelerator Voltage
CE	CE 24:6	742.7	369.3	8.3	0.7	10	5
Cer	Cer d16:1/C22:0	594.7	236.4	6.65	0.7	30	7
Cer	Cer d18:0/C22:0	624.7	266.4	6.87	0.7	30	7
Cer	Cer d18:0/C24:0	652.7	266.4	7.2	0.7	30	7
Cer	Cer d18:0/C24:1	650.7	266.4	6.95	0.7	30	7
Cer	Cer d18:1/19:0	581.5	264.3	6.45	0.7	29	5
Cer	Cer d18:1/C16:0	538.5	264.3	5.95	0.7	29	5
Cer	Cer d18:1/C17:0 (IS)	552.5	264.3	6.07	0.7	29	5
Cer	Cer d18:1/C18:0	566.6	264.3	6.32	0.7	29	5
Cer	Cer d18:1/C20:0	594.6	264.3	6.66	0.7	29	5
Cer	Cer d18:1/C22:0	622.6	264.3	6.95	0.7	29	5
Cer	Cer d18:1/C24:0	650.6	264.3	7.2	0.7	29	5
Cer	Cer d18:1/C24:1	648.6	264.3	6.95	0.7	29	5
Cer	Cer d18:1/C26:1	678.7	264.4	7.34	1	30	7
Cer	Cer d18:2/C16:0	536.7	262.4	5.592	1	30	7
Cer	Cer d18:2/C22:0	620.7	262.4	6.625	1	30	7
Cer	Cer d18:2/C24:1	646.7	262.4	6.617	1	30	7
COH	COH (161)	369.4	161.2	5.146	0.7	23	5
COH	COH (95)	369.4	95.2	5.146	1	38	5
COH	COH-d7 (IS) (161)	376.4	161.2	5.129	0.7	23	5
COH	COH-d7 (IS) (95)	376.4	95.2	5.129	0.7	38	5
TG	d5TG 16:0/16:0/16:0 (IS)	829.8	556.5	8.2	0.7	30	7
TG	d5TG 48:0 (IS)	829.8	829.8	8.2	0.7	5	5
DG	DG 15:0 15:0 (IS)	558.5	299.2	6.095	0.7	21	5
DG	DG 24:0 -(12:0) (IS)	474.7	257.1	4.92	0.7	10	7
DG	DG 30:0 -(14:0)	558.5	313.3	6.2	0.7	21	5
DG	DG 30:0 -(16:0)	558.5	285.2	6.2	0.7	21	5
DG	DG 30:1 -(14:0)	556.5	311.3	5.9	0.7	21	5
DG	DG 30:1 -(16:1)	556.5	285.2	5.9	0.7	21	5
DG	DG 32:0 -(14:0)	586.5	341.3	6.5	0.8	21	5
DG	DG 32:0 -(16:0)	586.5	313.2	6.5	0.8	21	5
DG	DG 32:0 -(18:0)	586.5	285.2	6.5	0.8	21	5
DG	DG 32:1 -(14:0)	584.5	339.3	6.2	0.8	21	5
DG	DG 32:1 -(16:0)	584.5	311.2	6.2	0.8	21	5
DG	DG 32:1 -(16:1)	584.5	313.2	6.3	0.8	21	5
DG	DG 32:1 -(18:1)	584.5	285.2	6.2	0.8	21	5
DG	DG 32:2 -(14:0)	582.5	337.3	5.845	0.7	21	5
DG	DG 32:2 -(16:1)	582.5	311.2	5.98	0.7	21	5
DG	DG 32:2 -(18:2)	582.5	285.2	5.95	0.7	21	5
DG	DG 34:0 -(16:0)	614.6	341.3	6.9	0.8	21	5
DG	DG 34:0 -(18:0)	614.6	313.3	6.7	0.8	21	5
DG	DG 34:1 -(16:0)	612.6	339.3	6.55	0.7	21	5
DG	DG 34:1 -(18:0)	612.6	311.3	6.5	0.7	21	5
DG	DG 34:1 -(18:1)	612.6	313.3	6.4	1	21	5
DG	DG 34:1 -(20:0)	612.6	283.3	6	0.7	21	5
DG	DG 34:2 -(16:0)	610.5	337.2	6.28	0.8	21	5
DG	DG 34:2 -(16:1)	610.5	339.2	6.21	0.8	21	5
DG	DG 34:2 -(18:1)	610.5	311.2	6.35	0.8	21	5
DG	DG 34:2 -(18:2)	610.5	313.2	6.35	0.8	21	5
DG	DG 36:0 -(16:0)	642.7	369.3	7.1	0.7	21	5
DG	DG 36:0 -(18:0)	642.6	341.3	7.1	0.7	21	5
DG	DG 36:0 -(20:0)	642.6	313.3	7.1	0.7	21	5
DG	DG 36:1 -(18:0)	640.6	339.3	6.7	0.8	21	5
DG	DG 36:1 -(18:1)	640.6	341.3	6.66	0.8	21	5
DG	DG 36:2 -(18:0)	638.6	337.3	6.5	0.8	21	5
DG	DG 36:2 -(18:1)	638.6	339.3	6.5	0.8	21	5
DG	DG 36:2 -(18:2)	638.6	341.3	6.5	0.8	21	5
DG	DG 36:3 -(18:1)	636.6	337.3	6.3	0.7	21	5
DG	DG 36:3 -(18:2)	636.6	339.3	6.3	0.7	21	5
DG	DG 36:3 -(20:3)	636.6	313.3	6.4	0.7	21	5

Compound Group	Compound Name	Precursor Ion	Product Ion	Ret Time (min)	Delta Ret Time	Collision Energy	Cell Accelerator Voltage
DG	DG 36:4 -(18:2)	634.5	337.2	6.15	0.7	21	5
DG	DG 36:4 -(18:3)	634.5	339.2	6.157	0.7	21	5
DG	DG 36:4 -(20:4)	634.5	313.2	6.229	0.7	21	5
DG	DG 38:1 -(18:1)	668.7	369.3	6.734	0.8	21	5
DG	DG 38:4 -(20:3)	662.6	339.3	6.5	0.7	21	5
DG	DG 38:4 -(20:4)	662.6	341.3	6.5	0.7	21	5
DG	DG 38:5 -(18:1)	660.6	361.3	6.174	0.8	21	5
DG	DG 38:5 -(20:3)	660.6	337.3	6.253	0.8	21	5
DG	DG 38:5 -(20:4)	660.6	339.3	6.38	0.8	21	5
DG	DG 38:5 -(22:5)	660.6	313.3	6.3515	0.8	21	5
DG	DG 38:6 -(20:4)	658.5	337.2	6.1285	0.8	21	5
DG	DG 38:6 -(22:6)	658.5	313.2	6.232	0.8	21	5
DHC	DHC 16:0	862.6	264.3	4.85	0.7	53	5
DHC	DHC 16:0d3 (IS)	865.6	264.3	4.85	0.7	53	5
DHC	DHC 18:0	890.7	264.3	5.17	0.7	53	5
DHC	DHC 20:0	918.7	264.3	5.55	0.7	53	5
DHC	DHC 22:0	946.7	264.3	5.85	0.7	53	5
DHC	DHC 24:0	974.8	264.3	6.15	0.7	53	5
DHC	DHC 24:1	972.7	264.3	5.85	0.7	53	5
dhCer	dhCer 16:0	540.5	522.5	6	0.7	21	5
dhCer	dhCer 16:0	540.5	284.3	6	0.7	30	5
dhCer	dhCer 18:0	568.6	550.6	6.3	1	21	5
dhCer	dhCer 18:0	568.6	284.3	6.3	1	30	5
dhCer	dhCer 20:0	596.6	578.6	6.7	0.7	21	5
dhCer	dhCer 20:0	596.6	284.3	6.6	0.7	30	5
dhCer	dhCer 22:0	624.6	606.6	6.95	0.8	21	5
dhCer	dhCer 22:0	624.6	284.3	6.95	0.8	30	5
dhCer	dhCer 24:0	652.7	634.7	7.2	0.7	21	5
dhCer	dhCer 24:0	652.7	284.3	7.2	0.7	30	5
dhCer	dhCer 24:1	650.6	632.6	7.1	0.7	21	5
dhCer	dhCer 24:1	650.6	284.3	7.1	0.7	30	5
dhCer	dhCer 8:0	428.4	410.4	4.359	0.7	21	5
dhCer	dhCer 8:0	428.4	284.3	4.359	0.7	30	5
PI	diC8 PI	604.6	327.6	1.76	1	17	7
GM3	GM3 16:0	1153.7	264.3	4.8	0.7	57	5
GM3	GM3 18:0	1181.8	264.3	5.2	0.7	57	5
GM3	GM3 20:0	1209.8	264.3	5.5	0.7	57	5
GM3	GM3 22:0	1237.8	264.3	5.8	0.7	57	5
GM3	GM3 24:0	1265.8	264.3	6.09	0.7	57	5
GM3	GM3 24:1	1263.8	264.3	5.8	0.7	57	5
LPC	LPC 14:0	468.3	184.1	2.18	0.8	21	5
LPC	LPC 15:0	482.3	184.1	2.55	0.8	21	5
LPC	LPC 16:0	496.3	184.1	2.85	0.8	21	5
LPC	LPC 16:1	494.3	184.1	2.5	1	21	5
LPC	LPC 17:0	510.35	184.1	3.17	0.8	21	5
LPC	LPC 17:1	508.4	184.1	2.75	1	21	5
LPC	LPC 18:0	524.4	184.1	3.46	0.8	21	5
LPC	LPC 18:1	522.4	184.1	3	0.8	21	5
LPC	LPC 18:2	520.3	184.1	2.63	1	21	5
LPC	LPC 18:3	518.3	184.1	2.3	1	21	5
LPC	LPC 19:0	538.4	184.1	3.63	0.8	21	5
LPC	LPC 20:0 (IS)	552.4	184.1	3.87	0.8	21	5
LPC	LPC 20:1	550.4	184.1	3.45	0.8	21	5
LPC	LPC 20:2	548.4	184.1	3	1	21	5
LPC	LPC 20:3	546.4	184.1	2.75	1.1	21	5
LPC	LPC 20:4	544.3	184.1	2.65	0.8	21	5
LPC	LPC 20:5	542.3	184.1	2.25	0.8	21	5
LPC	LPC 22:0	580.4	184.1	4.3	0.8	21	5
LPC	LPC 22:1	578.4	184.1	3.8	0.8	21	5
LPC	LPC 22:5	570.4	184.1	2.83	0.8	21	5

Compound Group	Compound Name	Precursor Ion	Product Ion	Ret Time (min)	Delta Ret Time	Collision Energy	Cell Accelerator Voltage
LPC	LPC 22:6	568.3	184.1	2.55	0.8	21	5
LPC	LPC 24:0	608.5	184.1	4.8	0.8	21	5
LPC	LPC 26:0	636.5	184.1	5.15	0.8	21	5
MHC	MHC d18:1/16:0	700.6	264.3	5.38	0.7	33	5
MHC	MHC d18:1/16:0d3 (IS)	703.6	264.3	5.28	0.7	33	5
MHC	MHC d18:1/18:0	728.6	264.3	5.8	1	33	5
MHC	MHC d18:1/20:0	756.6	264.3	6.34	0.7	33	5
MHC	MHC d18:1/22:0	784.7	264.3	6.6	0.7	33	5
MHC	MHC d18:1/24:0	812.7	264.3	6.93	0.7	33	5
MHC	MHC d18:1/24:1	810.7	264.3	6.6	0.7	33	5
MHC	MHC d18:1/8:0	588.8	264.3	4.04	0.7	33	5
PC	oddPC 29:0	692.5	184.1	5.1	1.2	21	5
Combo	oddPC 31:0\PC(O-32:0)	720.6	184.1	5.652	1.594	21	5
Combo	oddPC 31:1\PC(O-32:1)\ PC(P-32:0)	718.5	184.1	5.645	1.62	21	5
PC	oddPC 33:0	748.6	184.1	5.9	1.2	21	5
Combo	oddPC 33:1\PC(O-34:1)	746.6	184.1	5.9	1.553	21	5
Combo	oddPC 33:2\PC(O-34:2)\ PC(P-34:1)	744.6	184.1	5.4	1.5	21	5
Combo	oddPC 33:3\PC(O-34:3)\ PC(P-34:2)	742.5	184.1	5.5	1.5	21	5
Combo	oddPC 35:0\PC(O-36:0)	776.6	184.1	5.4	1.6	21	5
Combo	oddPC 35:1\PC(O-36:1)	774.6	184.1	5.3	1.6	21	5
Combo	oddPC 35:2\PC(O-36:2)	772.6	184.1	5.8	1.3	21	5
Combo	oddPC 35:3\PC(O-36:3)\ PC(P-36:2)	770.6	184.1	5.65	1.697	21	5
Combo	oddPC 35:4\PC(O-36:4)	768.6	184.1	5.567	1.18	21	5
PC	oddPC 35:5	766.5	184.1	5.65	0.7	21	5
Combo	oddPC 37:4\PC(O-38:4)	796.6	184.1	5.8	1.007	21	5
Combo	oddPC 37:5\PC(O-38:5)\ PC(P-38:4)	794.6	184.1	5.627	1.703	21	5
Combo	oddPC 37:6\PC(P-38:5)	792.6	184.1	5.596	1.613	21	5
Combo	oddPC 39:5\PC(O-40:5)	822.6	184.1	5.939	1.547	21	5
Combo	oddPC 39:6\PC(O-40:6)	820.6	184.1	5.8	1.566	21	5
Combo	oddPC 39:7\PC(O-40:7)\ PC(P-40:6)	818.6	184.1	5.611	1.685	21	5
PC	PC 13:0 13:0	650.5	184.1	4.5	0.7	21	5
PC	PC 14:0 14:0 (IS)	678.5	184.1	4.8	0.7	21	5
PC	PC 17:0 17:0	762.59	184.1	6	0.7	25	5
PC	PC 28:0	678.5	184.1	4.93	0.7	21	5
PC	PC 30:0	706.5	184.1	5.35	0.7	21	5
PC	PC 32:0	734.6	184.1	5.67	0.8	21	5
PC	PC 32:1	732.6	184.1	5.51	0.8	21	5
PC	PC 32:2	730.5	184.1	5.4	1	21	5
PC	PC 32:3	728.5	184.1	5.13	1	21	5
PC	PC 34:0	762.6	184.1	5.85	0.8	21	5
PC	PC 34:1	760.6	184.1	5.73	0.8	21	5
PC	PC 34:2	758.6	184.1	5.511	0.8	21	5
oxPC	PC 34:2 + 2O	790.6	184.1	5.6	1.2	21	5
oxPC	PC 34:2 + O/PC(O-34:3) +2O/PC(P-34:2) +2O	774.6	184.1	5.45	1.2	21	5
PC	PC 34:3	756.6	184.1	5.2145	0.8	21	5
PC	PC 34:4	754.5	184.1	4.95	1.2	21	5
PC	PC 34:5	752.5	184.1	4.65	1.2	21	5
Combo	PC 36:0\PC(P-38:6)	790.6	184.1	5.91	1.3	21	5
PC	PC 36:1	788.6	184.1	6.15	1.2	21	5
PC	PC 36:2	786.6	184.1	5.87	1	21	5
PC	PC 36:3	784.6	184.1	5.542	1	21	5
PC	PC 36:5	780.6	184.1	5.2	0.8	21	5
PC	PC 36:6	778.5	184.1	4.95	1.2	21	5
PC	PC 38:2	814.6	184.1	6.25	1	21	5
PC	PC 38:3	812.6	184.1	5.95	1	21	5
PC	PC 38:4	810.6	184.1	5.738	1	21	5

Compound Group	Compound Name	Precursor Ion	Product Ion	Ret Time (min)	Delta Ret Time	Collision Energy	Cell Accelerator Voltage
PC	PC 38:5	808.6	184.1	5.459	1	21	5
PC	PC 38:7	804.6	184.1	4.9	1	21	5
PC	PC 40:4	838.6	184.1	5.958	1	21	5
PC	PC 40:5	836.6	184.1	5.79	0.7	21	5
PC	PC 40:6	834.6	184.1	5.72	0.8	21	5
PC	PC 40:7	832.6	184.1	5.37	1	21	5
PC	PC 40:8	830.6	184.1	5.15	0.7	21	5
PC	PC(16:0/20:4)\PC(18:1/18:3)	782.6	184.1	5.592	0.8	21	5
Combo	PC(16:0/22:6)\PC(18:2/20:4)	806.6	184.1	5.225	1.14	21	5
LPAF	PC(O-16:0/0:0)	482.4	104.1	2.95	1	21	5
LPAF	PC(O-18:0/0:0)	510.4	104.1	3.4	1	21	5
LPAF	PC(O-18:1/0:0)	508.4	104.1	3.171	1.3	21	5
LPAF	PC(O-20:0/0:0)	538.4	104.1	3.622	1	21	5
LPAF	PC(O-20:1/0:0)	536.4	104.1	3.3	1.2	21	5
LPAF	PC(O-22:0/0:0)	566.5	104.1	4.6	0.8	21	5
LPAF	PC(O-22:1/0:0)	564.4	104.1	4.25	0.78	21	5
LPAF	PC(O-24:0/0:0)	594.5	104.1	5.1	1	21	5
LPAF	PC(O-24:1/0:0)	592.5	104.1	4.75	0.7	21	5
LPAF	PC(O-24:2/0:0)	590.5	104.1	4	0.88	21	5
Combo	PC(O-32:2)\PC(P-32:1)	716.6	184.1	5.388	1.339	21	5
Combo	PC(O-34:4)\PC(P-34:3)	740.6	184.1	5.508	1.089	21	5
Combo	PC(O-36:5)\PC(P-36:4)	766.6	184.1	5.536	1.003	21	5
PC(P)	PC(P-30:0)	690.4	184.1	5.16	0.7	21	5
PC(P)	PC(P-36:5)	764.6	184.1	5.4	0.7	21	5
PE	PE 14:0/14:0 (IS)	636.5	495.5	5.06	0.7	17	5
PE	PE 17:0/17:0	720.6	579.5	6.19	0.7	17	5
PE	PE 32:0	692.5	551.5	5.673	0.7	17	5
PE	PE 32:1	690.5	549.5	5.48	0.7	17	5
PE	PE 34:1	718.5	577.5	5.8	0.8	17	5
PE	PE 34:2	716.5	575.5	5.55	0.7	17	5
PE	PE 34:3	714.5	573.5	5.285	0.7	17	5
PE	PE 35:1	732.6	591.5	6.2	1.2	17	5
Combo	PE 35:2\PE(O-36:2)\ PE(P-18:0/18:1)	730.5	589.5	6.1	1.2	17	5
PE	PE 36:0	748.6	607.6	6.223	0.7	17	5
PE	PE 36:1	746.6	605.6	6.09	0.7	17	5
PE	PE 36:2	744.6	603.5	5.9	0.7	17	5
PE	PE 36:3	742.5	601.5	5.586	1	17	5
PE	PE 36:4	740.5	599.5	5.523	0.7	17	5
PE	PE 36:5	738.5	597.5	5.328	0.7	17	5
PE	PE 38:3	770.6	629.6	5.94	0.7	17	5
PE	PE 38:4	768.6	627.5	5.864	0.7	17	5
PE	PE 38:5	766.5	625.5	5.599	0.7	17	5
PE	PE 38:6	764.5	623.5	5.473	0.7	17	5
PE	PE 40:4	796.6	655.6	6.05	0.7	17	5
PE	PE 40:5	794.6	653.6	5.907	0.7	17	5
PE	PE 40:6	792.6	651.5	5.873	0.7	17	5
PE	PE 40:7	790.5	649.5	5.588	0.7	17	5
LPE	PE(14:0/0:0) (IS)	426.3	285.2	2.2	0.7	17	5
LPE	PE(16:0/0:0)	454.3	313.3	3	0.7	17	5
LPE	PE(18:0/0:0)	482.3	341.3	3.25	1	17	5
LPE	PE(18:1/0:0)	480.3	339.3	3.07	0.8	17	5
LPE	PE(18:2/0:0)	478.3	337.3	2.55	0.8	17	5
LPE	PE(20:4/0:0)	502.3	361.3	2.6	0.8	17	5
LPE	PE(22:6/0:0)	526.3	385.3	2.52	0.8	17	5
Combo	PE(O-18:0/22:5)\ PE(P-20:0/20:4)	780.6	639.6	6.142	1.158	17	5
Combo	PE(O-18:1/18:2)\ PE(P-18:0/18:2)	728.6	587.5	5.956	0.968	17	5
PE(O)	PE(O-18:1/20:3)	754.6	613.6	6.05	1	17	5
PE(O)	PE(O-18:2/18:2)	726.5	585.5	5.8	0.7	17	5

Compound Group	Compound Name	Precursor Ion	Product Ion	Ret Time (min)	Delta Ret Time	Collision Energy	Cell Accelerator Voltage
Combo	PE(O-18:2/20:3)\ PE(P-18:0/20:4)	752.6	611.5	6.083	1.043	17	5
Combo	PE(O-18:2/22:5)\ PE(P-18:0/22:6)	776.6	635.5	6.057	1.021	17	5
PE(O)	PE(O-34:1)	704.6	563.5	6.1	0.7	17	5
Combo	PE(O-34:2)\PE(P-16:0/18:1)	702.5	561.5	5.94	1.071	17	5
Combo	PE(O-36:5)\PE(P-16:0/20:4)	724.5	583.5	5.737	0.931	17	5
PE(O)	PE(O-36:6)	722.5	581.5	5.5	0.7	17	5
Combo	PE(O-40:6)\PE(P-18:0/22:5)	778.5	637.5	5.9	1.195	17	5
PE(P)	PE(P-16:0/18:1) FA	702.5	339.3	6	0.7	17	5
PE(P)	PE(P-16:0/18:1) head group	702.5	364.3	6	0.7	17	5
PE(P)	PE(P-16:0/18:2)	700.5	559.5	5.8	0.7	17	5
PE(P)	PE(P-16:0/18:2) FA	700.5	337.3	5.8	0.7	17	5
PE(P)	PE(P-16:0/18:2) head group	700.5	364.3	5.8	0.7	17	5
PE(P)	PE(P-16:0/20:4) FA	724.5	361.3	5.76	0.7	17	5
PE(P)	PE(P-16:0/20:4) head group	724.5	364.3	5.76	0.7	17	5
PE(P)	PE(P-16:0/22:5)	750.5	609.6	5.8	1	17	5
PE(P)	PE(P-16:0/22:5) FA	750.5	387.3	5.8	0.7	17	5
PE(P)	PE(P-16:0/22:5) head group	750.5	364.3	5.8	0.7	17	5
PE(P)	PE(P-16:0/22:6)	748.5	607.5	5.7	0.7	17	5
PE(P)	PE(P-16:0/22:6) FA	748.5	385.3	5.7	0.7	17	5
PE(P)	PE(P-16:0/22:6) head group	748.5	364.3	5.7	0.7	17	5
PE(P)	PE(P-18:0/18:1) FA	730.5	339.3	6.41	0.7	17	5
PE(P)	PE(P-18:0/18:1) head group	730.5	392.3	6.41	0.7	17	5
PE(P)	PE(P-18:0/18:2) FA	728.6	337.3	6.17	0.7	17	5
PE(P)	PE(P-18:0/18:2) head group	728.6	392.3	6.17	0.7	17	5
PE(P)	PE(P-18:0/20:4) FA	752.6	361.3	6.15	0.7	17	5
PE(P)	PE(P-18:0/20:4) head group	752.6	392.3	6.15	0.7	17	5
PE(P)	PE(P-18:0/22:5) FA	778.5	387.3	6.15	0.7	17	5
PE(P)	PE(P-18:0/22:5) head group	778.5	392.3	6.15	0.7	17	5
PE(P)	PE(P-18:0/22:6) FA	776.6	385.3	6.05	0.7	17	5
PE(P)	PE(P-18:0/22:6) head group	776.6	392.3	6.05	0.7	17	5
PE(P)	PE(P-20:0/20:4) FA	780.6	361.3	6.48	0.7	17	5
PE(P)	PE(P-20:0/20:4) head group	780.6	420.3	6.48	0.7	17	5
PG	PG 14:0 14:0 (IS)	684.6	495.5	4.58	0.7	21	5
PG	PG 16:0 18:1	766.6	577.5	5.35	0.7	21	5
PG	PG 17:0 17:0	768.6	579.5	5.65	0.7	21	5
PG	PG 18:0 18:1	794.6	605.6	5.485	0.7	21	5
PG	PG 18:1 18:1	792.6	603.5	5.395	0.7	21	5
LPI	PI (18:0/0:0)	618.3	341.3	2.7	0.8	17	5
LPI	PI (18:1/0:0)	616.3	339.3	2.4	0.8	17	5
LPI	PI (18:2/0:0)	614.3	337.3	1.995	0.98	17	5
LPI	PI (20:4/0:0)	638.3	361.3	2.026	1	17	5
PI	PI 12:0 13:0 (IS)	730.3	453.2	3.9	0.7	20	5
PI	PI 32:0	828.6	551.6	5.07	0.7	17	5
PI	PI 32:1	826.5	549.5	4.9	0.7	17	5
PI	PI 34:0	856.6	579.6	5.3	0.7	17	5
PI	PI 34:1	854.6	577.6	5.3	1	17	5
PI	PI 34:2	852.6	575.6	4.98	1	17	5
PI	PI 36:1	882.6	605.6	5.43	0.7	17	5
PI	PI 36:2	880.6	603.6	5.4	1	17	5
PI	PI 36:3	878.6	601.6	4.95	1	17	5
PI	PI 36:4	876.6	599.6	4.9	0.7	17	5
PI	PI 38:2	908.6	631.6	5.4	1	17	5
PI	PI 38:3	906.6	629.6	5.42	0.7	17	5
PI	PI 38:4	904.6	627.6	5.3	0.7	17	5
PI	PI 38:5	902.6	625.6	5.02	1	17	5
PI	PI 38:6	900.6	623.6	4.89	0.7	17	5
PI	PI 40:4	932.6	655.6	5.5	0.7	17	5
PI	PI 40:5	930.6	653.6	5.4	0.7	17	5
PI	PI 40:6	928.6	651.6	5.15	0.7	17	5

Compound Group	Compound Name	Precursor Ion	Product Ion	Ret Time (min)	Delta Ret Time	Collision Energy	Cell Accelerator Voltage
PS	PS 14:0 14:0 (IS)	680.5	495.5	4.42	1.2	25	5
PS	PS 17:0 17:0	764.5	579.5	5.5	1	25	5
PS	PS 34:1	762.6	577.6	5.23	1	25	5
PS	PS 34:2	760.6	575.6	5.02	1	25	5
PS	PS 36:1	790.6	605.6	5.512	1	25	5
PS	PS 36:2	788.5	603.5	5.292	1	25	5
PS	PS 38:3	814.6	629.6	5.342	1	25	5
PS	PS 38:4	812.5	627.5	5.342	1	25	5
PS	PS 38:5	810.5	625.5	5.092	1	25	5
PS	PS 40:5	838.6	653.6	5.342	1	25	5
PS	PS 40:6	836.5	651.5	5.292	1	25	5
SM	SM 30:1 (IS)	647.5	184.1	4.35	0.7	25	5
SM	SM 31:1	661.5	184.1	4.55	0.7	25	5
SM	SM 32:0	677.6	184.1	4.89	0.7	25	5
SM	SM 32:1	675.5	184.1	4.8	0.7	25	5
SM	SM 32:2	673.5	184.1	4.47	0.7	25	5
SM	SM 33:1	689.6	184.1	5.02	0.7	25	5
SM	SM 34:0	705.6	184.1	5.22	0.7	25	5
SM	SM 34:1	703.6	184.1	5.17	0.7	25	5
SM	SM 34:2	701.6	184.1	4.88	0.7	25	5
SM	SM 34:3	699.5	184.1	4.747	1	25	5
SM	SM 35:1	717.6	184.1	5.39	0.7	25	5
SM	SM 35:2	715.6	184.1	5.05	0.7	25	5
SM	SM 36:1	731.6	184.1	5.5	0.7	25	5
SM	SM 36:2	729.6	184.1	5.14	0.7	25	5
SM	SM 36:3	727.6	184.1	5.05	0.7	25	5
SM	SM 37:2	743.5	184.1	5.57	0.7	25	5
SM	SM 38:1	759.6	184.1	5.97	0.7	25	5
SM	SM 38:2	757.6	184.1	5.63	0.7	25	5
SM	SM 39:1	773.7	184.1	6.15	0.7	25	5
SM	SM 41:1	801.7	184.1	6.45	0.7	25	5
SM	SM 41:2	799.7	184.1	6.19	0.7	25	5
SM	SM 42:1	816.7	184.1	6.55	1	25	5
SM	SM d18:1/C12:0 (IS)	647.5123	184.1	4.35	1	25	5
Sph	Sphd16:1	272.24	254.2	1.9	1	5	5
Sph	Sphd16:1	272.24	236.1	1.9	1	15	5
Sph	Sphd18:0	302.32	284.2	2.82	1	10	5
Sph	Sphd18:0	302.32	266.2	2.82	1	15	5
Sph	Sphd18:0	302.32	254.2	2.82	1	20	5
Sph	Sphd18:0	302.32	60.2	2.82	1	17	5
Sph	Sphd18:0-D7	309.32	291.3	2.82	1	10	5
Sph	Sphd18:0-D7	309.32	273.2	2.82	1	15	5
Sph	Sphd18:0-D7	309.32	261.2	2.82	1	20	5
Sph	Sphd18:0-D7	309.32	60.2	2.82	1	17	5
Sph	Sphd18:1	300.3	282.2	2.7	1	5	5
Sph	Sphd18:1	300.3	264.2	2.7	1	15	5
Sph	Sphd18:1	300.3	252.2	2.7	1	15	5
Sph	Sphd18:1-D7	307.32	289.3	2.7	1	5	5
Sph	Sphd18:1-D7	307.32	271.2	2.7	1	15	5
Sph	Sphd18:1-D7	307.32	259.2	2.7	1	15	5
Sph	Sphd18:2	298.25	280.2	2	1	5	5
Sph	Sphd18:2	298.25	262.2	2	1	15	5
Sph	Sphd18:2	298.25	250.2	2	1	10	5
TG	TG 14:0 16:0 18:2	820.8	547.5	7.868	0.7	21	5
TG	TG 14:0 16:1 18:1	820.8	521.5	7.854	0.7	21	5
TG	TG 14:0 16:1 18:2	818.8	521.5	7.754	0.7	21	5
TG	TG 14:0 18:0 18:1	850.8	605.6	8.02	0.7	21	5
TG	TG 14:0 18:2 18:2	844.8	599.5	7.772	0.7	21	5
TG	TG 14:1 16:0 18:1	820.8	577.6	7.868	0.7	21	5
TG	TG 14:1 16:1 18:0	820.8	549.5	7.854	0.7	21	5

Compound Group	Compound Name	Precursor Ion	Product Ion	Ret Time (min)	Delta Ret Time	Collision Energy	Cell Accelerator Voltage
TG	TG 14:1 18:0 18:2	846.8	603.6	7.873	0.7	21	5
TG	TG 14:1 18:1 18:1	846.8	547.5	7.866	0.7	21	5
TG	TG 15:0 18:1 16:0	836.8	577.5	8.1	0.8	21	5
TG	TG 15:0 18:1 18:1	862.8	603.6	8.1	0.7	21	5
TG	TG 16:0 16:0 16:0	824.8	551.5	8.081	0.7	21	5
TG	TG 16:0 16:0 18:0	852.8	551.5	8.185	0.7	21	5
TG	TG 16:0 16:0 18:1	850.8	551.5	8.078	0.7	21	5
TG	TG 16:0 16:0 18:2	848.8	551.5	7.986	0.7	21	5
TG	TG 16:0 16:1 18:1	848.8	549.5	7.97	0.7	21	5
TG	TG 16:0 18:0 18:1	878.8	577.5	8.182	0.7	21	5
TG	TG 16:0 18:1 18:1	876.8	603.6	8.16	0.7	21	5
TG	TG 16:0 18:1 18:2	874.8	577.6	7.983	0.7	21	5
TG	TG 16:0 18:2 18:2	872.8	599.6	7.893	0.7	21	5
TG	TG 16:1 16:1 16:1	818.8	547.5	7.754	0.7	21	5
TG	TG 16:1 16:1 18:0	848.8	547.5	7.986	0.7	21	5
TG	TG 16:1 16:1 18:1	846.8	575.6	7.873	0.7	21	5
TG	TG 16:1 18:1 18:1	874.8	603.6	7.983	0.7	21	5
TG	TG 16:1 18:1 18:2	872.8	573.6	7.893	0.7	21	5
TG	TG 17:0 16:0 16:1	836.8	563.5	8.26	1	21	5
TG	TG 17:0 16:0 18:0	866.8	593.6	8.3	1	21	5
TG	TG 17:0 17:0 17:0	866.8	579.5	8.25	0.7	21	5
TG	TG 17:0 18:1 14:0	836.8	537.5	8.22	1	21	5
TG	TG 17:0 18:1 16:0	864.8	565.5	8.18	1	21	5
TG	TG 17:0 18:1 16:1	862.8	563.5	8.13	0.8	21	5
TG	TG 17:0 18:1 18:1	890.8	603.6	8.2	0.7	21	5
TG	TG 17:0 18:2 16:0	862.8	589.6	8.12	0.7	21	5
TG	TG 18:0 18:0 18:0	908.9	607.6	8.45	0.7	21	5
TG	TG 18:0 18:0 18:1	906.9	607.6	8.362	0.7	21	5
TG	TG 18:0 18:1 18:1	904.9	603.6	8.179	0.7	21	5
TG	TG 18:0 18:2 18:2	900.8	599.5	8.011	0.7	21	5
TG	TG 18:1 14:0 16:0	822.8	523.5	7.9655	0.7	21	5
TG	TG 18:1 18:1 18:1	902.9	603.6	8.18	0.7	21	5
TG	TG 18:1 18:1 18:2	900.9	603.9	8.06	0.7	21	5
TG	TG 18:1 18:1 20:4	924.9	603.6	8.01	0.7	21	5
TG	TG 18:1 18:1 22:6	948.9	603.7	7.903	0.7	21	5
TG	TG 18:1 18:2 18:2	898.9	599.6	7.905	0.7	21	5
TG	TG 18:2 18:2 18:2	896.9	599.6	7.804	0.7	21	5
TG	TG 18:2 18:2 20:4	920.9	599.6	7.76	0.7	21	5
TG	TG 48:0	824.8	824.8	8.081	0.7	5	5
TG	TG 48:1	822.8	822.8	7.973	0.7	5	5
TG	TG 48:2	820.7	820.7	7.854	0.7	5	5
TG	TG 48:3	818.7	818.7	7.754	0.7	5	5
TG	TG 49:1	836.8	836.8	8.1	0.8	5	5
TG	TG 50:0	852.8	852.8	8.185	0.7	5	5
TG	TG 50:1	850.8	850.8	8.078	0.7	5	5
TG	TG 50:2	848.8	848.8	7.97	0.7	5	5
TG	TG 50:3	846.8	846.8	7.866	0.7	5	5
TG	TG 50:4	844.7	844.7	7.78	0.7	5	5
TG	TG 51:0	866.8	866.8	8.4	0.7	5	5
TG	TG 51:1	864.8	864.8	8.18	0.7	5	5
TG	TG 51:2	862.8	862.8	8.1	0.7	5	5
TG	TG 52:1	878.8	878.8	8.17	0.8	5	5
TG	TG 52:2	876.8	876.8	8.074	0.7	5	5
TG	TG 52:3	874.8	874.8	7.983	0.7	5	5
TG	TG 52:4	872.8	872.8	7.893	0.7	5	5
TG	TG 53:2	890.8	890.8	8.15	0.7	5	5
TG	TG 54:0	908.9	908.9	8.25	1	5	5
TG	TG 54:1	906.8	906.8	8.28	1.1	5	5
TG	TG 54:2	904.9	904.8	8.16	0.8	5	5
TG	TG 54:3	902.8	902.8	8.088	0.7	5	5

Compound Group	Compound Name	Precursor Ion	Product Ion	Ret Time (min)	Delta Ret Time	Collision Energy	Cell Accelerator Voltage
TG	TG 54:4	900.8	900.8	7.996	0.7	5	5
TG	TG 54:5	898.8	898.8	7.913	0.7	5	5
TG	TG 54:6	896.8	896.8	7.847	0.7	5	5
TG	TG 56:6	924.8	924.8	7.9485	0.7	5	5
TG	TG 56:8	920.9	920.9	7.767	0.7	5	5
TG	TG 58:8	948.9	948.9	7.881	0.7	5	5
THC	THC 16:0	1024.7	264.3	5.2	0.7	57	5
THC	THC 18:0	1052.7	264.3	5.6	0.7	57	5
THC	THC 18:0 d3 (IS)	1055.7	264.3	5.6	0.7	57	5
THC	THC 20:0	1080.7	264.3	5.955	0.7	57	5
THC	THC 22:0	1108.8	264.3	6.25	0.7	57	5
THC	THC 24:0	1136.8	264.3	6.6	0.7	57	5
THC	THC 24:1	1134.8	264.3	6.3	0.7	57	5
ModCer	Acyl Cer 17:0 18:1	816.8	264.3	7.558	0.7	53	5

Table 5.10: MRM list of panel 2 including compound group, compound name, precursor ion and product ion (in unit respectively), retention time, collision energy and cell accelerator voltage settings

Compound Group	Compound Name	Precursor Ion	Product Ion	Ret Time (min)	Delta Ret Time	Collision Energy	Cell Accelerator Voltage
Cer d16:1	Cer d16:1/C16:0	510.5	236.2	4.392	1	17	5
Cer d16:1	Cer d16:1/C16:0(-H20)	492.5	236.2	4.392	1	17	5
Cer d16:1	Cer d16:1/C18:0	538.5	236.2	4.779	1	17	5
Cer d16:1	Cer d16:1/C18:0(-H20)	520.5	236.2	4.779	1	17	5
Cer d16:1	Cer d16:1/C20:0	566.5	236.2	5.12	0.88	17	5
Cer d16:1	Cer d16:1/C20:0(-H20)	548.5	236.2	5.12	0.88	17	5
Cer d16:1	Cer d16:1/C22:0	594.5	236.2	5.462	0.97	17	5
Cer d16:1	Cer d16:1/C22:0(-H20)	576.5	236.2	5.462	0.97	17	5
Cer d16:1	Cer d16:1/C22:1	592.5	236.2	5.12	0.97	17	5
Cer d16:1	Cer d16:1/C22:1(-H20)	574.5	236.2	5.12	0.97	17	5
Cer d16:1	Cer d16:1/C23:0	608.6	236.2	5.616	0.9	17	5
Cer d16:1	Cer d16:1/C23:0(-H20)	590.6	236.2	5.616	0.9	17	5
Cer d16:1	Cer d16:1/C24:0	622.6	236.2	5.76	0.9	17	5
Cer d16:1	Cer d16:1/C24:0(-H20)	604.6	236.2	5.76	0.9	17	5
Cer d16:1	Cer d16:1/C24:1	620.6	236.2	5.449	0.97	17	5
Cer d16:1	Cer d16:1/C24:1(-H20)	602.6	236.2	5.449	0.97	17	5
Cer d16:1	Cer d16:1/C25:1	634.6	236.2	5.65	0.68	17	5
Cer d16:1	Cer d16:1/C25:1(-H20)	616.6	236.2	5.65	0.68	17	5
Cer d16:1	Cer d16:1/C26:0	650.6	236.2	6.018	0.7	17	5
Cer d16:1	Cer d16:1/C26:0(-H20)	632.6	236.2	6.018	0.7	17	5
Cer d16:1	Cer d16:1/C26:1	648.6	236.2	5.801	0.91	17	5
Cer d16:1	Cer d16:1/C26:1(-H20)	630.6	236.2	5.801	0.91	17	5
Cer d18:0	Cer d18:0/C16:0	540.5	266.2	4.892	1	17	5
Cer d18:0	Cer d18:0/C16:0(-H20)	522.5	266.2	4.892	1	17	5
Cer d18:0	Cer d18:0/C18:0	568.5	266.2	5.1	1	17	5
Cer d18:0	Cer d18:0/C18:0(-H20)	550.5	266.2	5.1	1	17	5
Cer d18:0	Cer d18:0/C20:0	596.5	266.2	5.63	0.64	17	5
Cer d18:0	Cer d18:0/C20:0(-H20)	578.5	266.2	5.63	0.64	17	5
Cer d18:0	Cer d18:0/C22:0	624.6	266.2	5.83	0.67	17	5
Cer d18:0	Cer d18:0/C22:0(-H20)	606.6	266.2	5.83	0.67	17	5
Cer d18:0	Cer d18:0/C22:1	622.5	266.2	5.65	0.67	17	5
Cer d18:0	Cer d18:0/C22:1(-H20)	604.5	266.2	5.65	0.67	17	5
Cer d18:0	Cer d18:0/C23:0	638.6	266.2	5.95	0.9	17	5
Cer d18:0	Cer d18:0/C23:0(-H20)	620.6	266.2	5.95	0.9	17	5
Cer d18:0	Cer d18:0/C23:1	636.6	266.2	5.99	0.8	17	5
Cer d18:0	Cer d18:0/C23:1(-H20)	618.6	266.2	5.99	0.8	17	5
Cer d18:0	Cer d18:0/C24:0	652.6	266.2	6.17	1.03	17	5
Cer d18:0	Cer d18:0/C24:0(-H20)	634.6	266.2	6.17	1.03	17	5

Compound Group	Compound Name	Precursor Ion	Product Ion	Ret Time (min)	Delta Ret Time	Collision Energy	Cell Accelerator Voltage
Cer d18:0	Cer d18:0/C24:1	650.6	266.2	5.91	0.9	17	5
Cer d18:0	Cer d18:0/C24:1(-H20)	632.6	266.2	5.91	0.9	17	5
Cer d18:0	Cer d18:0/C25:0	666.6	266.2	6.29	1.02	17	5
Cer d18:0	Cer d18:0/C25:0(-H20)	648.6	266.2	6.29	1.02	17	5
Cer d18:0	Cer d18:0/C25:1	664.6	266.2	6	1.04	17	5
Cer d18:0	Cer d18:0/C25:1(-H20)	646.6	266.2	6	1.04	17	5
Cer d18:0	Cer d18:0/C26:0	680.6	266.2	6.45	0.7	17	5
Cer d18:0	Cer d18:0/C26:0(-H20)	662.6	266.2	6.45	0.7	17	5
Cer d18:0	Cer d18:0/C26:1	678.6	266.2	6.21	0.7	17	5
Cer d18:0	Cer d18:0/C26:1(-H20)	660.6	266.2	6.21	0.7	17	5
Cer d18:1	Cer d18:1/C14:0	510.5	264.2	4.46	1	17	5
Cer d18:1	Cer d18:1/C14:0(-H20)	492.5	264.2	4.46	1	17	5
Cer d18:1	Cer d18:1/C14:1	508.5	264.2	4.2	1	17	5
Cer d18:1	Cer d18:1/C14:1(-H20)	490.5	264.2	4.2	1	17	5
Cer d18:1	Cer d18:1/C16:0	538.5	264.2	4.756	0.85	17	5
Cer d18:1	Cer d18:1/C16:0(-H20)	520.5	264.2	4.756	0.85	17	5
Cer d18:1	Cer d18:1/C16:1	536.5	264.2	4.591	0.85	17	5
Cer d18:1	Cer d18:1/C16:1(-H20)	518.5	264.2	4.591	0.85	17	5
Cer d18:1	Cer d18:1/C17:0 (ISTD)	552.3	264.3	4.9	1	37	5
Cer d18:1	Cer d18:1/C17:0(-H20) (ISTD)	534.3	264.3	4.9	1	37	5
Cer d18:1	Cer d18:1/C18:0	566.5	264.2	5.12	1.03	17	5
Cer d18:1	Cer d18:1/C18:0(-H20)	548.5	264.2	5.12	1.03	17	5
Cer d18:1	Cer d18:1/C18:1	564.5	264.2	4.9	1.03	17	5
Cer d18:1	Cer d18:1/C18:1(-H20)	546.5	264.2	4.9	1.03	17	5
Cer d18:1	Cer d18:1/C20:0	594.5	264.2	5.437	0.97	17	5
Cer d18:1	Cer d18:1/C20:0(-H20)	576.5	264.2	5.437	0.97	17	5
Cer d18:1	Cer d18:1/C20:1	592.5	264.2	5.26	0.97	17	5
Cer d18:1	Cer d18:1/C20:1(-H20)	574.5	264.2	5.26	0.97	17	5
Cer d18:1	Cer d18:1/C22:0	622.6	264.2	5.738	0.9	17	5
Cer d18:1	Cer d18:1/C22:0(-H20)	604.6	264.2	5.738	0.9	17	5
Cer d18:1	Cer d18:1/C22:1	620.6	264.2	5.57	1.01	17	5
Cer d18:1	Cer d18:1/C22:1(-H20)	602.6	264.2	5.57	1.01	17	5
Cer d18:1	Cer d18:1/C23:0	636.6	264.2	5.88	1.03	17	5
Cer d18:1	Cer d18:1/C23:0(-H20)	618.6	264.2	5.88	1.03	17	5
Cer d18:1	Cer d18:1/C23:1	634.6	264.2	5.67	0.96	17	5
Cer d18:1	Cer d18:1/C23:1(-H20)	616.6	264.2	5.67	0.96	17	5
Cer d18:1	Cer d18:1/C24:0	650.6	264.2	6	0.9	17	5
Cer d18:1	Cer d18:1/C24:0(-H20)	632.6	264.2	6	0.9	17	5
Cer d18:1	Cer d18:1/C24:1	648.6	264.2	5.73	0.9	17	5
Cer d18:1	Cer d18:1/C24:1(-H20)	630.6	264.2	5.73	0.9	17	5
Cer d18:1	Cer d18:1/C25:0	664.6	264.2	6.12	0.9	17	5
Cer d18:1	Cer d18:1/C25:0(-H20)	646.6	264.2	6.12	0.9	17	5
Cer d18:1	Cer d18:1/C25:1	662.6	264.2	5.95	0.9	17	5
Cer d18:1	Cer d18:1/C25:1(-H20)	644.6	264.2	5.95	0.9	17	5
Cer d18:1	Cer d18:1/C26:0	678.6	264.2	6.24	0.9	17	5
Cer d18:1	Cer d18:1/C26:0(-H20)	660.6	264.2	6.24	0.9	17	5
Cer d18:1	Cer d18:1/C26:1	676.6	264.2	6	0.91	17	5
Cer d18:1	Cer d18:1/C26:1(-H20)	658.6	264.2	6	0.91	17	5
Cer d18:1	Cer d18:1/C8:0	426.4	264.2	3.257	0.72	17	5
Cer d18:1	Cer d18:1/C8:0(-H20)	408.4	264.2	3.257	0.72	17	5
Cer d18:2	Cer d18:2/C14:0	508.5	262.2	4	1	17	5
Cer d18:2	Cer d18:2/C14:0(-H20)	490.5	262.2	4	1	17	5
Cer d18:2	Cer d18:2/C16:0	536.5	262.2	4.45	0.68	17	5
Cer d18:2	Cer d18:2/C16:0(-H20)	518.5	262.2	4.45	0.68	17	5
Cer d18:2	Cer d18:2/C18:0	564.5	262.2	4.858	0.58	17	5
Cer d18:2	Cer d18:2/C18:0(-H20)	546.5	262.2	4.858	0.58	17	5
Cer d18:2	Cer d18:2/C18:1	562.5	262.2	4.6	1	17	5
Cer d18:2	Cer d18:2/C18:1(-H20)	544.5	262.2	4.6	1	17	5
Cer d18:2	Cer d18:2/C20:0	592.5	262.2	5.25	0.91	17	5
Cer d18:2	Cer d18:2/C20:0(-H20)	574.5	262.2	5.25	0.91	17	5

Compound Group	Compound Name	Precursor Ion	Product Ion	Ret Time (min)	Delta Ret Time	Collision Energy	Cell Accelerator Voltage
Cer d18:2	Cer d18:2/C20:1	590.5	262.2	5.05	0.91	17	5
Cer d18:2	Cer d18:2/C20:1(-H20)	572.5	262.2	5.05	0.91	17	5
Cer d18:2	Cer d18:2/C22:0	620.6	262.2	5.497	0.9	17	5
Cer d18:2	Cer d18:2/C22:0(-H20)	602.6	262.2	5.497	0.9	17	5
Cer d18:2	Cer d18:2/C22:1	618.6	262.2	5.25	0.9	17	5
Cer d18:2	Cer d18:2/C22:1(-H20)	600.6	262.2	5.25	0.9	17	5
Cer d18:2	Cer d18:2/C23:0	634.6	262.2	5.656	0.9	17	5
Cer d18:2	Cer d18:2/C23:0(-H20)	616.6	262.2	5.656	0.9	17	5
Cer d18:2	Cer d18:2/C23:1	632.6	262.2	5.4	0.9	17	5
Cer d18:2	Cer d18:2/C23:1(-H20)	614.6	262.2	5.4	0.9	17	5
Cer d18:2	Cer d18:2/C24:0	648.6	262.2	5.81	1.08	17	5
Cer d18:2	Cer d18:2/C24:0(-H20)	630.6	262.2	5.81	1.08	17	5
Cer d18:2	Cer d18:2/C24:1	646.6	262.2	5.6	1.03	17	5
Cer d18:2	Cer d18:2/C24:1(-H20)	628.6	262.2	5.6	1.03	17	5
Cer d18:2	Cer d18:2/C25:0	662.6	262.2	5.92	0.94	17	5
Cer d18:2	Cer d18:2/C25:0(-H20)	644.6	262.2	5.92	0.94	17	5
Cer d18:2	Cer d18:2/C25:1	660.6	262.2	5.6	0.74	17	5
Cer d18:2	Cer d18:2/C25:1(-H20)	642.6	262.2	5.6	0.74	17	5
Cer d18:2	Cer d18:2/C26:0	676.6	262.2	6	0.7	17	5
Cer d18:2	Cer d18:2/C26:0(-H20)	658.6	262.2	6	0.7	17	5
Cer d18:2	Cer d18:2/C26:1	674.6	262.2	5.75	0.8	17	5
Cer d18:2	Cer d18:2/C26:1(-H20)	656.6	262.2	5.75	0.8	17	5
DHCer	DHCer 16:0d3 (ISTD)	856.6	264.3	4.1	1	45	5
DHCer	DHCer 16:0d3(-H20) (ISTD)	847.6	264.3	4.1	1	45	5
DHCer	DHCer 8:0	428.4	284.3	3.359	1	45	5
DHCer	DHCer 8:0(-H2O)	410.4	284.3	3.359	1	45	5
DHCer d16:1	DHCer d16:1/C16:0	834.7	236.2	3.793	0.84	45	5
DHCer d16:1	DHCer d16:1/C16:0(-H20)	816.7	236.2	3.793	0.84	45	5
DHCer d18:1	DHCer d18:1/C14:0	834.7	264.2	3.781	0.55	45	5
DHCer d18:1	DHCer d18:1/C14:0(-H20)	816.7	264.2	3.781	0.55	45	5
DHCer d18:1	DHCer d18:1/C16:0	862.7	264.2	4.169	0.76	45	5
DHCer d18:1	DHCer d18:1/C16:0(-H20)	844.7	264.2	4.169	0.76	45	5
DHCer d18:1	DHCer d18:1/C18:0	890.7	264.2	4.52	0.55	45	5
DHCer d18:1	DHCer d18:1/C18:0(-H20)	872.7	264.2	4.52	0.55	45	5
DHCer d18:1	DHCer d18:1/C20:0	918.7	264.2	4.852	0.59	45	5
DHCer d18:1	DHCer d18:1/C20:0(-H20)	900.7	264.2	4.852	0.59	45	5
DHCer d18:1	DHCer d18:1/C22:0	946.7	264.2	5.195	0.73	45	5
DHCer d18:1	DHCer d18:1/C22:0(-H20)	928.7	264.2	5.195	0.73	45	5
DHCer d18:1	DHCer d18:1/C22:1	944.7	264.2	4.9	0.73	45	5
DHCer d18:1	DHCer d18:1/C22:1(-H20)	926.7	264.2	4.9	0.73	45	5
DHCer d18:1	DHCer d18:1/C23:0	960.7	264.2	5.335	0.63	45	5
DHCer d18:1	DHCer d18:1/C23:0(-H20)	942.7	264.2	5.335	0.63	45	5
DHCer d18:1	DHCer d18:1/C24:0	974.7	264.2	5.465	0.8	45	5
DHCer d18:1	DHCer d18:1/C24:0(-H20)	956.7	264.2	5.465	0.8	45	5
DHCer d18:1	DHCer d18:1/C24:1	972.7	264.2	5.183	0.91	45	5
DHCer d18:1	DHCer d18:1/C24:1(-H20)	954.7	264.2	5.183	0.91	45	5
DHCer d18:2	DHCer d18:2/C16:0	860.7	262.2	3.855	0.91	45	5
DHCer d18:2	DHCer d18:2/C16:0(-H20)	842.7	262.2	3.855	0.91	45	5
DHCer d18:2	DHCer d18:2/C18:1	886.7	262.2	4	1	45	5
DHCer d18:2	DHCer d18:2/C18:1(-H20)	868.7	262.2	4	1	45	5
DHCer d18:2	DHCer d18:2/C22:0	944.7	262.2	4.93	1	45	5
DHCer d18:2	DHCer d18:2/C22:0(-H20)	926.7	262.2	4.93	1	45	5
DHCer d18:2	DHCer d18:2/C24:0	972.7	262.2	5.241	0.8	45	5
DHCer d18:2	DHCer d18:2/C24:0(-H20)	954.7	262.2	5.241	0.8	45	5
DHCer d18:2	DHCer d18:2/C24:1	970.7	262.2	4.931	0.8	45	5
DHCer d18:2	DHCer d18:2/C24:1(-H20)	952.7	262.2	4.931	0.8	45	5
GM3 d16:1	GM3 d16:1/C14:0	1097.7	236.2	2.978	0.51	55	5
GM3 d16:1	GM3 d16:1/C14:0	1095.7	290.2	2.978	0.51	55	5
GM3 d16:1	GM3 d16:1/C16:0	1125.7	236.2	3.29	0.51	55	5
GM3 d16:1	GM3 d16:1/C16:0	1123.7	290.2	3.29	0.51	55	5

Compound Group	Compound Name	Precursor Ion	Product Ion	Ret Time (min)	Delta Ret Time	Collision Energy	Cell Accelerator Voltage
GM3 d16:1	GM3 d16:1/C18:0	1153.7	236.2	3.64	0.78	55	5
GM3 d16:1	GM3 d16:1/C18:0	1151.7	290.2	3.64	0.78	55	5
GM3 d16:1	GM3 d16:1/C20:0	1181.8	236.2	3.98	0.59	55	5
GM3 d16:1	GM3 d16:1/C20:0	1179.8	290.2	3.98	0.59	55	5
GM3 d16:1	GM3 d16:1/C22:0	1209.8	236.2	4.318	0.59	55	5
GM3 d16:1	GM3 d16:1/C22:0	1207.8	290.2	4.318	0.59	55	5
GM3 d16:1	GM3 d16:1/C24:0	1237.8	236.2	4.638	0.59	55	5
GM3 d16:1	GM3 d16:1/C24:0	1235.8	290.2	4.638	0.59	55	5
GM3 d16:1	GM3 d16:1/C24:1	1235.8	236.2	4.4	0.59	55	5
GM3 d16:1	GM3 d16:1/C24:1	1233.8	290.2	4.4	0.59	55	5
GM3 d18:1	GM3 d18:1/C14:0	1125.7	264.2	3.301	0.7	55	5
GM3 d18:1	GM3 d18:1/C14:0	1123.7	290.2	3.301	0.7	55	5
GM3 d18:1	GM3 d18:1/C16:0	1153.7	264.2	3.604	1.02	55	5
GM3 d18:1	GM3 d18:1/C16:0	1151.7	290.2	3.604	1.02	55	5
GM3 d18:1	GM3 d18:1/C18:0	1181.8	264.2	3.98	0.74	55	5
GM3 d18:1	GM3 d18:1/C18:0	1179.8	290.2	3.98	0.74	55	5
GM3 d18:1	GM3 d18:1/C20:0	1209.8	264.2	4.36	0.74	55	5
GM3 d18:1	GM3 d18:1/C20:0	1207.8	290.2	4.36	0.74	55	5
GM3 d18:1	GM3 d18:1/C22:0	1237.8	264.2	4.638	0.59	55	5
GM3 d18:1	GM3 d18:1/C22:0	1235.8	290.2	4.638	0.59	55	5
GM3 d18:1	GM3 d18:1/C24:0	1265.8	264.2	4.939	1.02	55	5
GM3 d18:1	GM3 d18:1/C24:0	1263.8	290.2	4.939	1.02	55	5
GM3 d18:1	GM3 d18:1/C24:1	1263.8	264.2	4.648	0.86	55	5
GM3 d18:1	GM3 d18:1/C24:1	1261.8	290.2	4.648	0.86	55	5
GM3 d18:2	GM3 d18:2/14:0	1123.7	262.2	3	0.7	55	5
GM3 d18:2	GM3 d18:2/14:0	1121.7	290.2	3	0.7	55	5
GM3 d18:2	GM3 d18:2/16:0	1151.7	262.2	3.382	0.7	55	5
GM3 d18:2	GM3 d18:2/16:0	1149.7	290.2	3.382	0.7	55	5
GM3 d18:2	GM3 d18:2/18:0	1179.8	262.2	3.71	0.82	55	5
GM3 d18:2	GM3 d18:2/18:0	1177.8	290.2	3.71	0.82	55	5
GM3 d18:2	GM3 d18:2/20:0	1207.8	262.2	4.06	0.67	55	5
GM3 d18:2	GM3 d18:2/20:0	1205.8	290.2	4.06	0.67	55	5
GM3 d18:2	GM3 d18:2/22:0	1235.8	262.2	4.395	0.78	55	5
GM3 d18:2	GM3 d18:2/22:0	1233.8	290.2	4.395	0.78	55	5
GM3 d18:2	GM3 d18:2/24:0	1263.8	262.2	4.627	0.98	55	5
GM3 d18:2	GM3 d18:2/24:0	1261.8	290.2	4.627	0.98	55	5
GM3 d18:2	GM3 d18:2/24:1	1261.8	262.2	4.405	0.74	55	5
GM3 d18:2	GM3 d18:2/24:1	1259.8	290.2	4.405	0.74	55	5
MHCer d16:1	MHCer d16:1/C16:0	672.6	236.2	3.988	0.67	30	5
MHCer d16:1	MHCer d16:1/C16:0(-H20)	654.6	236.2	3.988	0.67	30	5
MHCer d16:1	MHCer d16:1/C20:0	728.6	236.2	4.754	0.57	30	5
MHCer d16:1	MHCer d16:1/C20:0(-H20)	710.6	236.2	4.754	0.57	30	5
MHCer d16:1	MHCer d16:1/C22:0	756.6	236.2	5.084	0.67	30	5
MHCer d16:1	MHCer d16:1/C22:0(-H20)	738.6	236.2	5.084	0.67	30	5
MHCer d16:1	MHCer d16:1/C22:1	754.6	236.2	4.98	0.67	30	5
MHCer d16:1	MHCer d16:1/C22:1(-H20)	736.6	236.2	4.98	0.67	30	5
MHCer d16:1	MHCer d16:1/C23:0	770.6	236.2	5.258	0.62	30	5
MHCer d16:1	MHCer d16:1/C23:0(-H20)	752.6	236.2	5.258	0.62	30	5
MHCer d16:1	MHCer d16:1/C23:1	768.6	236.2	5	1	30	5
MHCer d16:1	MHCer d16:1/C23:1(-H20)	750.6	236.2	5	1	30	5
MHCer d16:1	MHCer d16:1/C24:0	784.6	236.2	5.399	0.64	30	5
MHCer d16:1	MHCer d16:1/C24:0(-H20)	766.6	236.2	5.399	0.64	30	5
MHCer d16:1	MHCer d16:1/C24:1	782.6	236.2	5.071	0.68	30	5
MHCer d16:1	MHCer d16:1/C24:1(-H20)	764.6	236.2	5.071	0.68	30	5
MHCer d16:1	MHCer d16:1/C26:0	812.7	236.2	5.6	1	30	5
MHCer d16:1	MHCer d16:1/C26:0(-H20)	794.7	236.2	5.6	1	30	5
MHCer d18:0	MHCer d18:0/C16:0	702.6	266.2	4.4	1	30	5
MHCer d18:0	MHCer d18:0/C16:0(-H20)	684.6	266.2	4.4	1	30	5
MHCer d18:0	MHCer d18:0/C16:1	700.6	266.2	4.645	0.68	30	5
MHCer d18:0	MHCer d18:0/C16:1(-H20)	682.6	266.2	4.645	0.68	30	5

Compound Group	Compound Name	Precursor Ion	Product Ion	Ret Time (min)	Delta Ret Time	Collision Energy	Cell Accelerator Voltage
MHCer d18:0	MHCer d18:0/C22:0	786.6	266.2	5.363	0.63	30	5
MHCer d18:0	MHCer d18:0/C22:0(-H20)	768.6	266.2	5.363	0.63	30	5
MHCer d18:0	MHCer d18:0/C22:1	784.6	266.2	5.269	0.63	30	5
MHCer d18:0	MHCer d18:0/C22:1(-H20)	766.6	266.2	5.269	0.63	30	5
MHCer d18:0	MHCer d18:0/C23:0	800.7	266.2	5.517	0.66	30	5
MHCer d18:0	MHCer d18:0/C23:0(-H20)	782.7	266.2	5.517	0.66	30	5
MHCer d18:0	MHCer d18:0/C24:0	814.7	266.2	5.651	0.66	30	5
MHCer d18:0	MHCer d18:0/C24:0(-H20)	796.7	266.2	5.651	0.66	30	5
MHCer d18:0	MHCer d18:0/C24:1	812.7	266.2	5.372	0.74	30	5
MHCer d18:0	MHCer d18:0/C24:1(-H20)	794.7	266.2	5.372	0.74	30	5
MHCer d18:1	MHCer d18:1/16:0d3 (ISTD)	703.6	264.3	4.28	0.7	37	5
MHCer d18:1	MHCer d18:1/16:0d3(-H20) (ISTD)	685.6	264.3	4.28	0.7	37	5
MHCer d18:1	MHCer d18:1/C14:0	672.6	264.2	3.95	1	30	5
MHCer d18:1	MHCer d18:1/C14:0(-H20)	654.6	264.2	3.95	1	30	5
MHCer d18:1	MHCer d18:1/C16:0	700.6	264.2	4.357	0.96	30	5
MHCer d18:1	MHCer d18:1/C16:0(-H20)	682.6	264.2	4.357	0.96	30	5
MHCer d18:1	MHCer d18:1/C16:1	698.6	264.2	4.237	0.96	30	5
MHCer d18:1	MHCer d18:1/C16:1(-H20)	680.6	264.2	4.237	0.96	30	5
MHCer d18:1	MHCer d18:1/C18:0	728.6	264.2	4.721	0.8	30	5
MHCer d18:1	MHCer d18:1/C18:0(-H20)	710.6	264.2	4.721	0.8	30	5
MHCer d18:1	MHCer d18:1/C18:1	726.6	264.2	4.43	0.8	30	5
MHCer d18:1	MHCer d18:1/C18:1(-H20)	708.6	264.2	4.43	0.8	30	5
MHCer d18:1	MHCer d18:1/C20:0	756.6	264.2	5.061	0.72	30	5
MHCer d18:1	MHCer d18:1/C20:0(-H20)	738.6	264.2	5.061	0.72	30	5
MHCer d18:1	MHCer d18:1/C20:1	754.6	264.2	4.946	0.72	30	5
MHCer d18:1	MHCer d18:1/C20:1(-H20)	736.6	264.2	4.946	0.72	30	5
MHCer d18:1	MHCer d18:1/C22:0	784.6	264.2	5.364	0.9	30	5
MHCer d18:1	MHCer d18:1/C22:0(-H20)	766.6	264.2	5.364	0.9	30	5
MHCer d18:1	MHCer d18:1/C22:1	782.6	264.2	5.28	1.02	30	5
MHCer d18:1	MHCer d18:1/C22:1(-H20)	764.6	264.2	5.28	1.02	30	5
MHCer d18:1	MHCer d18:1/C23:0	798.6	264.2	5.5	0.85	30	5
MHCer d18:1	MHCer d18:1/C23:0(-H20)	780.6	264.2	5.5	0.85	30	5
MHCer d18:1	MHCer d18:1/C23:1	796.6	264.2	5.45	1	30	5
MHCer d18:1	MHCer d18:1/C23:1(-H20)	778.6	264.2	5.45	1	30	5
MHCer d18:1	MHCer d18:1/C24:0	812.7	264.2	5.641	0.9	30	5
MHCer d18:1	MHCer d18:1/C24:0(-H20)	794.7	264.2	5.641	0.9	30	5
MHCer d18:1	MHCer d18:1/C24:1	810.7	264.2	5.361	0.9	30	5
MHCer d18:1	MHCer d18:1/C24:1(-H20)	792.7	264.2	5.361	0.9	30	5
MHCer d18:1	MHCer d18:1/C25:0	826.7	264.2	5.8	1	30	5
MHCer d18:1	MHCer d18:1/C25:0(-H20)	808.7	264.2	5.8	1	30	5
MHCer d18:1	MHCer d18:1/C25:1	824.7	264.2	5.52	0.74	30	5
MHCer d18:1	MHCer d18:1/C25:1(-H20)	806.7	264.2	5.52	0.74	30	5
MHCer d18:1	MHCer d18:1/C26:0	840.7	264.2	5.908	0.69	30	5
MHCer d18:1	MHCer d18:1/C26:0(-H20)	822.7	264.2	5.908	0.69	30	5
MHCer d18:1	MHCer d18:1/C26:1	838.7	264.2	5.65	1	30	5
MHCer d18:1	MHCer d18:1/C26:1(-H20)	820.7	264.2	5.65	1	30	5
MHCer d18:1	MHCer d18:1/C8:0 (ISTD)	588.5	264.2	2.91	1.02	30	5
MHCer d18:1	MHCer d18:1/C8:0 (ISTD) (-H20)	570.5	264.2	2.91	1.02	30	5
MHCer d18:2	MHCer d18:2/C16:0	698.6	262.2	4.04	0.61	30	5
MHCer d18:2	MHCer d18:2/C16:0(-H20)	680.6	262.2	4.04	0.61	30	5
MHCer d18:2	MHCer d18:2/C16:1	696.6	262.2	3.932	1	30	5
MHCer d18:2	MHCer d18:2/C16:1(-H20)	678.6	262.2	3.932	1	30	5
MHCer d18:2	MHCer d18:2/C20:0	754.6	262.2	4.799	0.62	30	5
MHCer d18:2	MHCer d18:2/C20:0(-H20)	736.6	262.2	4.799	0.62	30	5
MHCer d18:2	MHCer d18:2/C22:0	782.6	262.2	5.14	0.8	30	5
MHCer d18:2	MHCer d18:2/C22:0(-H20)	764.6	262.2	5.14	0.8	30	5
MHCer d18:2	MHCer d18:2/C22:1	780.6	262.2	5.036	0.8	30	5
MHCer d18:2	MHCer d18:2/C22:1(-H20)	762.6	262.2	5.036	0.8	30	5
MHCer d18:2	MHCer d18:2/C23:0	796.6	262.2	5.291	0.73	30	5

Compound Group	Compound Name	Precursor Ion	Product Ion	Ret Time (min)	Delta Ret Time	Collision Energy	Cell Accelerator Voltage
MHCer d18:2	MHCer d18:2/C23:0(-H20)	778.6	262.2	5.291	0.73	30	5
MHCer d18:2	MHCer d18:2/C24:0	810.7	262.2	5.44	0.74	30	5
MHCer d18:2	MHCer d18:2/C24:0(-H20)	792.7	262.2	5.44	0.74	30	5
MHCer d18:2	MHCer d18:2/C24:1	808.7	262.2	5.138	0.68	30	5
MHCer d18:2	MHCer d18:2/C24:1(-H20)	790.7	262.2	5.138	0.68	30	5
MHCer d18:2	MHCer d18:2/C25:0	824.7	262.2	5.619	0.68	30	5
MHCer d18:2	MHCer d18:2/C25:0(-H20)	806.7	262.2	5.619	0.68	30	5
SM C24:1	SM C24:1	563.42	184.1	2.443	0.69	25	5
SM C30:1	SM C30:1 (ISTD)	647.6	184.1	3.389	1	25	5
SM C32:1	SM C32:1	675.53	184.1	3.773	1	25	5
SM C32:2	SM C32:2	673.52	184.1	3.46	1	25	5
SM C34:0	SM C34:0	705.58	184.1	4.159	1	25	5
SM C34:1	SM C34:1	703.58	184.1	4.171	1	25	5
SM C34:2	SM C34:2	701.56	184.1	3.857	1	25	5
SM C36:0	SM C36:0	733.58	184.1	4.5	0.8	25	5
SM C36:1	SM C36:1	731.61	184.1	4.52	1	25	5
SM C36:2	SM C36:2	729.59	184.1	4.246	1	25	5
SM C38:0	SM C38:0	761.6	184.1	4.598	1	25	5
SM C38:1	SM C38:1	759.64	184.1	4.88	1	25	5
SM C38:2	SM C38:2	757.61	184.1	4.62	1	25	5
SM C39:1	SM C39:1	773.6	184.1	5.094	1	25	5
SM C40:0	SM C40:0	789.67	184.1	4.9	1	25	5
SM C40:1	SM C40:1	787.67	184.1	5.25	1	25	5
SM C40:2	SM C40:2	785.65	184.1	4.95	1	25	5
SM C41:1	SM C41:1	801.68	184.1	5.397	1	25	5
SM C41:2	SM C41:2	799.67	184.1	5.138	1	25	5
SM C42:0	SM C42:0	817.7	184.1	5.64	1	25	5
SM C42:1	SM C42:1	815.7	184.1	5.5	1	25	5
SM C42:2	SM C42:2	813.68	184.1	5.23	1	25	5
SM C42:3	SM C42:3	811.67	184.1	4.988	1	25	5
SM C43:1	SM C43:1	829.7	184.1	5.6	1	25	5
SM C43:2	SM C43:2	827.7	184.1	5.34	1	25	5
SM C44:1	SM C44:1	843.7	184.1	5.99	1	25	5
SM C32:1	SM d16:1/C16:0	675.53	236.2	3.77	0.8	37	5
SM C34:1	SM d16:1/C18:0	703.58	236.2	4.16	0.8	37	5
SM C36:1	SM d16:1/C20:0	731.61	236.2	4.53	0.8	37	5
SM C38:1	SM d16:1/C22:0	759.64	236.2	4.922	0.8	37	5
SM C39:1	SM d16:1/C23:0	773.6	236.2	5.094	0.8	37	5
SM C40:1	SM d16:1/C24:0	787.67	236.2	5.256	0.8	37	5
SM C40:2	SM d16:1/C24:1	785.65	236.2	4.95	0.8	37	5
SM C34:0	SM d18:0/C16:0	705.58	266.2	4.159	0.8	37	5
SM C36:0	SM d18:0/C18:0	733.58	266.2	4.5	0.8	37	5
SM C38:0	SM d18:0/C20:0	761.6	266.2	4.609	0.8	37	5
SM C40:0	SM d18:0/C22:0	789.67	266.2	4.943	0.8	37	5
SM C42:0	SM d18:0/C24:0	817.7	266.2	5.536	0.8	37	5
SM C30:1	SM d18:1/C12:0	647.6	264.2	3.389	0.8	37	5
SM C32:1	SM d18:1/C14:0	675.53	264.2	3.772	0.8	37	5
SM C34:1	SM d18:1/C16:0	703.58	264.2	4.149	0.8	37	5
SM C36:1	SM d18:1/C18:0	731.61	264.2	4.52	0.8	37	5
SM C38:1	SM d18:1/C20:0	759.64	264.2	4.888	0.8	37	5
SM C40:1	SM d18:1/C22:0	787.67	264.2	5.233	0.8	37	5
SM C40:2	SM d18:1/C22:1	785.65	264.2	4.95	0.8	37	5
SM C41:1	SM d18:1/C23:0	801.68	264.2	5.397	0.8	37	5
SM C41:2	SM d18:1/C23:1	799.67	264.2	5.069	0.8	37	5
SM C42:1	SM d18:1/C24:0	815.7	264.2	5.527	0.8	37	5
SM C42:2	SM d18:1/C24:1	813.68	264.2	5.231	0.8	37	5
SM C43:1	SM d18:1/C25:0	829.7	264.2	5.6	0.8	37	5
SM C43:2	SM d18:1/C25:1	827.7	264.2	5.53	0.8	37	5
SM C44:1	SM d18:1/C26:0	843.7	264.2	5.99	0.8	37	5
SM C24:1	SM d18:1/C6:0	563.42	264.2	2.442	0.69	37	5

Compound Group	Compound Name	Precursor Ion	Product Ion	Ret Time (min)	Delta Ret Time	Collision Energy	Cell Accelerator Voltage
SM C32:2	SM d18:2/C14:0	673.52	262.2	3.459	0.8	37	5
SM C34:2	SM d18:2/C16:0	701.56	262.2	3.857	0.8	37	5
SM C36:2	SM d18:2/C18:0	729.59	262.2	4.246	0.8	37	5
SM C38:2	SM d18:2/C20:0	757.61	262.2	4.62	0.8	37	5
SM C40:2	SM d18:2/C22:0	785.65	262.2	4.989	0.8	37	5
SM C41:2	SM d18:2/C23:0	799.67	262.2	5.15	0.8	37	5
SM C42:2	SM d18:2/C24:0	813.68	262.2	5.301	0.8	37	5
SM C42:3	SM d18:2/C24:1	811.67	262.2	4.988	0.84	37	5
SM C43:2	SM d18:2/C25:0	827.7	262.2	5.5	0.8	37	5

Table 5.11: MRM list of panel 4 including compound group, compound name, precursor ion and product ion (in unit respectively), retention time, collision energy and cell accelerator voltage settings

Compound Group	Compound Name	Precursor Ion	Product Ion	Collision Energy	Cell Accelerator Voltage
S1P	S1P (d24:0)	522.39	60.08	29	3
S1P	S1P (d24:0)	522.39	113	29	3
S1P	S1P (d24:1)	520.39	60.08	29	3
S1P	S1P (d24:1)	520.39	113	29	3
S1P	S1P (d24:2)	518.39	60.08	29	3
S1P	S1P (d24:2)	518.39	113	29	3
S1P	S1P (d22:0)	494.37	60.08	29	3
S1P	S1P (d22:0)	494.37	113	29	3
S1P	S1P (d22:1)	492.36	60.08	29	3
S1P	S1P (d22:1)	492.36	113	29	3
S1P	S1P (22:2)	490.36	60.08	29	3
S1P	S1P (22:2)	490.36	113	29	3
S1P	S1P (t20:0)	482.35	60.08	29	3
S1P	S1P (t20:0)	482.35	113	29	3
S1P	S1P (d21:0)	480.35	60.08	29	3
S1P	S1P (d21:0)	480.35	113	29	3
S1P	S1P (d21:1)	478.35	60.08	29	3
S1P	S1P (d21:1)	478.35	113	29	3
S1P	S1P (d20:0)	466.35	60.08	29	3
S1P	S1P (d20:0)	466.35	113	29	3
S1P	S1P (d20:1)	464.35	60.08	29	3
S1P	S1P (d20:1)	464.35	113	29	3
S1P	S1P (d20:2)	462.35	60.08	29	3
S1P	S1P (d20:2)	462.35	113	29	3
S1P	S1P (t18:0)	454.35	60.08	29	3
S1P	S1P (t18:0)	454.35	113	29	3
S1P	S1P (d19:0)	452.35	60.08	29	3
S1P	S1P (d19:0)	452.35	113	29	3
S1P	S1P (d19:1)	450.35	60.08	29	3
S1P	S1P (d19:1)	450.35	113	29	3
S1P	S1P (d19:2)	448.35	60.08	29	3
S1P	S1P (d19:2)	448.35	113	29	3
S1P ISTD	13C2D2_S1P	440.33	60.08	29	3
S1P ISTD	13C2D2_S1P	440.33	113	29	3
S1P	S1P (d18:0)	438.34	60.08	29	3
S1P	S1P (d18:0)	438.34	113	29	3
S1P	S1P (d18:1)	436.31	60.08	29	3
S1P	S1P (d18:1)	436.31	113	29	3
S1P	S1P (d18:2)	434.29	60.08	29	3
S1P	S1P (d18:2)	434.29	113	29	3
S1P	S1P (t16:0)	426.3	60.08	29	3
S1P	S1P (t16:0)	426.3	113	29	3
S1P	S1P (d17:0)	424.3	60.08	29	3

Compound Group	Compound Name	Precursor Ion	Product Ion	Collision Energy	Cell Accelerator Voltage
S1P	S1P (d17:0)	424.3	113	29	3
S1P	S1P (d17:1)	422.3	60.08	29	3
S1P	S1P (d17:1)	422.3	113	29	3
S1P	S1P (d17:2)	420.3	60.08	29	3
S1P	S1P (d17:2)	420.3	113	29	3
S1P	S1P (d16:0)	410.3	60.08	29	3
S1P	S1P (d16:0)	410.3	113	29	3
S1P	S1P (d16:1)	408.28	60.08	29	3
S1P	S1P (d16:1)	408.28	113	29	3
S1P	S1P (d16:2)	406.27	60.08	29	3
S1P	S1P (d16:2)	406.27	113	29	3
S1P	S1P (d14:0)	382.2	60.08	29	3
S1P	S1P (d14:0)	382.2	113	29	3
S1P	S1P (d14:1)	380.2	60.08	29	3
S1P	S1P (d14:1)	380.2	113	29	3
S1P	S1P (d14:2)	378.2	60.08	29	3
S1P	S1P (d14:2)	378.2	113	29	3

Table 5.12: Measured quantifier lipid species included in MRM-list of panel 1 and their corresponding ISTD for the calculation of ratios and concentration calculations. DGs were excluded from report due to high technical variance.

Measured lipid	Corresponding ISTD		Measured lipid	Corresponding ISTD
CE 15:0	PC 14:0 14:0		**LPC 16:1**	LPC 20:0
CE 16:0	PC 14:0 14:0		**LPC 17:0**	LPC 20:0
CE 16:1	PC 14:0 14:0		**LPC 17:1**	LPC 20:0
CE 17:0	PC 14:0 14:0		**LPC 18:0**	LPC 20:0
CE 17:1	PC 14:0 14:0		**LPC 18:1**	LPC 20:0
CE 18:0	PC 14:0 14:0		**LPC 18:2**	LPC 20:0
CE 18:1	PC 14:0 14:0		**LPC 18:3**	LPC 20:0
CE 18:2	PC 14:0 14:0		**LPC 19:0**	LPC 20:0
CE 18:3	PC 14:0 14:0		**LPC 20:1**	LPC 20:0
CE 20:1	PC 14:0 14:0		**LPC 20:2**	LPC 20:0
CE 20:2	PC 14:0 14:0		**LPC 20:3**	LPC 20:0
CE 20:3	PC 14:0 14:0		**LPC 20:4**	LPC 20:0
CE 20:4	PC 14:0 14:0		**LPC 20:5**	LPC 20:0
CE 20:5	PC 14:0 14:0		**LPC 22:0**	LPC 20:0
CE 22:4	PC 14:0 14:0		**LPC 22:1**	LPC 20:0
CE 22:5	PC 14:0 14:0		**LPC 22:5**	LPC 20:0
CE 22:6	PC 14:0 14:0		**LPC 22:6**	LPC 20:0
CE 24:4	PC 14:0 14:0		**LPC 24:0**	LPC 20:0
Cer d16:1/C22:0	Cer d 18:1 / C17:0		**LPC 26:0**	LPC 20:0
Cer d18:0/C22:0	Cer d 18:1 / C17:0		**MHC d18:1/16:0**	MHC d18:1/16:0d3
Cer d18:0/C24:0	Cer d 18:1 / C17:0		**MHC d18:1/18:0**	MHC d18:1/16:0d3
Cer d18:0/C24:1	Cer d 18:1 / C17:0		**MHC d18:1/20:0**	MHC d18:1/16:0d3
Cer d18:1/19:0	Cer d 18:1 / C17:0		**MHC d18:1/22:0**	MHC d18:1/16:0d3
Cer d18:1/C16:0	Cer d 18:1 / C17:0		**MHC d18:1/24:0**	MHC d18:1/16:0d3
Cer d18:1/C18:0	Cer d 18:1 / C17:0		**MHC d18:1/24:1**	MHC d18:1/16:0d3
Cer d18:1/C20:0	Cer d 18:1 / C17:0		**MHC d18:1/8:0**	MHC d18:1/16:0d3
Cer d18:1/C22:0	Cer d 18:1 / C17:0		**oddPC 29:0**	PC 14:0 14:0
Cer d18:1/C24:0	Cer d 18:1 / C17:0		**oddPC 31:1**	PC 14:0 14:0
Cer d18:1/C24:1	Cer d 18:1 / C17:0		**oddPC 33:1**	PC 14:0 14:0
Cer d18:1/C26:1	Cer d 18:1 / C17:0		**oddPC 35:2**	PC 14:0 14:0
Cer d18:2/C16:0	Cer d 18:1 / C17:0		**oddPC 35:3**	PC 14:0 14:0
Cer d18:2/C22:0	Cer d 18:1 / C17:0		**oddPC 37:4**	PC 14:0 14:0
Cer d18:2/C24:1	Cer d 18:1 / C17:0		**oddPC 37:5**	PC 14:0 14:0
DG 15:0 15:0	DG 24:0 (12:0)		**oddPC 39:5**	PC 14:0 14:0
DG 30:0 -(16:0)	DG 24:0 (12:0)		**oddPC 39:6**	PC 14:0 14:0
DG 30:1 -(16:1)	DG 24:0 (12:0)		**oddPC 39:7**	PC 14:0 14:0
DG 32:0 -(16:0)	DG 24:0 (12:0)		**PC(O-32:1)**	PC 14:0 14:0
DG 32:1 -(14:0 18:1)	DG 24:0 (12:0)		**PC(O-34:1)**	PC 14:0 14:0
DG 32:1 -(16:0 16:1)	DG 24:0 (12:0)		**PC(O-34:2)**	PC 14:0 14:0
DG 32:2 -(16:1)	DG 24:0 (12:0)		**PC(O-36:1)**	PC 14:0 14:0
DG 34:0 -(16:0 18:0)	DG 24:0 (12:0)		**PC(O-36:2)**	PC 14:0 14:0
DG 34:1 -(16:0 18:1)	DG 24:0 (12:0)		**PC(O-36:5)**	PC 14:0 14:0
DG 34:2 -(16:0 18:2)	DG 24:0 (12:0)		**PC(O-38:4)**	PC 14:0 14:0
DG 34:2 -(16:1 18:1)	DG 24:0 (12:0)		**PC(O-38:5)**	PC 14:0 14:0
DG 36:0 -(18:0)	DG 24:0 (12:0)		**PC(O-40:5)**	PC 14:0 14:0
DG 36:1	DG 24:0 (12:0)		**PC(O-40:6)**	PC 14:0 14:0
DG 36:2	DG 24:0 (12:0)		**PC(O-40:7)**	PC 14:0 14:0
DG 36:2 -(18:2)	DG 24:0 (12:0)		**PC 13:0 13:0**	PC 14:0 14:0
DG 36:3	DG 24:0 (12:0)		**PC 28:0**	PC 14:0 14:0
DG 36:4 -(18:2)	DG 24:0 (12:0)		**PC 30:0**	PC 14:0 14:0
DG 36:4 -(18:3)	DG 24:0 (12:0)		**PC 32:0**	PC 14:0 14:0
DG 36:4 -(20:4)	DG 24:0 (12:0)		**PC 32:1**	PC 14:0 14:0
DG 38:4 -(20:4)	DG 24:0 (12:0)		**PC 32:2**	PC 14:0 14:0
DG 38:5	DG 24:0 (12:0)		**PC 32:3**	PC 14:0 14:0
DG 38:6 -(20:4)	DG 24:0 (12:0)		**PC 34:0**	PC 14:0 14:0
DHC 16:0	MHC d18:1/16:0d3		**PC 34:1**	PC 14:0 14:0
DHC 18:0	MHC d18:1/16:0d3		**PC 34:2**	PC 14:0 14:0
DHC 20:0	MHC d18:1/16:0d3		**PC 34:2 + 2O**	PC 14:0 14:0
DHC 22:0	MHC d18:1/16:0d3		**PC 34:4**	PC 14:0 14:0
DHC 24:0	MHC d18:1/16:0d3		**PC 36:0\PC(P-38:6)**	PC 14:0 14:0
DHC 24:1	MHC d18:1/16:0d3		**PC 36:1**	PC 14:0 14:0
GM3 16:0	SM 30:1		**PC 36:2**	PC 14:0 14:0
GM3 18:0	SM 30:1		**PC 36:3**	PC 14:0 14:0
LPC 14:0	LPC 20:0		**PC 38:2**	PC 14:0 14:0
LPC 15:0	LPC 20:0		**PC 38:3**	PC 14:0 14:0
LPC 16:0	LPC 20:0		**PC 38:4**	PC 14:0 14:0
PC 38:5	PC 14:0 14:0		**SM 32:2**	SM 30:1
PC 38:7	PC 14:0 14:0		**SM 33:1**	SM 30:1

Measured lipid	Corresponding ISTD		Measured lipid	Corresponding ISTD
PC 40:4	PC 14:0 14:0		**SM 34:0**	SM 30:1
PC 40:5	PC 14:0 14:0		**SM 34:1**	SM 30:1
PC 40:6	PC 14:0 14:0		**SM 34:2**	SM 30:1
PC 40:7	PC 14:0 14:0		**SM 34:3**	SM 30:1
PC 40:8	PC 14:0 14:0		**SM 35:1**	SM 30:1
PC(16:0/20:4)\PC(18:1/18:3)	PC 14:0 14:0		**SM 35:2**	SM 30:1
PC(16:0/22:6)\PC(18:2/20:4)	PC 14:0 14:0		**SM 36:1**	SM 30:1
PC(O-16:0/0:0)	PC 14:0 14:0		**SM 36:2**	SM 30:1
PC(O-18:0/0:0)	PC 14:0 14:0		**SM 36:3**	SM 30:1
PC(O-18:1/0:0)	PC 14:0 14:0		**SM 37:2**	SM 30:1
PC(O-20:0/0:0)	PC 14:0 14:0		**SM 38:1**	SM 30:1
PC(O-20:1/0:0)	PC 14:0 14:0		**SM 38:2**	SM 30:1
PC(O-32:2)\PC(P-32:1)	PC 14:0 14:0		**SM 39:1**	SM 30:1
PC(O-34:4)\PC(P-34:3)	PC 14:0 14:0		**SM 41:1**	SM 30:1
PC(P-30:0)	PC 14:0 14:0		**SM 41:2**	SM 30:1
PC(P-36:5)	PC 14:0 14:0		**SM 42:1**	SM 30:1
PE 34:1	PE 14:0 14:0		**TG 14:0 16:0 18:2**	d5TAG 48:0 /16:0 16:0 16:0
PE 34:2	PE 14:0 14:0		**TG 14:0 16:1 18:1**	d5TAG 48:0 /16:0 16:0 16:0
PE 36:1	PE 14:0 14:0		**TG 14:0 16:1 18:2**	d5TAG 48:0 /16:0 16:0 16:0
PE 36:2	PE 14:0 14:0		**TG 14:0 18:0 18:1**	d5TAG 48:0 /16:0 16:0 16:0
PE 36:3	PE 14:0 14:0		**TG 14:0 18:2 18:2**	d5TAG 48:0 /16:0 16:0 16:0
PE 36:4	PE 14:0 14:0		**TG 14:1 16:0 18:1**	d5TAG 48:0 /16:0 16:0 16:0
PE 38:3	PE 14:0 14:0		**TG 14:1 16:1 18:0**	d5TAG 48:0 /16:0 16:0 16:0
PE 38:4	PE 14:0 14:0		**TG 14:1 18:0 18:2**	d5TAG 48:0 /16:0 16:0 16:0
PE 38:5	PE 14:0 14:0		**TG 14:1 18:1 18:1**	d5TAG 48:0 /16:0 16:0 16:0
PE 38:6	PE 14:0 14:0		**TG 15:0 18:1 16:0**	d5TAG 48:0 /16:0 16:0 16:0
PE 40:4	PE 14:0 14:0		**TG 15:0 18:1 18:1**	d5TAG 48:0 /16:0 16:0 16:0
PE 40:5	PE 14:0 14:0		**TG 16:0 16:0 16:0**	d5TAG 48:0 /16:0 16:0 16:0
PE 40:6	PE 14:0 14:0		**TG 16:0 16:0 18:0**	d5TAG 48:0 /16:0 16:0 16:0
PE(16:0/0:0)	PE 14:0 (0:0)		**TG 16:0 16:0 18:1**	d5TAG 48:0 /16:0 16:0 16:0
PE(18:0/0:0)	PE 14:0 (0:0)		**TG 16:0 16:0 18:2**	d5TAG 48:0 /16:0 16:0 16:0
PE(18:1/0:0)	PE 14:0 (0:0)		**TG 16:0 16:1 18:1**	d5TAG 48:0 /16:0 16:0 16:0
PE(18:2/0:0)	PE 14:0 (0:0)		**TG 16:0 18:0 18:1**	d5TAG 48:0 /16:0 16:0 16:0
PE(20:4/0:0)	PE 14:0 (0:0)		**TG 16:0 18:1 18:1**	d5TAG 48:0 /16:0 16:0 16:0
PE(22:6/0:0)	PE 14:0 14:0		**TG 16:0 18:1 18:2**	d5TAG 48:0 /16:0 16:0 16:0
PE(O-18:1/20:3)	PC 14:0 14:0		**TG 16:0 18:2 18:2**	d5TAG 48:0 /16:0 16:0 16:0
PE(P-16:0/18:1) FA	PC 14:0 14:0		**TG 16:1 16:1 16:1**	d5TAG 48:0 /16:0 16:0 16:0
PE(P-16:0/18:2) FA	PC 14:0 14:0		**TG 16:1 16:1 18:0**	d5TAG 48:0 /16:0 16:0 16:0
PE(P-16:0/20:4) FA	PC 14:0 14:0		**TG 16:1 16:1 18:1**	d5TAG 48:0 /16:0 16:0 16:0
PE(P-16:0/22:5) FA	PC 14:0 14:0		**TG 16:1 18:1 18:1**	d5TAG 48:0 /16:0 16:0 16:0
PE(P-16:0/22:6) FA	PC 14:0 14:0		**TG 16:1 18:1 18:2**	d5TAG 48:0 /16:0 16:0 16:0
PE(P-18:0/18:1) FA	PC 14:0 14:0		**TG 17:0 16:0 16:1**	d5TAG 48:0 /16:0 16:0 16:0
PE(P-18:0/18:2) FA	PC 14:0 14:0		**TG 17:0 16:0 18:0**	d5TAG 48:0 /16:0 16:0 16:0
PE(P-18:0/20:4) FA	PC 14:0 14:0		**TG 17:0 17:0 17:0**	d5TAG 48:0 /16:0 16:0 16:0
PE(P-18:0/22:5) FA	PC 14:0 14:0		**TG 17:0 18:1 14:0**	d5TAG 48:0 /16:0 16:0 16:0
PE(P-18:0/22:6) FA	PC 14:0 14:0		**TG 17:0 18:1 16:0**	d5TAG 48:0 /16:0 16:0 16:0
PE(P-20:0/20:4) FA	PC 14:0 14:0		**TG 17:0 18:1 16:1**	d5TAG 48:0 /16:0 16:0 16:0
PE(P-20:0/20:4) head group	PC 14:0 14:0		**TG 17:0 18:1 18:1**	d5TAG 48:0 /16:0 16:0 16:0
PG 16:0 18:1	PG 14:0 14:0		**TG 17:0 18:2 16:0**	d5TAG 48:0 /16:0 16:0 16:0
PI 32:1	PI 12:0 13:0		**TG 18:0 18:0 18:0**	d5TAG 48:0 /16:0 16:0 16:0
PI 34:1	PI 12:0 13:0		**TG 18:0 18:0 18:1**	d5TAG 48:0 /16:0 16:0 16:0
PI 34:2	PI 12:0 13:0		**TG 18:0 18:1 18:1**	d5TAG 48:0 /16:0 16:0 16:0
PI 36:1	PI 12:0 13:0		**TG 18:0 18:2 18:2**	d5TAG 48:0 /16:0 16:0 16:0
PI 36:2	PI 12:0 13:0		**TG 18:1 14:0 16:0**	d5TAG 48:0 /16:0 16:0 16:0
PI 36:3	PI 12:0 13:0		**TG 18:1 18:1 18:1**	d5TAG 48:0 /16:0 16:0 16:0
PI 36:4	PI 12:0 13:0		**TG 18:1 18:1 18:2**	d5TAG 48:0 /16:0 16:0 16:0
PI 38:2	PI 12:0 13:0		**TG 18:1 18:1 20:4**	d5TAG 48:0 /16:0 16:0 16:0
PI 38:3	PI 12:0 13:0		**TG 18:1 18:1 22:6**	d5TAG 48:0 /16:0 16:0 16:0
PI 38:4	PI 12:0 13:0		**TG 18:1 18:2 18:2**	d5TAG 48:0 /16:0 16:0 16:0
PI 38:5	PI 12:0 13:0		**TG 18:2 18:2 18:2**	d5TAG 48:0 /16:0 16:0 16:0
PI 38:6	PI 12:0 13:0		**TG 18:2 18:2 20:4**	d5TAG 48:0 /16:0 16:0 16:0
PI 40:4	PI 12:0 13:0		**TG 48:0**	d5TAG 48:0 /16:0 16:0 16:0
PI 40:5	PI 12:0 13:0		**TG 48:1**	d5TAG 48:0 /16:0 16:0 16:0
PI 40:6	PI 12:0 13:0		**TG 48:2**	d5TAG 48:0 /16:0 16:0 16:0
PS 38:4	PS 14:0 14:0		**TG 48:3**	d5TAG 48:0 /16:0 16:0 16:0
SM 31:1	SM 30:1		**TG 49:1**	d5TAG 48:0 /16:0 16:0 16:0
SM 32:0	SM 30:1		**TG 50:0**	d5TAG 48:0 /16:0 16:0 16:0
SM 32:1	SM 30:1		**TG 50:1**	d5TAG 48:0 /16:0 16:0 16:0
TG 50:2	d5TAG 48:0 /16:0 16:0 16:0			
TG 50:3	d5TAG 48:0 /16:0 16:0 16:0			
TG 50:4	d5TAG 48:0 /16:0 16:0 16:0			
TG 51:0	d5TAG 48:0 /16:0 16:0 16:0			
TG 51:1	d5TAG 48:0 /16:0 16:0 16:0			

Measured lipid	Corresponding ISTD		Measured lipid	Corresponding ISTD
TG 51:2	d5TAG 48:0 /16:0 16:0 16:0			
TG 52:1	d5TAG 48:0 /16:0 16:0 16:0			
TG 52:2	d5TAG 48:0 /16:0 16:0 16:0			
TG 52:3	d5TAG 48:0 /16:0 16:0 16:0			
TG 52:4	d5TAG 48:0 /16:0 16:0 16:0			
TG 53:2	d5TAG 48:0 /16:0 16:0 16:0			
TG 54:0	d5TAG 48:0 /16:0 16:0 16:0			
TG 54:1	d5TAG 48:0 /16:0 16:0 16:0			
TG 54:2	d5TAG 48:0 /16:0 16:0 16:0			
TG 54:3	d5TAG 48:0 /16:0 16:0 16:0			
TG 54:4	d5TAG 48:0 /16:0 16:0 16:0			
TG 54:5	d5TAG 48:0 /16:0 16:0 16:0			
TG 54:6	d5TAG 48:0 /16:0 16:0 16:0			
TG 56:6	d5TAG 48:0 /16:0 16:0 16:0			
TG 56:8	d5TAG 48:0 /16:0 16:0 16:0			
TG 58:8	d5TAG 48:0 /16:0 16:0 16:0			
THC 16:0	THC 18:0 d3			

Table 5.13.: Measured quantifier lipid species included in MRM-list of panel 2 and their corresponding ISTD for the calculation of ratios and concentration calculations

Measured Lipid	Corresponding ISTD		Measured Lipid	Corresponding ISTD
Cer d16:1/C18:0	Cer d18:1/C17:0		**MHCer d18:1/C24:1**	MHCer d18:1/16:0d3
Cer d16:1/C20:0	Cer d18:1/C17:0		**MHCer d18:1/C25:0**	MHCer d18:1/16:0d3
Cer d16:1/C22:0	Cer d18:1/C17:0		**MHCer d18:1/C26:0**	MHCer d18:1/16:0d3
Cer d16:1/C23:0	Cer d18:1/C17:0		**MHCer d18:1/C8:0**	MHCer d18:1/16:0d3
Cer d16:1/C24:0	Cer d18:1/C17:0		**MHCer d18:2/C20:0**	MHCer d18:1/16:0d3
Cer d18:0/C18:0	Cer d18:1/C17:0		**MHCer d18:2/C24:0**	MHCer d18:1/16:0d3
Cer d18:0/C22:0	Cer d18:1/C17:0		**SM C32:1**	SM C30:1
Cer d18:0/C23:0	Cer d18:1/C17:0		**SM C32:2**	SM C30:1
Cer d18:0/C24:0	Cer d18:1/C17:0		**SM C34:0**	SM C30:1
Cer d18:0/C24:1	Cer d18:1/C17:0		**SM C34:1**	SM C30:1
Cer d18:1/C16:0	Cer d18:1/C17:0		**SM C34:2**	SM C30:1
Cer d18:1/C16:1	Cer d18:1/C17:0		**SM C36:0**	SM C30:1
Cer d18:1/C18:0	Cer d18:1/C17:0		**SM C36:1**	SM C30:1
Cer d18:1/C18:1	Cer d18:1/C17:0		**SM C36:2**	SM C30:1
Cer d18:1/C20:0	Cer d18:1/C17:0		**SM C38:0**	SM C30:1
Cer d18:1/C20:1	Cer d18:1/C17:0		**SM C38:1**	SM C30:1
Cer d18:1/C22:0	Cer d18:1/C17:0		**SM C38:2**	SM C30:1
Cer d18:1/C22:1	Cer d18:1/C17:0		**SM C39:1**	SM C30:1
Cer d18:1/C23:0	Cer d18:1/C17:0		**SM C40:0**	SM C30:1
Cer d18:1/C24:0	Cer d18:1/C17:0		**SM C40:1**	SM C30:1
Cer d18:1/C24:1	Cer d18:1/C17:0		**SM C40:2**	SM C30:1
Cer d18:1/C25:0	Cer d18:1/C17:0		**SM C41:1**	SM C30:1
Cer d18:1/C25:1	Cer d18:1/C17:0		**SM C41:2**	SM C30:1
Cer d18:1/C26:0	Cer d18:1/C17:0		**SM C42:0**	SM C30:1
Cer d18:1/C26:1	Cer d18:1/C17:0		**SM C42:1**	SM C30:1
Cer d18:2/C20:0	Cer d18:1/C17:0		**SM C42:2**	SM C30:1
Cer d18:2/C22:0	Cer d18:1/C17:0		**SM C42:3**	SM C30:1
Cer d18:2/C23:0	Cer d18:1/C17:0		**SM C43:1**	SM C30:1
Cer d18:2/C24:0	Cer d18:1/C17:0		**SM C43:2**	SM C30:1
Cer d18:2/C24:1	Cer d18:1/C17:0		**SM C44:1**	SM C30:1
Cer d18:2/C25:0	Cer d18:1/C17:0		**SM d16:1/C16:0**	SM C30:1
DHCer d16:1/C16:0	DHCer 16:0d3		**SM d16:1/C18:0**	SM C30:1
DHCer d18:1/C14:0	DHCer 16:0d3		**SM d16:1/C20:0**	SM C30:1
DHCer d18:1/C16:0	DHCer 16:0d3		**SM d16:1/C22:0**	SM C30:1
DHCer d18:1/C18:0	DHCer 16:0d3		**SM d18:0/C16:0**	SM C30:1
DHCer d18:1/C20:0	DHCer 16:0d3		**SM d18:0/C22:0**	SM C30:1
DHCer d18:1/C22:0	DHCer 16:0d3		**SM d18:1/C14:0**	SM C30:1
DHCer d18:1/C23:0	DHCer 16:0d3		**SM d18:1/C16:0**	SM C30:1
DHCer d18:1/C24:0	DHCer 16:0d3		**SM d18:1/C18:0**	SM C30:1
DHCer d18:1/C24:1	DHCer 16:0d3		**SM d18:1/C20:0**	SM C30:1
DHCer d18:2/C16:0	DHCer 16:0d3		**SM d18:1/C22:0**	SM C30:1
DHCer d18:2/C22:0	DHCer 16:0d3		**SM d18:1/C22:1**	SM C30:1
DHCer d18:2/C24:0	DHCer 16:0d3		**SM d18:1/C23:0**	SM C30:1
GM3 d16:1/C18:0	SM C30:1		**SM d18:1/C24:1**	SM C30:1
GM3 d16:1/C20:0	SM C30:1		**SM d18:2/C16:0**	SM C30:1
GM3 d16:1/C22:0	SM C30:1		**SM d18:2/C18:0**	SM C30:1
GM3 d16:1/C24:0	SM C30:1		**SM d18:2/C20:0**	SM C30:1
GM3 d18:1/C14:0	SM C30:1		**SM d18:2/C23:0**	SM C30:1
GM3 d18:1/C16:0	SM C30:1			

Measured Lipid	Corresponding ISTD		Measured Lipid	Corresponding ISTD
GM3 d18:1/C18:0	SM C30:1			
GM3 d18:1/C20:0	SM C30:1			
GM3 d18:1/C22:0	SM C30:1			
GM3 d18:1/C24:0	SM C30:1			
GM3 d18:1/C24:1	SM C30:1			
GM3 d18:2/16:0	SM C30:1			
GM3 d18:2/18:0	SM C30:1			
GM3 d18:2/20:0	SM C30:1			
GM3 d18:2/24:0	SM C30:1			
GM3 d18:2/24:1	SM C30:1			
MHCer d18:1/C16:0	MHCer d18:1/16:0d3			
MHCer d18:1/C16:1	MHCer d18:1/16:0d3			
MHCer d18:1/C18:0	MHCer d18:1/16:0d3			
MHCer d18:1/C20:0	MHCer d18:1/16:0d3			
MHCer d18:1/C22:0	MHCer d18:1/16:0d3			
MHCer d18:1/C23:0	MHCer d18:1/16:0d3			
MHCer d18:1/C24:0	MHCer d18:1/16:0d3			

Table 5.14.: Measured quantifier lipid species included in MRM-list of panel 3 and their corresponding ISTD for the calculation of ratios and concentration calculations

Measured lipids	Corresponding ISTD
TG 46:2	d5TAG 48:0 /16:0 16:0 16:0
TG 46:1	d5TAG 48:0 /16:0 16:0 16:0
TG 46:0	d5TAG 48:0 /16:0 16:0 16:0
TG 48:3	d5TAG 48:0 /16:0 16:0 16:0
TG 48:2	d5TAG 48:0 /16:0 16:0 16:0
TG 48:1	d5TAG 48:0 /16:0 16:0 16:0
TG 48:0	d5TAG 48:0 /16:0 16:0 16:0
TG 49:1	d5TAG 48:0 /16:0 16:0 16:0
TG 50:4	d5TAG 48:0 /16:0 16:0 16:0
TG 50:3	d5TAG 48:0 /16:0 16:0 16:0
TG 50:2	d5TAG 48:0 /16:0 16:0 16:0
TG 50:1	d5TAG 48:0 /16:0 16:0 16:0
TG 50:0	d5TAG 48:0 /16:0 16:0 16:0
TG 51:3	d5TAG 48:0 /16:0 16:0 16:0
TG 51:2	d5TAG 48:0 /16:0 16:0 16:0
TG 51:1	d5TAG 48:0 /16:0 16:0 16:0
TG 51:0	d5TAG 48:0 /16:0 16:0 16:0
TG 52:5	d5TAG 48:0 /16:0 16:0 16:0
TG 52:4	d5TAG 48:0 /16:0 16:0 16:0
TG 52:3	d5TAG 48:0 /16:0 16:0 16:0
TG 52:2	d5TAG 48:0 /16:0 16:0 16:0
TG 52:1	d5TAG 48:0 /16:0 16:0 16:0
TG 53:2	d5TAG 48:0 /16:0 16:0 16:0
TG 54:6	d5TAG 48:0 /16:0 16:0 16:0
TG 54:5	d5TAG 48:0 /16:0 16:0 16:0
TG 54:4	d5TAG 48:0 /16:0 16:0 16:0
TG 54:3	d5TAG 48:0 /16:0 16:0 16:0
TG 54:2	d5TAG 48:0 /16:0 16:0 16:0
TG 54:1	d5TAG 48:0 /16:0 16:0 16:0
TG 54:0	d5TAG 48:0 /16:0 16:0 16:0
TG 56:8	d5TAG 48:0 /16:0 16:0 16:0
TG 56:7	d5TAG 48:0 /16:0 16:0 16:0
TG 56:6	d5TAG 48:0 /16:0 16:0 16:0
TG 56:5	d5TAG 48:0 /16:0 16:0 16:0
TG 58:11	d5TAG 48:0 /16:0 16:0 16:0
TG 58:10	d5TAG 48:0 /16:0 16:0 16:0
TG 58:9	d5TAG 48:0 /16:0 16:0 16:0
TG 58:8	d5TAG 48:0 /16:0 16:0 16:0

Table 5.15.: Measured quantifier lipid species included in MRM-list of panel 4 and their corresponding ISTD for the calculation of ratios and concentration calculations

Measured lipids	Corresponding ISTD
S1P (d14:0)	13C2D2–S1P
S1P (d14:1)	13C2D2–S1P
S1P (d14:2)	13C2D2–S1P
S1P (d16:0)	13C2D2–S1P
S1P (d16:1)	13C2D2–S1P
S1P (d16:2)	13C2D2–S1P
S1P (d17:0)	13C2D2–S1P
S1P (d18:0)	13C2D2–S1P
S1P (d18:1)	13C2D2–S1P
S1P (d18:2)	13C2D2–S1P
S1P (d19:0)	13C2D2–S1P
S1P (d19:1)	13C2D2–S1P
S1P (d19:2)	13C2D2–S1P
S1P (t18:0)	13C2D2–S1P
S1P (d20:0)	13C2D2–S1P
S1P (d20:1)	13C2D2–S1P
S1P (d20:2)	13C2D2–S1P
S1P (d21:0)	13C2D2–S1P
S1P (d21:1)	13C2D2–S1P
S1P (t20:0)	13C2D2–S1P
S1P (d22:0)	13C2D2–S1P
S1P (d22:1)	13C2D2–S1P
S1P (d22:2)	13C2D2–S1P
S1P (d24:0)	13C2D2–S1P
S1P (d24:1)	13C2D2–S1P
S1P (d24:2)	13C2D2–S1P

Acknowledgments

I am grateful to all people involved in the success of this thesis.
Firstly, I would like to thank Prof. Dr. Boretti and Prof. Dr. Sieber-Ruckstuhl for accepting me as their graduate student, for giving me the opportunity to travel to Singapore for the practical part of this project as well as their support, help and corrections during the write-up of the thesis. Moreover I am thankful to Prof. Dr. Markus Wenk for allowing me to learn and work in his laboratory in Singapore. Furthermore, I would like to thank Prof. Lutz for taking his time reading, correcting and evaluating this thesis.
Secondly, I would like to express my sincere gratitude to my supervisor Bo Burla, PhD, in Singapore for his great guidance, supervision and patience during practical laboratory work especially because I was new to this field and needed to learn lipidomics from scratch: Deep thanks for spending evenings together adjusting retention times before starting the MS run, explaining all the technical details and enormous amounts of possible settings, guiding me through the manual chromatographic integration and its calculations, helping me to organize a big data project and its statistical interpretation as well as the evaluation of the results and their presentation and the constant helpful suggestions and fruitful discussions.
Many thanks to assistant professor Amaury Cazenave Gassiot for the helpful advice during manual integration as well as the guidance and supervision during the practical work of panel 3 and its correction. Moreover, I would like to thank assistant professor Federico Torta for his advice during trouble shooting and for the guidance during the untargeted trials.
Furthermore, special thanks go to Shanshan Ji, PhD, for her helpful tutorials in the complex world of statistics.
Moreover, many thanks to Florence Schmid, who conducted the long-term animal experiment. Without her diligent work, I would not have been able to process the samples. Thanks goes also to Dr. Venzin, who helped with the surgeries during the experiment.
Moreover, I would like to thank Anke Willing for her support and her organization of lipid extraction in Zurich.
Deep thanks goes out to every single SLING lab member in Singapore, as I felt very welcome and for creating a great working atmosphere with fun and laughter paired with busy work in the laboratory. They were always happy to answer my questions on lipidomics.
During the writing of this thesis my colleagues Lena Zwickl and Catia Musella and my friend Iva Cvitaš were a great support and always had a sympathetic ear.
Last but not least my most heartfelt thanks go to my parents for their constant support during my studies and this thesis.

Curriculum Vitae

Susanne Spoerel, Tierärztin

Persönliche Daten:

Geburtsdatum	28.01.1990
Geburtsort	Hamburg
Nationalität	Deutsch

Bildungsweg:

Seit 2016	Dissertation, Kleintierklinik Vetsuisse Fakultät Zürich (CH) in Kooperation mit National University of Singapore (SGP)
2009 bis 2015	Studium der Veterinärmedizin an der Tierärztlichen Hochschule Hannover (DEU)
2000 bis 2009	Johann-Rist-Gymnasium, Wedel (DEU)

Berufserfahrung:

Seit 2017	Tierärztin, Klinik für Kleintiere, Universität Gießen (DEU)
2016 - 2017	Dissertation, Klinik für Kleintiermedizin, Vetsuisse Fakultät Zürich, Universität Zürich (CHE) in Kooperation mit Singapore Lipidomics Incubator, National University of Singapore, Singapore (SGP)
2015	Wissenschaftliche Mitarbeiterin am Heinrich-Pette-Institut, Leibniz Institut für Experimentelle Virologie, Hamburg (DEU)
2011, 2013	Wissenschaftliche Hilfskraft im Physiologischen Institut der Tierärztlichen Hochschule Hannover (DEU)

Extracurriculäre Weiterbildung:

2014	Leadership Program for Veterinary Students, Cornell University (USA) Research project: CD8+ T-cell response in neonatal mice infected with murine cytomegalovirus
2013	Wahlpraktikum Institut für neue und neuartige Tierseuchenerreger, Friedrich-Loeffler-Institut, Insel Riems (DEU)
2012	Fundamentals of Veterinary Science Summer School, Cambridge University (UK) Research project: Sites of replication of a persistent murine norovirus strain